AD-A131 118 HEAT TRANSFER AND EROSION IN THE ARES 75MM HIGH VELOCITY CANNON VOLUME 2(U) ARES INC PORT CLINTON OH F A VASSALLO ET AL. OCT 77 DAAA09-76-C-2082 1/2

UNCLASSIFIED F/G 20/13 NL

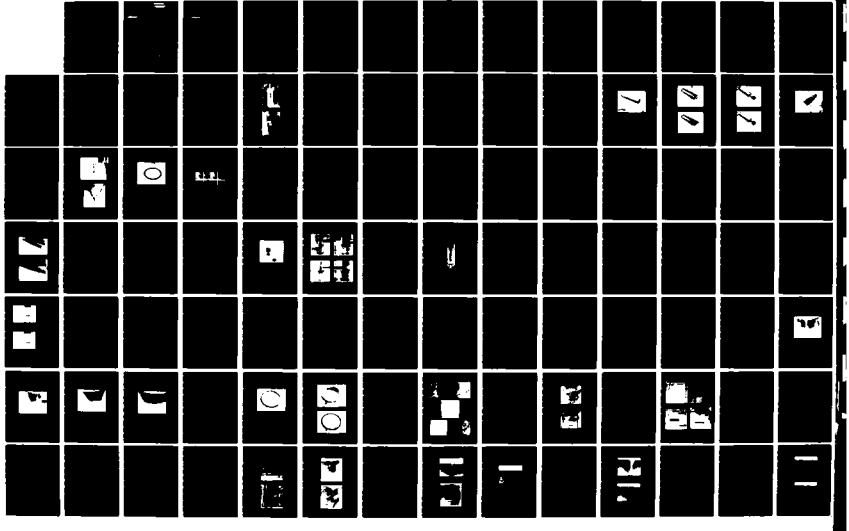

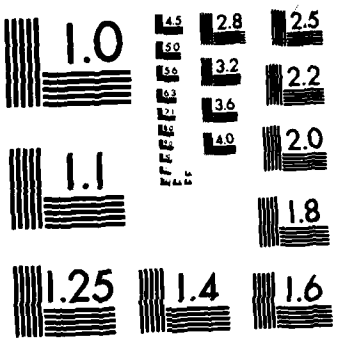

[redacted]

(2)

Calspan

Technical Report

HEAT TRANSFER AND EROSION IN THE ARES 75 MM HIGH VELOCITY CANNON – VOL II

F.A. Vassallo and W.R. Brown

Calspan Technical Report No. VL-5873-D-1

Calspan Corporation
Buffalo, New York 14221

Calspan

HEAT TRANSFER AND EROSION IN THE ARES 75 MM HIGH VELOCITY CANNON – VOL II

F.A. Vassallo and W.R. Brown

Calspan Technical Report No. VL-5873-D-1

Prepared For:

ARES, INC.
PORT CLINTON, OHIO

OCTOBER 1977
PURCHASE ORDER NO. 1438

PREPARED BY: F.A. Vassallo
F.A. Vassallo
Principal Engineer
Thermal Research Center

APPROVED BY: Gerald A. Sterbutzel
G.A. Sterbutzel, Director
Thermal Research Center

W. Richard Brown
W.R. Brown
Principal Engineer
Thermal Research Center

Calspan Corporation
Buffalo, New York 14221

FOREWORD

This report was prepared for Ares, Incorporated under Purchase Order No. 1438. The work was monitored by Mr. Duane Somers of Ares, and was performed in the period from December 1975 to October 1977.

The aid of Mr. A.K. Ashby in conducting the firing tests and Mr. D.E. Adams in the thermal analysis of barrel bending is gratefully acknowledged.

TABLE OF CONTENTS

Section	Title	Page
	FOREWORD	i
I	INTRODUCTION AND SUMMARY	1
	A. THERMAL EFFECTS	2
	B. EROSION	2
	C. FATIGUE	2
II	EXPERIMENTAL FIXTURES AND INSTRUMENTATION	4
	A. SINGLE-SHOT TEST FIXTURE	4
	B. INSTRUMENTED SHORT BARREL	4
	C. EROSION SENSING RINGS	10
	D. EROSION RING PREPARATION AND DISCUSSION	19
	1. Vascomax 300 Maraging Steel	19
	2. Low Alloy Steels	19
	3. Low Carbon Steel	20
	4. Chromium Plate	21
	5. Refractory Coatings	24
	6. Summary of Ring Specimens	24
	E. BARREL LINERS	27
	1. Refractory Metals	27
	2. Replaceable 4340 Liner	28
	F. AMMUNITION	30
	1. Propellant Charge	30
	2. Ablator Composition	31
	3. Ablative Ammunition	32
III	SINGLE-SHOT TEST RESULTS AND DISCUSSION	37
	A. BALLISTICS PERFORMANCE	37
	B. HEAT INPUT	45
	C. EROSION	51
	1. Entrance End - M26 Stick Propellant	51

TABLE OF CONTENTS (CONT.)

Section	Title	Page
	2. Entrance End - M26/M30 Propellant	65
	3. Exit End	67
	D. FATIGUE	69
	1. Short Barrel Insert Ring Surface Cracking	74
	a. 4340 Steel Observations	74
	b. Vascomax 300 Observations	83
	c. Extended Short Barrel Firing Experience	86
	2. Low Carbon Steel Liners	86
	3. Main Barrel Fatigue	88
	a. Surface Cracking	88
	b. Extended Main Barrel Firing Experience	88
	4. Summary of Fatigue Considerations	89
	E. LINER TESTS	90
	1. Tantalum Liner	90
	2. Replaceable 4340 Liner	92
IV	RAPID FIRE RESULTS	94
	A. BARREL TEMPERATURES AND HEAT INPUT	94
	B. EROSION	100
	REFERENCES	104
	APPENDIX	105
	A. BRAZING STUDIES	105
	B. THERMALLY INDUCED BARREL BENDING	114

LIST OF FIGURES

Figure	Title	Page
1	SINGLE-SHOT 75MM TEST FIXTURE	5
2	INSTRUMENTED SHORT BARREL	6
3	SHORT BARREL RETAINING COLLAR	7
4	IN-WALL THERMOCOUPLE DESIGN	9
5	INSTRUMENTED VASCOMAX 300 SHORT BARREL SHOWING TYPICAL EROSION RINGS	11
6	VIEW OF INSTRUMENTED VASCOMAX SHORT BARREL (ENTRANCE END)	12
7	VIEW OF INSTRUMENTED VASCOMAX SHORT BARREL (EXIT END)	13
8	SHORT BARREL THERMAL AND EROSION INSTRUMENTATION	14
9	VASCOMAX 300 RING (R IX) PLATED WITH LC CHROME AND GROUND TO SIZE (FINAL PLATING THICKNESS = 6.5 MILS)	16
10	SAME SPECIMEN AS ABOVE (R IX) SHOWING AN EROSION INDEX MARK BEFORE FIRING (INDIUM REPLICA, SEM)	16
11	MODIFIED EROSION RING INSERT.	17
12	COMPOSITE REPLICA OF SURFACE GROOVES BEFORE TEST	18
13	VASCOMAX SHORT BARREL WITH REPLACEABLE 4340 LINER	29
14	75MM ABLATIVE AMMUNITION COMPONENTS	33
15	METHOD OF ASSEMBLY OF ABLATIVE ROUND COMPONENTS	34
16	ABLATIVE AMMUNITION ASSEMBLY IN PARTIAL CROSS-SECTION	36
17	REPRESENTATIVE PRESSURE DATA FOR M26 AND M26/M30 CHARGES	43
18	VIEW OF SURFACE OF 4340 ENTRANCE RING AFTER THREE SHOTS	56
19	VIEW OF VASCOMAX ENTRANCE RING AFTER 5 STANDARD PLUS 3 ABLATIVE SHOTS	57

DEFENSE LOGISTICS AGENCY
DEFENSE DOCUMENTATION CENTER
CAMERON STATION
ALEXANDRIA, VIRGINIA 22314

IN REPLY REFER TO DTIC-DDAL 83-1052(a)
(AC 202-274-6847 or AUTOVON 284-6847)

10 May 83

SUBJECT: Request for Scientific and Technical Reports

TO:

Commander
US Army Armament Res & Dev Command
ATTN: DRDAR-TSS
Dover, NJ 07801

1. We have been unable to locate the report referenced below in the DDC collection, although we believe it to be DoD-funded and available to us under DoD Instruction 5100.38. We ask that you send us copies in compliance with that instruction.

2. In the event that the instruction specifies more than two copies for this report, and it would create a hardship to send the required number, we ask that you send only two copies. If two copies are unavailable, DDC will accept one copy or a loan copy which will be returned in 30 days. All copies must be suitable for photographic reproduction.

3. UNCLASSIFIED REPORTS MUST BE MARKED WITH A DISTRIBUTION STATEMENT, see DoD Directive 5200.20 (AR 70-31, NAVMATINST 5200.29 or AFR 80-45). Check reverse side of this letter for proper distribution statement.

4. A franked mailing label for shipping the reports and a DDC Form 50 to obtain the AD number after processing are enclosed.

5. If for any reason you cannot furnish the report, please return the copy of this letter annotating your reason on the reverse side.

FOR THE ADMINISTRATOR:

HARRY A. SCHLESINGER, Jr.
Chief, Acquisition Section

2 Encl
1. Franked Label
2. DDC Form 50

AD A131 118

83-1052(a)

Calspan Corp - Buffalo, NY

Heat Transfer and Erosion in the Area 75 mm
High- Velocity Cannon, Vol. II

Rpt. #VL-5073-P-1 - Oct 77

DAAA09-76-C-2082

Return this copy to DDC with reports or as reply.

fml 00304
83-130

FL-88
SEP 77

DISTRIBUTION STATEMENTS
(DoD Directive 5200.20)

Please check appropriate block:

☑ 1. ____ Copies are being forwarded.
If the report is unclassified, indicate whether Statement A or B applies.

Statement A.

☑ Approved for public release; distribution unlimited.

Statement B.

☐ Distribution limited to U.S. Government agencies only; (fill in reason); (date statement applied). Other requests for this document must be referred to (insert controlling DoD office).

☐ 2. This document was previously forwarded to DDC on _____ (date) and the AD number is _____.

☐ 3. In accordance with the provisions of Department of Defense instructions, the document requested is not supplied because:

☐ It is TOP SECRET.

☐ It is excepted in accordance with DoD instructions pertaining to communications and electronic intelligence.

☐ It is a registered publication.

☐ It is a contract or grant proposal, or an order.

☐ Will be published at a later date. (Enter approximate date, if known.)

☐ Other (Give reason).

Dr. Arthur J. Bracuti
Print or Type Name

Arthur J Bracuti
Authorized Signature

X 3788
Telephone Number

LIST OF FIGURES (CONT.)

Figure	Title	Page
20	VIEW OF SURFACES OF PLASMA SPRAYED TANTALUM ENTRANCE RING AFTER ONE SHOT (SHOWS "BLISTERING" OF TANTALUM COATING)	58
21	VIEW OF SURFACE OF PLASMA SPRAYED NiAl ENTRANCE RING AFTER 2 SHOTS	59
22	VIEW OF 1010 STEEL LINED ENTRANCE RING R VII AFTER 5 SHOTS (CLEANED WITH HOPPES NO. 9 SOLVENT)	61
23	VIEWS OF SOFT (LC) CHROME ENTRANCE RING	62
24	SURFACE CONDITION OF TEST RINGS AFTER FIRING	64
25	COMPARISON OF SURFACE CRACKING	66
26	SURFACE CONDITION OF VASCOMAX 300 ENTRANCE RINGS BEFORE AND AFTER FIRING	68
27	FRACTURE TOUGHNESS VS. YIELD STRENGTH IN THE 18 PERCENT NICKEL MARAGING STEELS (AFTER HALL[4])	71
28	FRACTURE TOUGHNESS VS. STRENGTH FOR "GUN STEELS" AND VACUUM MELTED MARAGING STEELS (AFTER ZACKAY, ET. AL.[6])	73
29	4340 STEEL EXIT RING (F II) SHOWING EXTENSIVE FATIGUE CRACKING AFTER 19 SHOTS (SEM)	75
30	SAME SPECIMEN AS ABOVE AT HIGHER MAGNIFICATION (SEM)	75
31	4340 EXIT RING NO. 11 LATERAL SECTION SHOWING TYPICAL CRACK APPEARANCE IN THE SEM	76
32	SAME CRACK AS ABOVE AT 1000X. PROPELLANT GASES HAVE ERODED CRACK WIDTH TO 10-15μ = 0.5 MIL	76
33	4340 STEEL EXIT RING NO. 11, LATERAL SECTION SHOWING FATIGUE CRACK AFTER 19 SHOTS (ALSO SHOWS HARD MARTENSITE LAYER ABOUT 75μ DEEP)(LIGHT MICROSCOPE, 40X, NO ETCH)	78
34	SAME SPECIMEN AS ABOVE SHOWING REDUCED LENGTH OF MICRO HARDNESS INDENTATIONS NEAR SURFACE (SEM)	78

LIST OF FIGURES (CONT.)

Figure	Title	Page
35	4340 STEEL ENTRANCE RING V, LATERAL SECTION SHOWING WHITE -- ETCHING LAYER AT BORE SURFACE (LIGHT MICROSCOPE, 130X, NITAL ETCH)	79
36	4340 STEEL EXIT RING CROSS-SECTION AFTER 19 SINGLE SHOTS (80X)	81
37	VASCOMAX 300 EXIT RING CROSS-SECTION AFTER 19 "BURST" SHOTS (80X)	81
38	VASCOMAX 300 EXIT RING CROSS-SECTION AFTER 15 "BURST" SHOTS WITH ABLATIVE AMMUNITION (80X)	84
39	VASCOMAX 300 ENTRANCE RING CROSS-SECTION AFTER 15 "BURST" SHOTS WITH ABLATIVE AMMUNITION (80X)	84
40	VASCOMAX ENTRANCE RING CROSS-SECTION SHOWING SURFACE SOFTENING AFTER 15 SHOTS SEM	85
41	LOW CARBON (1010) STEEL ENTRANCE RING NO. VII SECTION SHOWING NO CRACKING AFTER FIVE SHOTS (130X LIGHT MICROSCOPE, NITAL ETCH)	87
42	SAME SPECIMEN AS ABOVE SHOWING LITTLE INCREASE IN MICROHARDNESS NEAR SURFACE (500X SEM)	87
43	SPECIAL VASCOMAX 300 SHORT BARREL AND ASSOCIATED TANTALUM-2 1/2% TUNGSTEN LINER	91
44	VIEW OF INSTRUMENTED SHORT BARREL AS INSTALLED IN ARES RAPID-FIRE FIXTURE	95
45	TEMPERATURE HISTORY DURING BURST FIRE AT ENTRANCE END OF SHORT BARREL (5 ROUNDS - NON-ABLATIVE)	96
46	TEMPERATURE HISTORY DURING BURST FIRE AT EXIT END OF SHORT BARREL (5 ROUNDS - NON-ABLATIVE)	97
47	PREDICTED AVERAGE BARREL TEMPERATURES DURING RAPID FIRE AT 120 RPM - 145 INCHES FROM BREECH END OF SHORT BARREL	101

LIST OF FIGURES (CONT.)

Figure	Title	Page
A1	THERMAL SIZE CHANGES IN VASCOMAX 300 AND LOW CARBON STEEL	111
A2	ARES 75MM BARREL COOL-DOWN, NATURAL CONVECTION, RADIATION LOSS INCLUDED	117
A3	ARES 75MM BARREL COOL-DOWN, 60 FT/SEC WIND VELOCITY, RADIATION LOSS INCLUDED	119

LIST OF TABLES

Table	Title	Page
I	NOMINAL STEEL COMPOSITIONS	20
II	TEST RING SUMMARY	25
III	BALLISTIC RESULTS	38
IV	SUMMARY OF BALLISTIC RESULTS (AVERAGES)	42
V	RESIDUAL CHAMBER PRESSURES	45
VI	BARREL HEAT INPUT	46
VII	BARREL HEAT INPUT SUMMARY (AVERAGES)	49
VIII	EROSION PERFORMANCE AT ENTRANCE TO SHORT BARREL	52
IX	EROSION PERFORMANCE AT EXIT OF SHORT BARREL	54
X	BARREL HEAT INPUT DURING RAPID-FIRE TESTS	99
XI	RAPID-FIRE EROSION RESULTS	102
A1	IRREVERSIBLE THERMAL SIZE CHANGES IN VASCOMAX 300	112

I. INTRODUCTION AND SUMMARY

Single-shot firings of the 75mm high velocity cannon conducted at Ares during initial weapon development, indicated potentially severe erosion of the breech end of the barrel (short barrel). Extended burst sequences were expected to aggravate the erosion thus threatening to shorten, intolerably, the practical barrel life. In an effort to improve longevity, Calspan conducted a study[1] of the actual heating and erosion in the short barrel through experimental single-shot firing investigations using a fixture similar to that of the Ares Phase I cannon. Primary efforts in that study were directed to an assessment of the expected heating and erosion in the present 75mm cannon during rapid fire and the evaluation of potential solutions to indicated problems by use of barrel materials changes, and/or ammunition modifications. It was found that erosion in the short barrel could be lowered substantially by use of:

1. Addition of about 110 gms. of thickened silicone ablator at the base of the projectile in the round,
2. Refractory metal liners fabricated of tantalum-10%, tungsten or columbium-1% zirconium,
3. Surface platings of chromium in thicknesses up to 0.010 inches.

In the present work, the ablative concept has been further developed and optimized. Practical problems associated with utilization of liners in the short barrel to improve erosion performance were also addressed. Possible use of surface platings and/or coatings in the short barrel was briefly explored through additional firing tests.

In addition, basic thermal information associated with each charge type fired was obtained as a secondary measure of performance as well as to be used as a guide to improved barrel thermal design.

A. THERMAL EFFECTS

Through both single-shot and burst firing of non-ablative and ablative ammunition, tube temperature data were obtained and analyzed with regard to the indicated bore heat input. It was found that bore heating conditions for all charges tested were generally less severe than those found in the earlier work above. This result was due in part to change in propellant charge and in part to better application of the ablative concept.

Analysis of measured heat input with respect to barrel temperature increase and thermal gradients indicates no expected stress-deformation failures of the barrel as presently configured in any practical burst length.

B. EROSION

Erosion testing of several materials and ammunition changes was performed through the use of a special instrumented short barrel in which test ring inserts could be installed. Firing results indicate impressive reductions in short barrel erosion with use of 100 gms. of thickened silicone ablator. Rapid-fire test results of the current round which includes the ablative composition show negligible erosion throughout the short barrel.

A low contraction "soft" chrome plated Vascomax 300 test ring was found to exhibit negligible erosion in twenty shots. Post test bond integrity of the plating was found to be excellent. The crack pattern developed due to firing differs greatly from that in conventional hard chrome such that very long erosion life should be favored; there is also good prospect of further improvements in this direction.

C. FATIGUE

Fatigue was considered primarily from the standpoint of observed surface crack initiation in test rings and possible implications of this surface cracking in a fracture mechanics context. While surface cracks up to four mils deep in Vascomax rings and up to about 30 mils deep in 4340 rings

appear after 19 shots, firing experience at Ares clearly shows that crack growth does not continue at rates even approaching those that might be inferred from these findings. A Vascomax 300 short barrel at Ares has fired over 500 rounds with minimal crack growth and a 4340 main barrel has similarly fired over 700 rounds. Further study is required to relate the crack initiation information obtained to the actual crack growth rates prevailing in continued firing. Vascomax 300 appears to be superior to conventional steels in terms of both general resistance to crack growth (fracture toughness) and resistance to bore surface crack initiation, when both types are compared at high yield strength levels.

II. EXPERIMENTAL FIXTURES AND INSTRUMENTATION

The primary thrust of the work was experimental with sufficient analysis to allow meaningful data interpretation. Hence, considerable effort in the work involved modification and/or design and fabrication of a number of test fixtures, specimens, erosion sensors, thermal instrumentation, and ammunition.

A. SINGLE-SHOT TEST FIXTURE

Field tests conducted at Calspan's Ashford Test Site were performed using a single-shot test fixture representative of the Ares rapid-fire cannon. This fixture (Figure 1) was used in the earlier Calspan work as reported in Reference 1. Chief modification of this fixture for the present work was change of firing pin construction to accommodate the change from the M59 low voltage to the M52 high voltage primer, and provision for high voltage circuitry.

B. INSTRUMENTED SHORT BARREL

The basic experimental component used in the field test evaluations was a Calspan fabricated special short barrel. The earlier 4340 short barrel which had been utilized in the preliminary studies of Reference 1 was deemed inappropriate for use in this optimization study which was to include burst fire testing. Also, it was considered most desirable to perform tests on larger surfaces than those provided by the smaller more locally sensitive erosion sensors of the preliminary work. For this reason, an instrumented short barrel fabricated of Vascomax 300 maraging steel was designed and constructed in this program. Details of construction are shown in Figure 2. As shown, the basic cylindrical short barrel was made in accordance with chief dimensions of Ares P/N 3010. In an effort to reduce both materials and labor costs, however, a two-part short barrel construction was adopted. In this construction, the basic cylindrical short barrel element of Figure 2 is used in combination with the retaining collar of Figure 3 to form a short barrel typical of that used at Ares. With this construction technique, 5 1/4 inch diameter maraging steel stock could be used in place of 7 1/2 inch diameter stock. Additional advantage is gained because the retaining collar is common

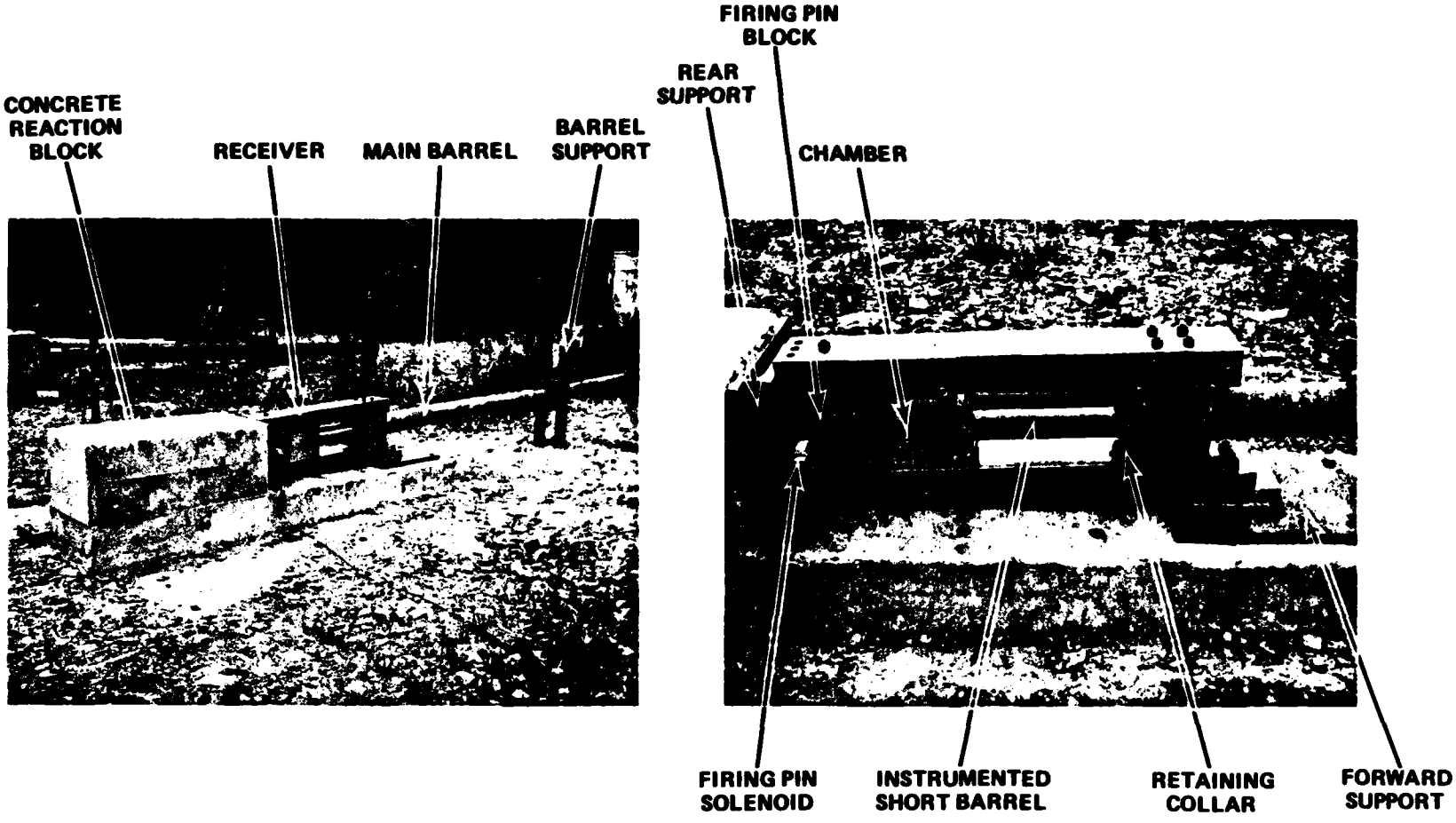

Figure 1 SINGLE-SHOT 75 mm TEST FIXTURE

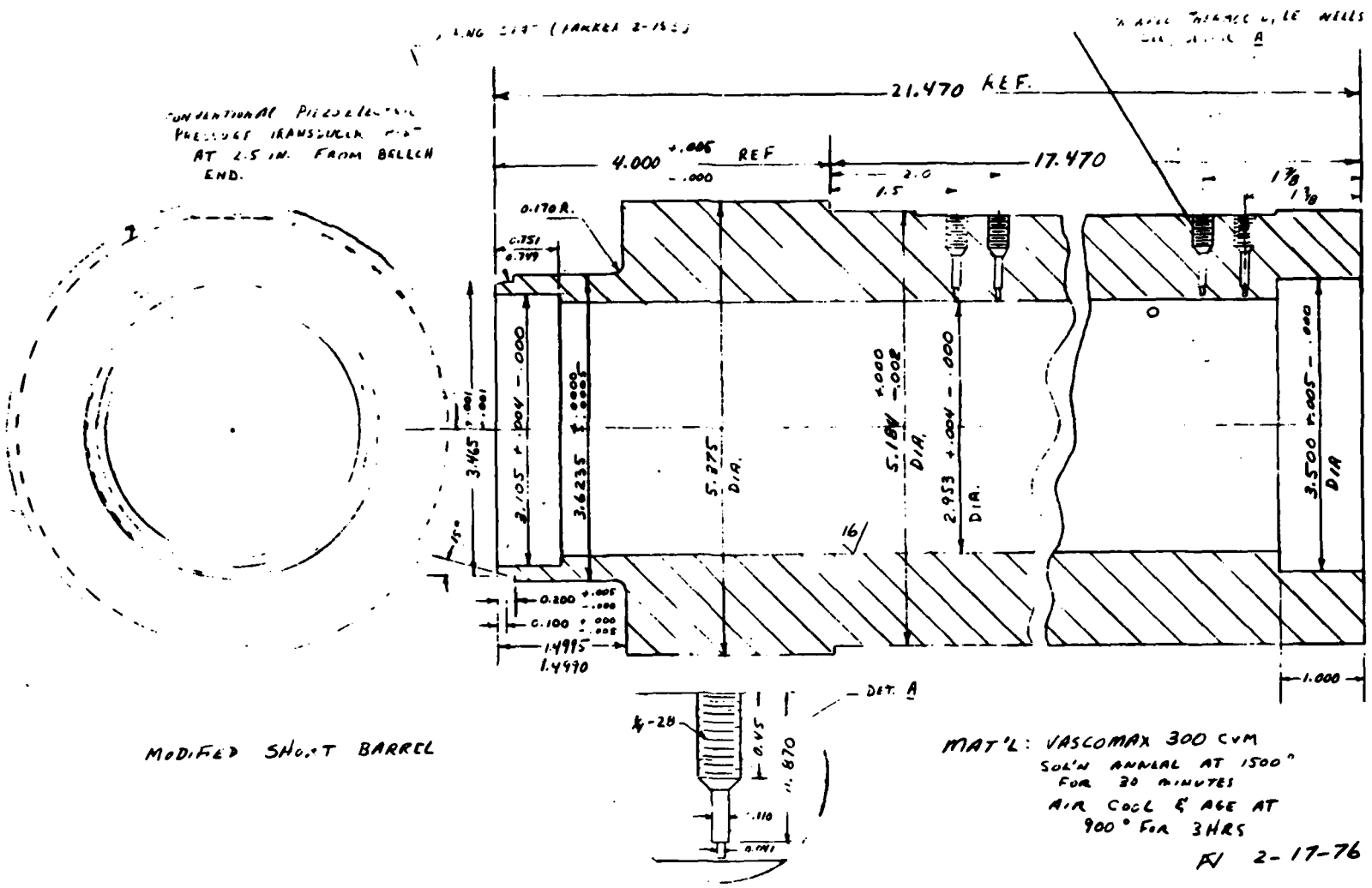

Figure 2 INSTRUMENTED SHORT BARREL

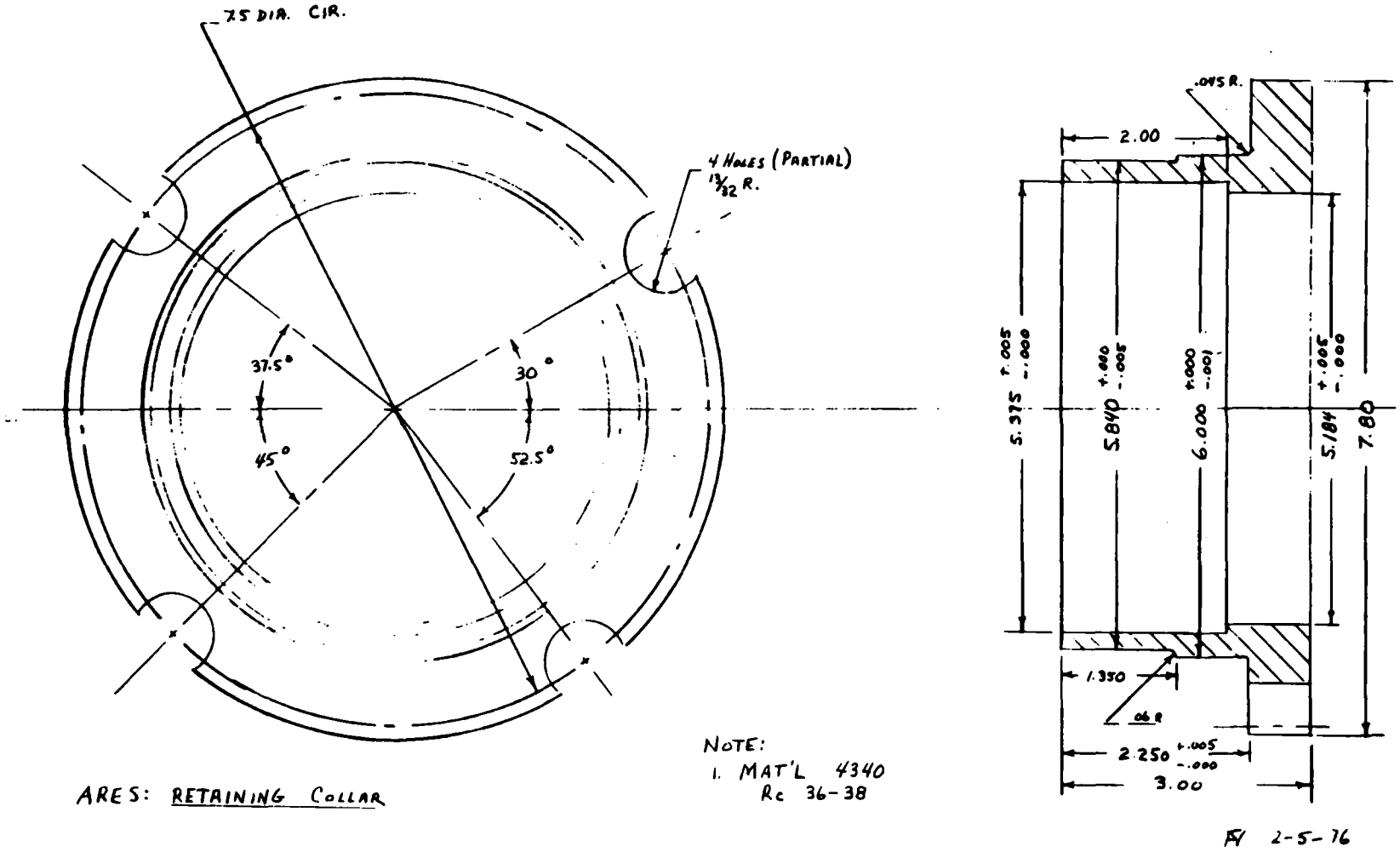

Figure 3 SHORT BARREL RETAINING COLLAR

to all short barrels utilized in the work. A further advantage of this construction is the lowering of effective weight of material to be handled inasmuch as the two parts can be separately transported.*

The short barrel was fitted with both in-wall thermocouple wells for heat transfer measurements, and a piezoelectric pressure transducer port for pressure measurement. Design and installation of the thermocouple wells was made with the thought that they be applicable for use in rapid fire. A shallow flat (about 0.070 inch) deep is provided axially, along the surface of the short barrel. Each thermocouple well is installed at the center of this flat. Thermocouple wires can thus be routed axially along the flat allowing free motion of the chamber sleeve over the short barrel as required in rapid fire.

In-wall thermocouples were fabricated as illustrated in Figure 4 using 0.040 inch diameter stainless steel sheath chromel-alumel thermocouples. These were constructed according to conventional design previously used by Calspan utilizing an 8-32 screw and spring. At the thermocouple tip, the bared 40 gauge chromel and alumel wires are forced under the action of the spring to contact the bottom of the thermocouple well placed in the short barrel thus forming a thermocouple circuit having negligible response lag; hence, thermoelectric output of the thermocouple is identically related to the temperature at the contact point. Interpretation of the output of this thermocouple after firing can result in a measure of total heat input to the bore per shot, as described in Reference 1. Furthermore, use of the thermocouples in rapid fire can allow a demonstration of the adequacy of computer solutions such as those of Reference 2 for predicting thermal gradients in the short barrel during burst fire.

As shown, in-wall thermocouple pairs may be used at each end of the short barrel. Initial depths from the bore surface are 0.025 and 0.042 inches

*Recognizing the benefits of this two-piece construction, Ares has adopted this design in its rapid-fire cannon.

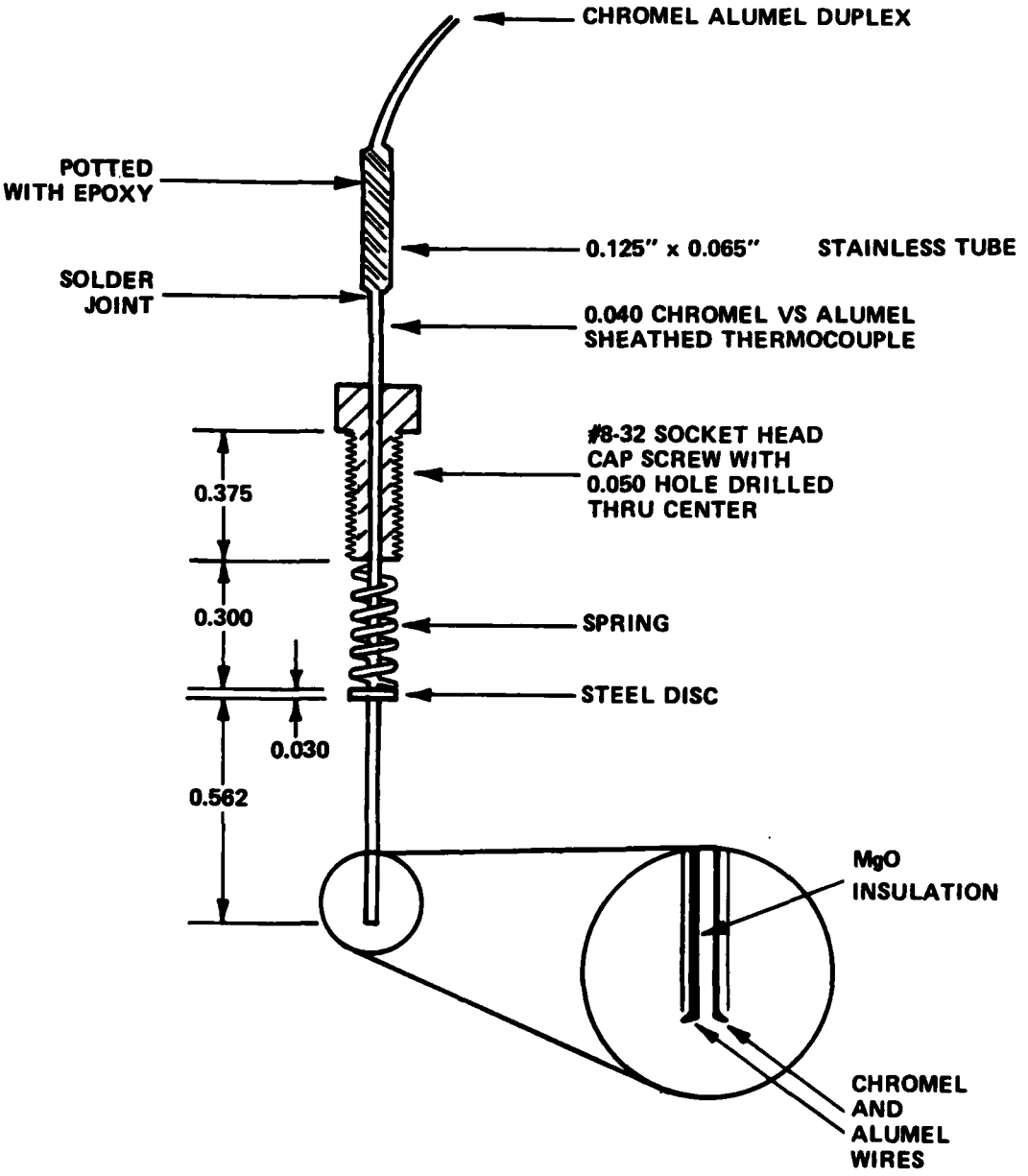

Figure 4 IN-WALL THERMOCOUPLE DESIGN

for each pair. Although sufficient information can be obtained from a single thermocouple regarding the amount of total heat input, the second thermocouple position provides a backup in the event that sufficient erosion takes place to produce burnthrough to the 0.025 in. depth. A single pressure port is installed near the entrance of the short barrel as shown to permit the use of a piezoelectric pressure transducer for evaluation of important pressure history in the short barrel.

Each end of the short barrel is provided with a cutout to permit insertion of an erosion sensing ring for evaluation of ammunition and/or materials erosion performance.

Typical erosion ring inserts and their method of installation are shown in Figures 5, 6, and 7. Each ring prior to test is characterized by use of indium surface replicas and the Scanning Electron Microscope and by weight and diameter measurements. Because each ring has a significant area exposed to the erosive environment, the ability to judge the erosion performance of any selected modification in a very few shots is greatly enhanced over that of the small erosion sensors of earlier work (Ref. 1). Entrance rings are readily changed at the test site. The method is illustrated in Figure 6. Change of the exit ring as shown in Figure 7 is somewhat more difficult inasmuch as it involves removal of the short barrel, but has been found to require only a few minutes of on-site effort.

Figure 8 illustrates the short barrel thermal and erosion instrumentation as installed for the rapid-fire tests conducted at Ares. The thermocouple probes are shown as well as the clamping procedure which was used in the routing of the thermocouple lead wires. The erosion ring inserts under test are held in place using a flat head screw retainer as shown.

C. EROSION SENSING RINGS

Measurement of erosion in the short barrel was obtained by use of ring inserts placed at each end of the short barrel. These rings replaced the smaller erosion sensors of earlier work. Each ring specimen was provided,

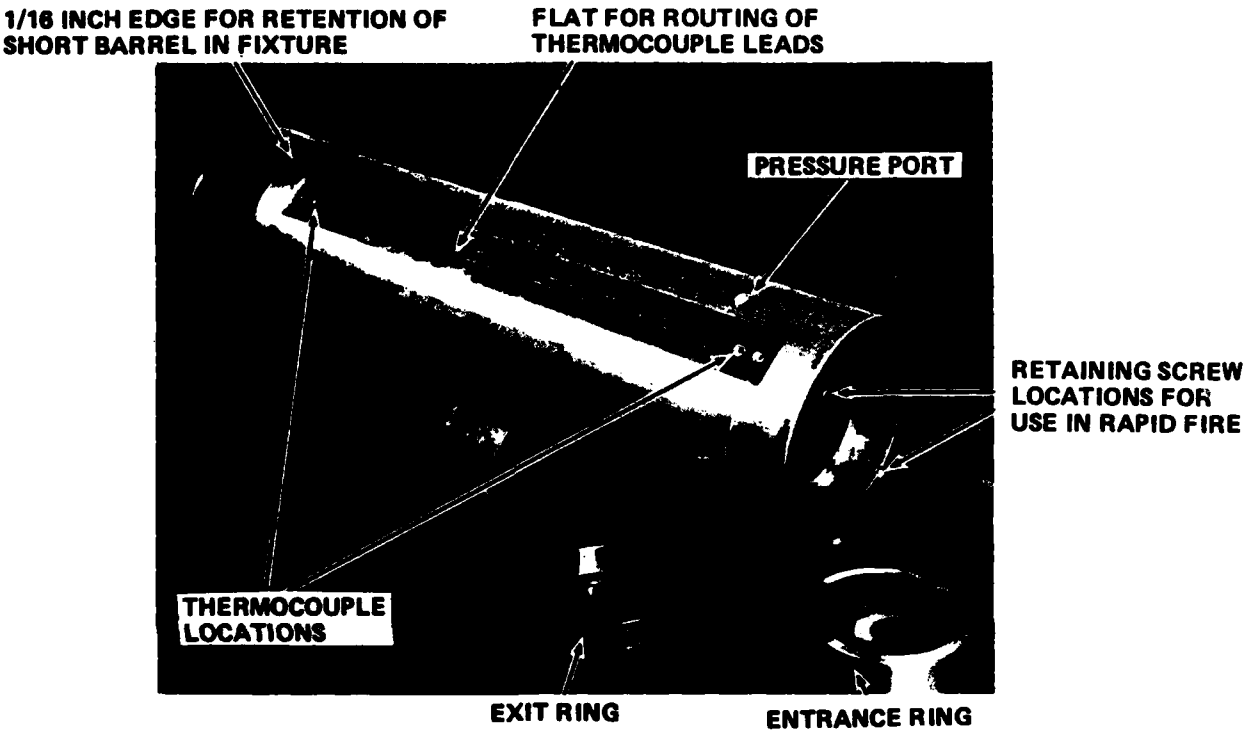

Figure 5 INSTRUMENTED VASCOMAX 300 SHORT BARREL SHOWING TYPICAL EROSION RINGS

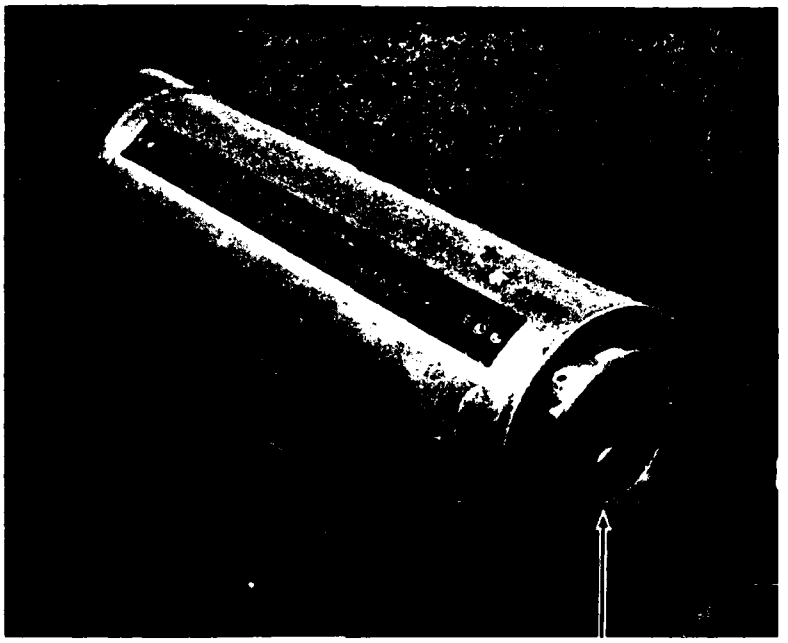

EROSION RING
PARTIALLY INSERTED

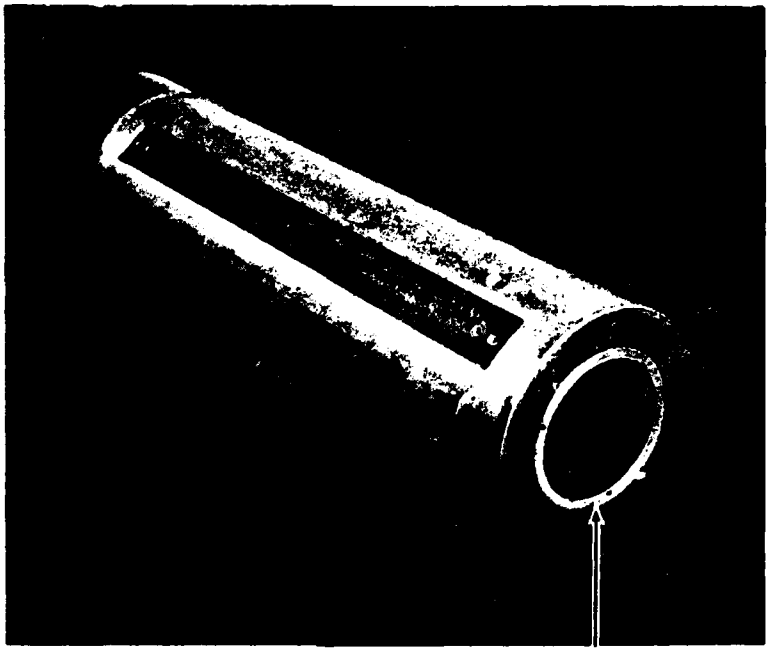

EROSION RING
FULLY INSERTED

Figure 6 VIEW OF INSTRUMENTED VASCOMAX SHORT BARREL (ENTRANCE END)

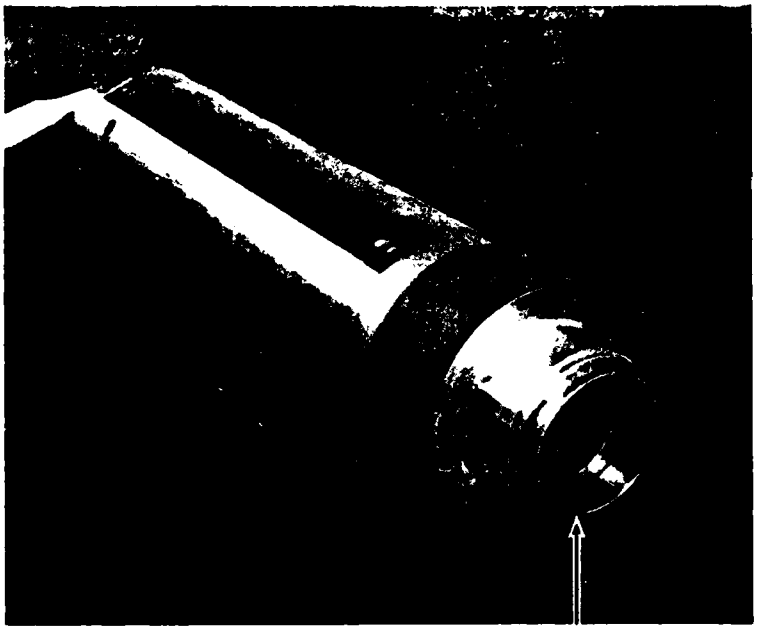

EROSION RING
PARTIALLY INSERTED

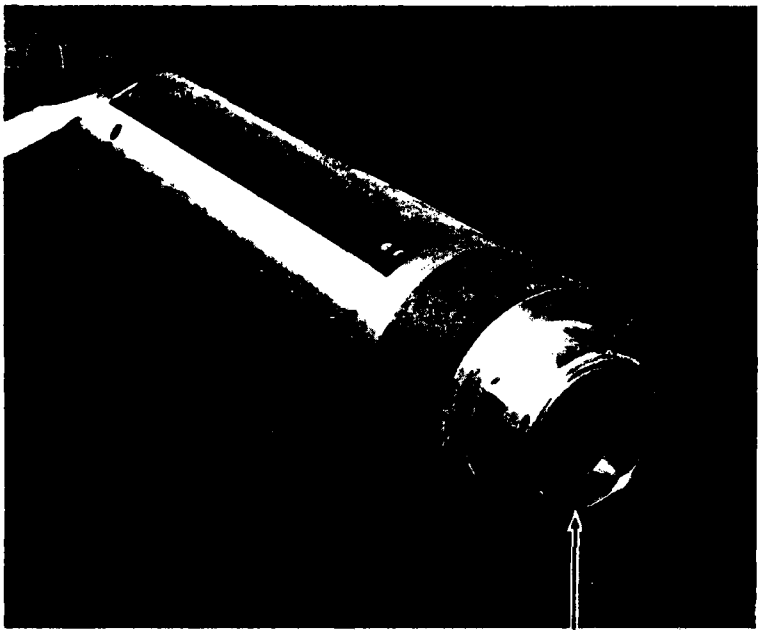

EROSION RING
FULLY INSERTED

Figure 7 VIEW OF INSTRUMENTED VASCOMAX SHORT BARREL (EXIT END)

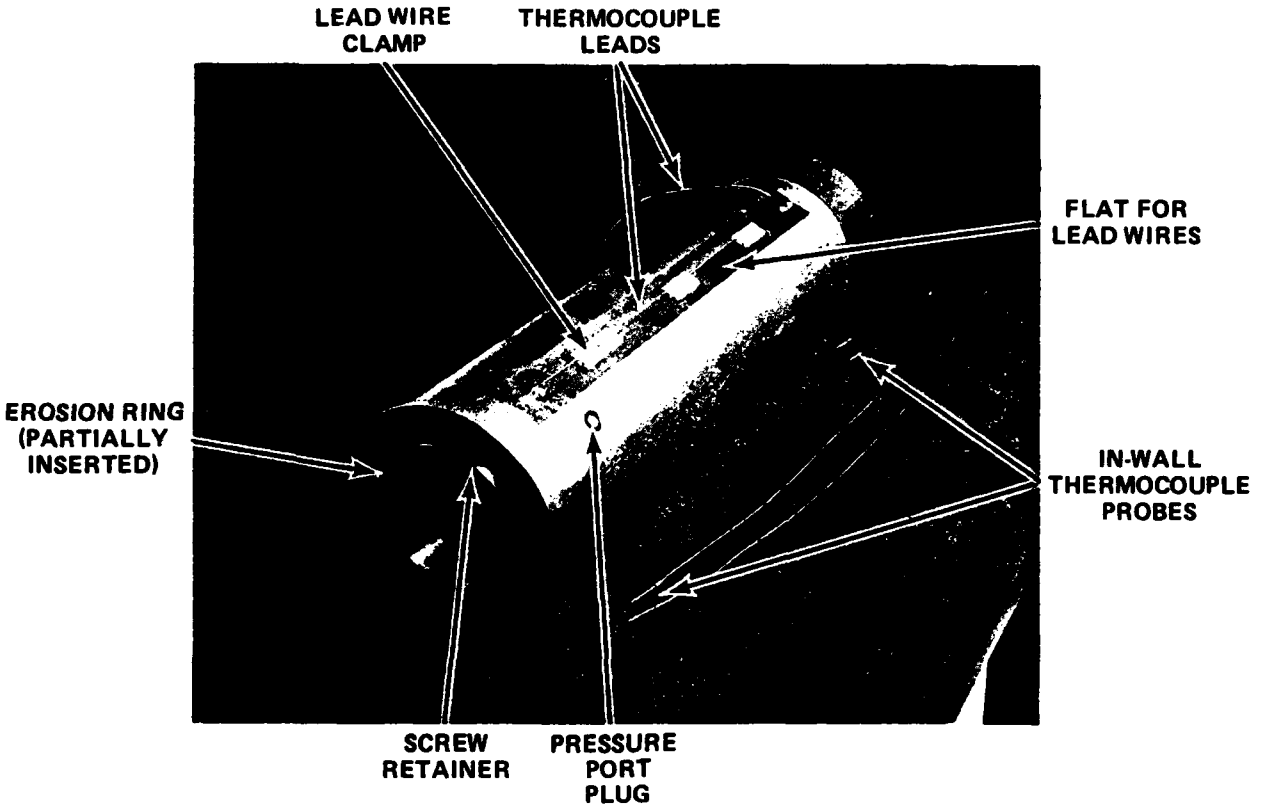

Figure 8 SHORT BARREL THERMAL AND EROSION INSTRUMENTATION

at selected circumferential locations, with surface impressions, the size of which would change in proportion to the amount of material removed during firing. Initial testing was conducted with rings having very small microhardness Knoop impressions placed in its surface in similar fashion to those used in the earlier work (Ref. 1). It was soon found that impression depths attainable from the hardness tester were insufficient to accommodate the gross erosion experienced. Hence, further testing was conducted using a surface scribe mark implaced by a carbide tool having a 90° included angle such that the depth of the scribe mark was equal to one-half its width. With this system, scribe mark depths up to .002 inches could readily be produced. Figure 9 illustrates a typical scribe mark on the bore surface of a chrome plated ring. Detailed characterization of the surface scribe marks was obtained by use of a replication technique by which indium metal was forced into intimate contact with the ring surface at the scribe location, thus forming a mirror image of the impression. This image could then be photographed at high magnification in the Scanning Electron Microscope (SEM), resulting in an excellent characterization of the surface scribe mark as illustrated in Figure 10. Indium replicas were taken for each sample prior to and after test. These were subsequently photographed in the SEM.

A third erosion indicating technique was also applied in testing toward the conclusion of the study. As illustrated in Figure 11, a number of circumferential erosion indicating grooves were cut into the bore surface of the ring. These were cut with a 90° included angle carbide tool so that, again, the groove depth is one-half its width. Control of tool pressure allows variation in groove depth which can be then measured optically using indium surface replicas and the SEM. Figure 12 illustrates typical appearance of surface grooves at 25:1 magnification. As shown, groove depths of a few tenths of a thousandth are readily characterized. The axial grooves function as referencing marks to specify location. Loss of material through erosion results in "thinning" of the grooves which is readily measured optically.

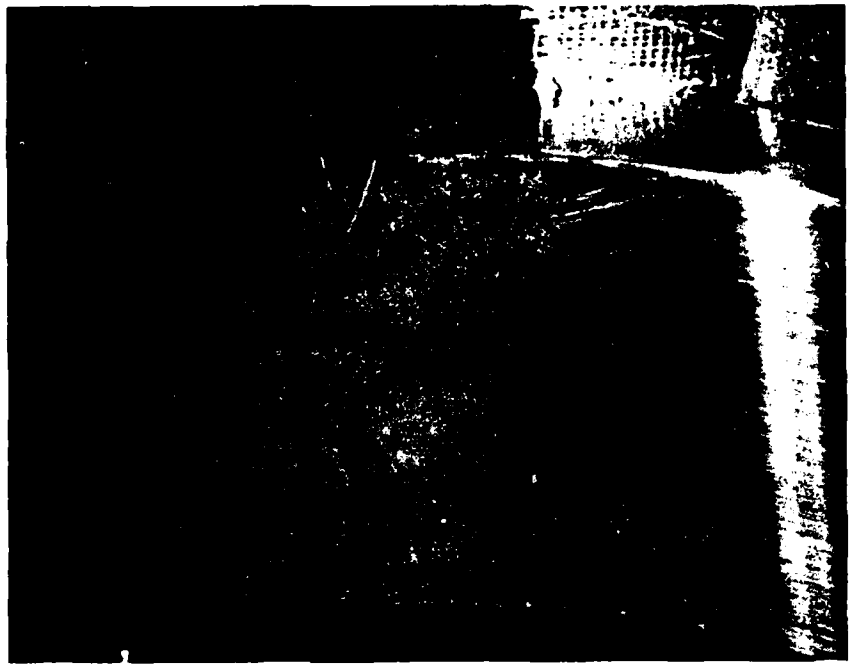

Figure 9 VASCOMAX 300 RING (R IX) PLATED WITH LC CHROME AND GROUND TO SIZE (FINAL PLATING THICKNESS = 6.5 MILS)

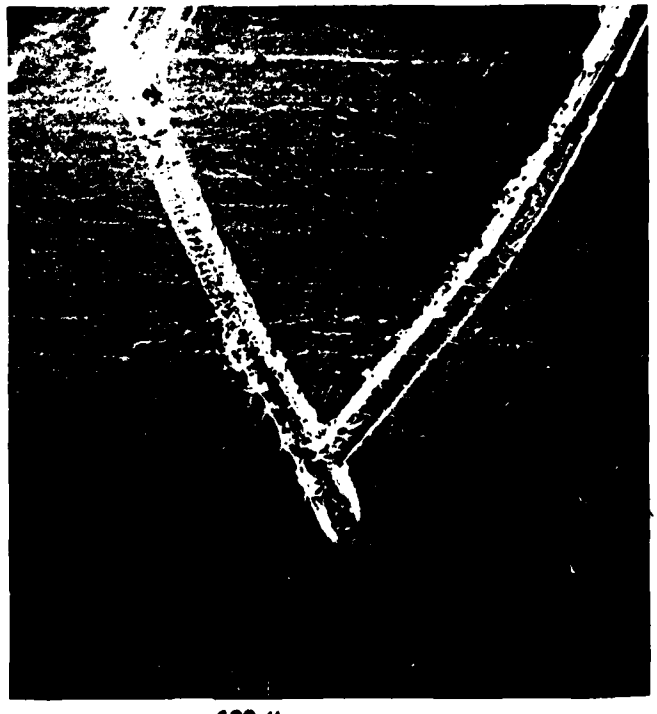

100 μ

Figure 10 SAME SPECIMEN AS ABOVE (R IX) SHOWING AN EROSION INDEX MARK BEFORE FIRING (INDIUM REPLICA, SEM)

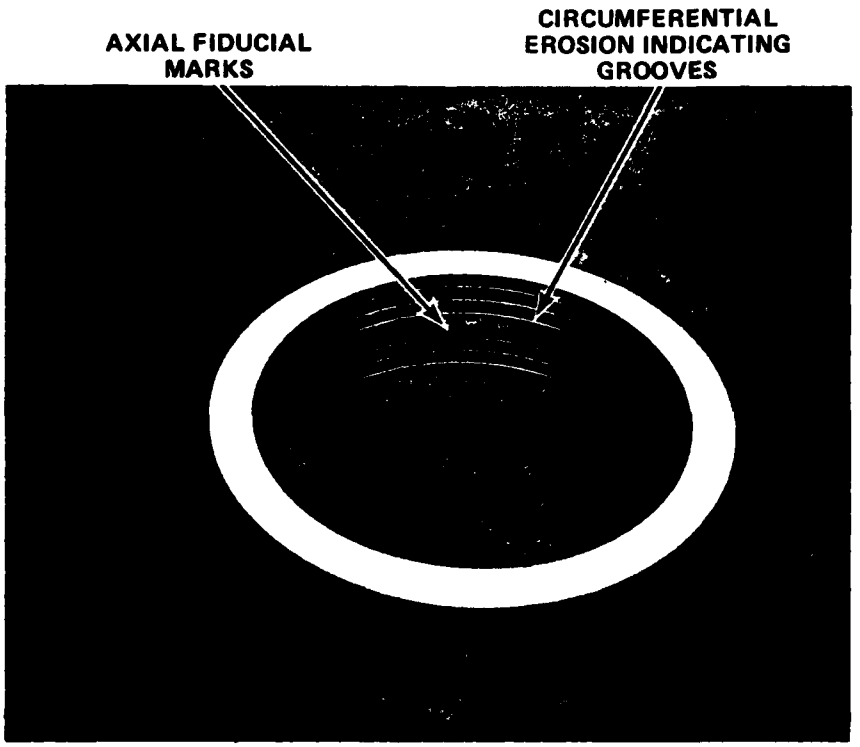

Figure 11 MODIFIED EROSION RING INSERT

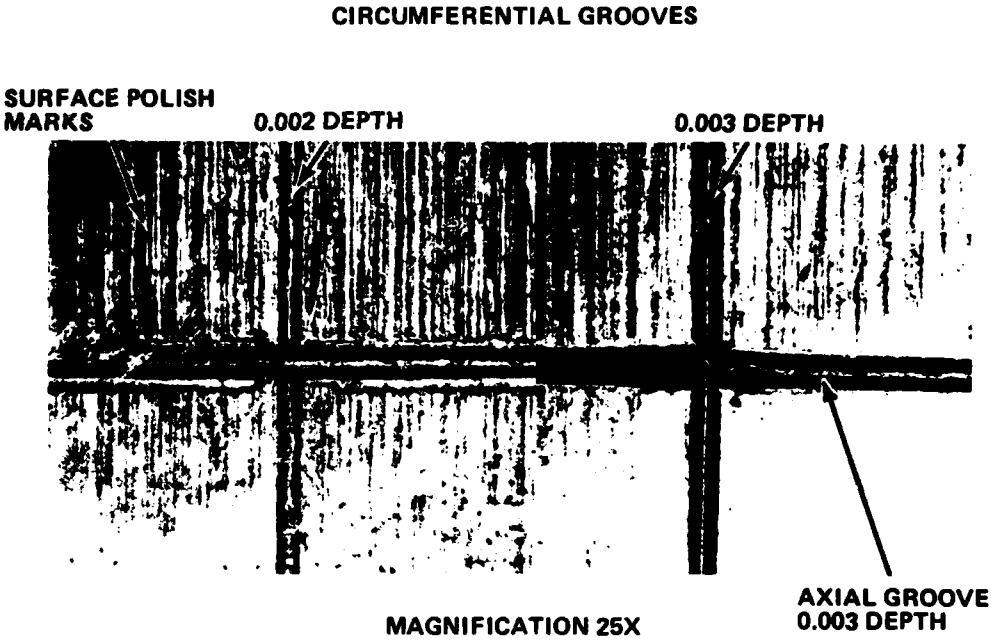

Figure 12 COMPOSITE REPLICA OF SURFACE GROOVES BEFORE TEST

Final characterization of the test rings was, of course, obtained by recording the ring weight. Because the ring has a relatively large area exposed to the erosive environment, very meaningful weight loss measurements can be made in only a few shots, thus enhancing ability to judge the erosion performance of any selected modification.

D. EROSION RING PREPARATION AND DISCUSSION

Candidate erosion ring inserts were selected from among those materials and/or coatings having practical utility for use in the short barrel. Generally, candidates were chosen on the basis of one or more characteristics promising to improve erosion performance of the cannon. Rings were fabricated to allow exploration of ammunition modifications, barrel materials changes, and surface coatings/platings regarding their effect on erosion.

1. Vascomax 300 Maraging Steel

Of primary interest for use in the short barrel are the tough ultra high strength precipitation hardened steels inasmuch as short barrel outer diameter must be kept to a minimum for proper functioning of the weapon. These high strength alloys are adequately represented by the Vascomax 300 maraging steel which is currently used in the Ares rapid-fire system. Therefore, a number of Vascomax 300 rings were fabricated to be used for the purpose of establishing baseline erosion conditions in the present short barrel and for evaluation of the effectiveness of ammunition modifications, such as the ablative ammunition approach. All Vascomax rings were fabricated and heat treated according to recommended practice (i.e., 3 hours at 900°F yielding R_C 51).

2. Low Alloy Steels

The preliminary work of Reference 1 indicated some modest benefit of a change to low-alloy, medium-carbon steel for the short barrel. Nominal compositions for large gun tube steels (modified 4330), small arms steels (chrome-moly-vanadium) and 4340 steel are tabulated below along with that for maraging steel to be used for later reference.

TABLE I

NOMINAL STEEL COMPOSITIONS

Element	Vascomax 300 Maraging Steel	Modified 4330 Gun Tube Steel	Chrome-moly-vanadium Small Arms Steel	4340 Steel
Carbon	<0.03	0.30%	0.40	0.40%
Nickel	18.50	2.40	0.0	1.80
Chromium	0.0	1.0	1.10	0.80
Molybdenum	4.80	0.50	0.65	0.25
Vanadium	0.0	0.10	0.25	0.0
Manganese	<0.10	0.55	0.90	0.70
Phosphorus	<0.01	<0.40	<0.40	<0.42
Sulfur	<0.01	<0.40	<0.40	<0.40
Silicon	<0.10	0.25	0.30	0.25
Cobalt	9.00	0.0	0.0	0.0

In the Ares cannon, 4340 steel is, of course, employed in the main barrel, and has been tested as a short barrel candidate. There are certain thermochemical reasons (to be discussed in the next section headed "Low Carbon Steel Test Rings") why the lower alloy content of 4340 might cause it to resist erosion somewhat better than the two gun steels tabulated, and much better than Vascomax 300. Low-alloy, medium-carbon steels such as 4340 continue, therefore, to be of importance in the present work. It was noted in Reference 1 that 4340 erosion sensors eroded more slowly than did Vascomax 300. There is, however, greater likelihood of fatigue failure with use of 4340 because of the severe surface stress levels which prevail in the short barrel, and hence, further evaluation of this material was deemed necessary. Test rings fabricated of this material were machined and heat treated to R_C 42-44; this hardness being necessary to achieve sufficient strength in this material for use as a monolithic short barrel.

3. Low Carbon Steel

In the erosion test results of the present program and in the literature dating back to World War II, there is much to suggest that in "high heat

flux" guns, the predominant erosion mechanism is a thermochemical reaction between the gun gases and steel bore surfaces. This reaction (whatever its exact nature may be) results in surface melting at temperatures well below the melting point of the metal or alloy in question. In brief, there is evidence that one or more of the following occur:

1. The carbon content of the surface is increased due to carburization such that the melting (mushy state) temperature is driven down from ~2700°F to ~2100°F.

2. Nickel reacts with some constituent of the gases (possibly sulfur) to accelerate erosion (note that Vascomax 300 contains 18 percent nickel).

3. Alloying elements decrease the melting point of iron and decrease the thermal conductivity such that bore surface melting is favored.

Considerations such as the above lead to the conclusion that pure iron or low-carbon steel should be superior in erosion resistance to alloy steels. Since low-carbon steel can be very readily fabricated into a liner for the strong maraging steel short barrel, and since there are no spin-up stresses (no rifling) to contend with, low-carbon steel could in fact be a practical liner material in the Ares cannon. Thus, a test ring insert having a flux brazed 1010 low-carbon steel liner was fabricated for test purposes.

4. Chromium Plate

In both small and large caliber guns, chromium plate has been found to essentially eliminate erosion while the chromium remains on the surface. Earlier work (Reference 1) also has shown very superior erosion performance of chromium-plated erosion sensors placed in the Ares short barrel. There was, however, in that work some early evidence of substantial surface cracking which promised to shorten the useful life of the plating.

Chromium plating can be applied under various plating bath conditions such that the as-plated hardness ranges from K 1000* (R_c 72) down to K 540 (R_c 50). Concurrent with the hardness variation is a large variation in the irreversible thermal contraction behavior exhibited by the plating upon initial heating. Thus, the hard ($\sim R_c$ 68) plating normally applied to gun barrels is termed high contraction (HC) chrome because it undergoes a 1.0 percent linear shrinkage on initial heating to ~1800°F (~1000°C). This thermal shrinkage results in a multiplication and further opening of the microcracks which form in the chrome during plating.

In contrast, "soft" ($\sim R_c$ 50) chrome plate upon heating to 1800°F is found to shrink only about 0.1 percent and is termed low contraction (LC) chrome. The microcrack system in LC chrome is minimal as-plated and most importantly, Calspan postulates that the combination of "softness" (ductility) and low thermal contraction in the LC chrome will result in a much reduced rate of crack proliferation and growth in a plated gun bore. Since the loss of chrome plate in gun bores is largely due to the undermining of the substrate steel through cracks in the plate, it is further postulated that LC chrome will be more resistant to erosion in the Ares 75mm cannon than is HC chrome.

It should perhaps be noted that LC chrome has been tried in guns in the past, with mixed results. However, to Calspan's knowledge it has not been tried in a smooth-bore barrel, i.e., where there is no rifling, and where the extreme mechanical stresses associated with rifling functioning are absent.

Further credence is lent to the idea that LC chrome will resist crack proliferation when the exact cause of extreme hardness and brittleness in HC chrome is considered. Studies have shown that HC chrome has hydrated oxide films in the microcracks which form during plating. These films, which certainly promote brittleness, are much reduced in extent in LC chrome.

---

*"K" will be used to designate "Knoop diamond pyramid microhardness at 500 grams load" in this report, and R_c for Rockwell "C" scale hardness equivalent.

Typically, HC chrome has an oxygen content of the order of 400 ppm (parts per million) while in LC chrome the oxygen level is reduced to 50 ppm. In addition, there is evidence that nitrogen dispersed in the atomic lattice of electrolytic chrome has a strong hardening effect and that LC chrome contains less nitrogen. Therefore, LC (soft) chrome was selected for test as applied to a Vascomax 300 substrate.

In the interest of controlling plating conditions and metal pretreatment carefully such that maximum adhesion could be obtained, the LC chrome of the present study was applied in a laboratory plating line set up for that purpose at Calspan. The plating procedure was as follows:

1. Degrease Vascomax ring in hot alkaline cleaner.

2. Electropolish 1 hour at 150°F and 500 amp/ft^2 in a bath composed of 56% phosphoric acid, 12% CrO_3 (chromic acid) and 32% water. In this step the ring was made the anode and the cathode consisted of a pure lead cylinder about two inches in diameter positioned in the center of the ring.

3. The above electropolishing tends to leave a passive hydrated oxide film on the steel surface which must be removed before adherent plating can be applied. Removal of the film (activation) was accomplished in the chrome plating bath itself by treating the ring for 45 seconds at 190°F and 1000 amp/ft^2 "reverse current," i.e., with the ring as anode.

4. Plate 6.5 hours at 190°F and 1000 amp/ft^2 in a bath composed of 250 gram/liter CrO_3 (chromic acid) and 2.5 gram/liter H_2SO_4 (sulfuric acid).

By the above treatment, about two mils per side were removed from the steel ring I.D. in the electropolishing step and six mils per side of LC chrome was applied. Electropolishing has been shown in past studies to be essential for maximum plating adherence.

Plating hardness, determined from indium replicas of Knoop indentations, was K 590 (R_c 53). Hardness and cracking proclivity can be reduced still further by vacuum annealing, but was considered beyond the scope of the present study.

Vascomax test rings were also prepared for the application of conventional hard (HC) chromium plate. These rings were forwarded to Watervliet for plating. Watervliet found it necessary to nickel plate these test rings prior to application of their conventional chrome because adherence directly to the Vascomax substrate was found inadequate. The as-received plating on nickel although probably adequate for test purposes still appears to lack the needed adhesion for long life operation in this cannon. Unfortunately, the difficulties in plating these rings experienced at Watervliet delayed their availability to the extent that these rings were not able to be tested at Calspan in this phase. They will, however, be tested in future work.

5. Refractory Coatings

As an alternative to chromium plating, plasma-sprayed coatings were selected to investigate possible utility of thin refractory metal coatings as used for rocket nozzle protection under similar high-heating, high-shear conditions. Two plasma sprayed coatings of tantalum and NiAl were chosen as representative of the best candidate materials presently available. These coatings were applied to entrance rings by Hitemco, Inc. in thicknesses of about 0.005 in. on Vascomax 300 substrates. These plasma-sprayed coatings were later tested in the instrumented short barrel.

6. Summary of Ring Specimens

In the work reported here, erosion test rings as discussed above were prepared for test of both ammunition and/or barrel material modifications. Table II summarizes the test rings prepared in this work and briefly describes their purpose and present status of testing.

TABLE II

TEST RING SUMMARY

Short Barrel Position	Designation	Description	Present Status
Entrance	R I	Vascomax 300, Rc 51	Test Fired
Entrance	R II	Vascomax 300, Rc 51	Fired and Sectioned
Entrance	R III	Vascomax 300, with 0.005 in. plasma sprayed tantalum	Test Fired
Entrance	R IV	Vascomax 300, with 0.005 in. plasma sprayed NiAl	Test Fired
Entrance	R V	4340, Rc 42-44	Fired and Sectioned
Entrance	R VI	4340, Rc 42-44	Ready for Test
Entrance	R VII	Vascomax 300, 1010 steel liner	Fired and Sectioned
Entrance	R VIII	Vascomax 300, with 0.005 in. "soft" chrome plating	Plated
Entrance	R IX	Vascomax 300, with 0.0065 in. "soft" chrome plating	Single Shot and Burst Fire Tested
Entrance	R X	Vascomax 300, with "soft" chrome for destructive metallographic examination	Ready for Plating
Entrance	R XI R XII	Vascomax 300, 0.010 in oversize for plating at Watervliet	Ready for Test
Entrance	R XIII	Vascomax 300, Rc 51-52	Single Shot and Burst Fire Tested
Entrance	R XIV R XV	Vascomax 300, solution annealed preparatory to brazing in liner	Nickel plated, ready to braze
Entrance	R XVI	Vascomax 300	Test Fired
Entrance	R XVII	1020 Steel	Test Fired

TABLE II (CONT.)

TEST RING SUMMARY

Short Barrel Position	Designation	Description	Present Status
Exit	F I	Vascomax 300, Rc 49-50	Fired and Sectioned
Exit	F II	4340 Steel	Fired and Sectioned
Exit	F III	Vascomax 300, Rc 49-50	Test Fired
Exit	F IV	Vascomax 300, Rc 49-50	Fired and Sectioned
Exit	F V	1010 Steel	Test Fired
Exit	F VI	Vascomax 300, Rc 49-50	Test Fired

E. BARREL LINERS

1. Refractory Metals

In the preliminary work of Reference 1, it was found that the refractory metals tantalum-10% tungsten and columbium-1% zirconium exhibited excellent resistance to the erosive propellant gases of the 75mm round. Some effort in the present work was therefore directed toward evaluation of these materials as liners within the Vascomax short barrel.

Communications with a number of possible vendors revealed that fabrication of tantalum-10% tungsten tubing suitable for shrink fit assembly within a Vascomax outer housing would not be attempted by reliable sources. Fansteel Special Structures, Torrence, California, suggested change to tantalum-2 1/2% tungsten which they indicated could be fabricated within tolerable cost by a rolling and welding operation. Inasmuch as no basic difference in thermal/erosion properties were evident in comparing the two alloys TA-10W with TA-2 1/2W, a purchase order was issued to Fansteel for delivery of both the tantalum alloy and columbium alloy tubes. Tube wall thickness was 0.090 inch with an inner diameter of 2.953 inches.

A short barrel housing into which either liner can be placed was fabricated. To be most appropriate for use in the Ares rapid-fire fixture, the housing was constructed of Vascomax 300 maraging steel. The overall dimensions of the housing were essentially those of the instrumented short barrel discussed above but without need of cylindrical ring cutouts at the barrel ends.

After receipt of the liners from Fansteel, each was ground on their outer diameter to permit heat shrink assembly within the Vascomax housing. Although difficult, because of the softness of the material (tensile measured at 39,000 psi), surface grinding was necessary to "true" the O.D. of the liner and was accomplished to the extent believed adequate for heat shrink retention of the liner. The outer surface was, however, far from that desired in an application of this type. In addition, the inner liner surface condition

showed greater roughness than desired, and in fact, the longitudinal weld resulting from the fabrication of the liner from rolled sheet was visible over a short length. Fortunately, the gas seal on the projectile allows for considerable latitude in bore diameter and roughness. Therefore, it was believed prudent to subject this liner to test recognizing it to be less than the best installation.

After preparation of the tantalum-2 1/2% tungsten liner through grinding, it was given detailed inspection for size. The bore of the Vascomax 300 short barrel housing was honed to a diameter of 0.0025 inches less than that of the measured average liner outer diameter. Heat shrink fit at this condition would allow some interference between liner and housing at an average temperature of 400°F. The housing was then heated to 800°F after which the tantalum liner was easily inserted. On cooling, the liner was found to be firmly held in position. A two-degree taper was machined at the entrance end and the bore was machined to permit passage of the projectile.

As an indicator of erosion, three indexing scribe marks several thousandths of an inch deep were made at the entrance and exit ends of the liner using a 90° carbide tipped stylus. Indium replicas of these marks were made and the lined short barrel was then ready for installation into the single-shot fixture.

The columbium liner was also prepared for insertion into the Vascomax housing but completion of this liner assembly was to await the conclusion of testing of the tantalum liner which uses the same short barrel housing.

2. Replaceable 4340 Liner

In this program, some effort was devoted to the design fabrication and initial proof testing of a Vascomax 300 short barrel housing containing a replaceable 4340 steel liner. The resulting housing-liner combination is shown in Figure 13. The Vascomax liner housing was constructed by reworking a previously used and eroded short barrel S/N 2. This barrel was solution

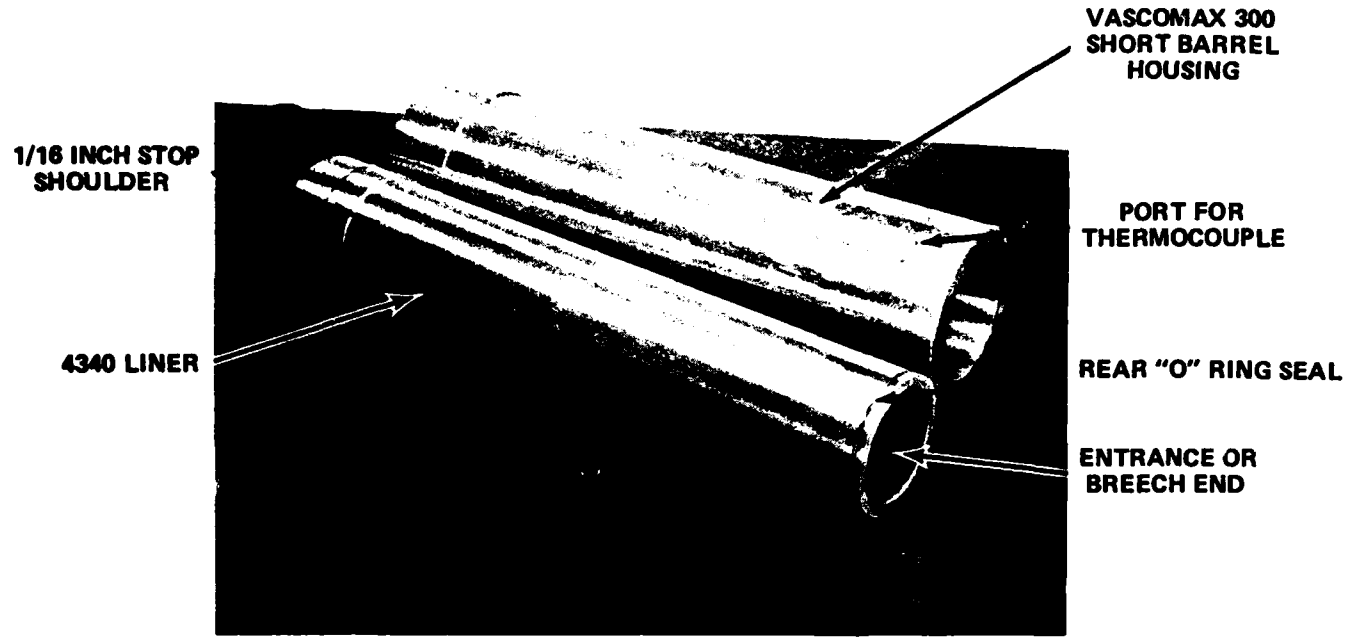

LINER REMOVED

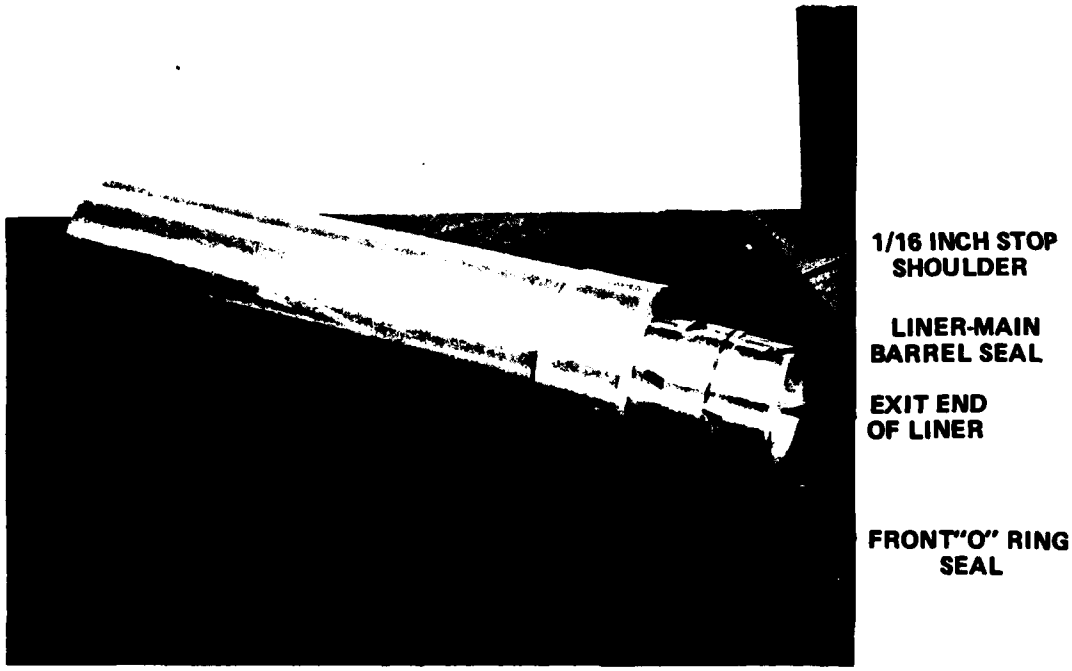

LINER PARTIALLY INSERTED

Figure 13 VASCOMAX SHORT BARREL WITH REPLACABLE 4340 LINER

annealed, machined, and hardened to accept a full cylindrical 4340 liner, as illustrated in Figure 13. The liner thickness (0.336 inch) was selected as the best compromise between loss of short barrel strength due to the liner and liner temperature rise per shot. In this connection, it must be noted that, for the design selected, short barrel integrity is substantially that due to the housing and this, in fact, can withstand the ballistic pressures with no assistance by the liner. Margin of safety is about 0.45. With the added support of the liner, the margin of safety increases somewhat. A thermal expansion problem does arise with the incorporation of the liner, however. Thermal resistance at the interface between liner and main housing reduces loss of heat from the liner, thus resulting in increased liner average temperature over that of the main housing. Further, because axial movement between liner and housing is permitted, thermal expansion will result in increased liner length compared to that of the main housing. The selected liner thickness reduces this expansion difference to the greatest extent possible within the strength limitations of the combined assembly. A further improvement in assembly strength is gained by the application of "O" rings at each end of the liner as shown in Figure 13. These prevent or at least reduce leakage of gases to the inner surface of the housing, thus allowing the liner to provide greater support of the internal pressure.

F. AMMUNITION

Ballistics, heating, erosion, and fatigue data were gathered for both conventional and ablative ammunition configurations. Components for all rounds tested were supplied by AAI Corporation.

1. Propellant Charge

Basically, two propellant loadings were used, the first (designated M26) consisted of 2380 gms. of M26 stick propellant with 250 grains of black powder booster. The second (designated M26/M30) consisted of 512 gms. of M26 stick propellant added to 1678 gms. of M30 chopped propellant with the same booster charge. In the test program, rounds were received either as loaded

by AAI or as prepackaged propellant increments assembled by Calspan personnel. Calspan loading procedures were, in essential detail, the same as those utilized at AAI.

All rounds fired at Calspan utilized the current standard 4.9 lb TP aluminum/steel projectile configuration.

2. Ablator Composition

The Type I ablator composition employed in the bulk of the testing reported herein consisted of 92.5 percent dimethylsilicone fluid of 60,000 cstks, viscosity plus 7.5 percent Cabosil* Grade M-5 fumed silica. This formulation is prepared by mixing the prescribed amount of Cabosil (dried at 110°C for three hours minimum) and the silicone fluid for 30 minutes in a Hobart type mixer. As a quality control check, the ASTM D217 Cone Penetrometer reading of each batch is determined immediately after mixing. A Type II formulation consisting of 92.5 percent dimethylsilicone fluid of 1000 cstks. viscosity and 7.5 percent of M-5 Cabosil was also prepared in similar fashion. This second mix Type II has practical advantage over the Type I in ease of pumping which is desirable for rapid loading in many rounds.

Both of the above compositions were subjected to a high temperature stability test at 250°F as a means of establishing that they will be completely stable under 165°F high temperature storage test conditions. No separation or softening was found after seven days at 250°F. This stability stems from the nature of the methyl silicone molecule which may be represented as below;

$$\begin{array}{c} CH_3 \\ CH_3 - Si - O - \\ CH_3 \end{array} \left[\begin{array}{c} CH_3 \\ Si - O \\ CH_3 \end{array} \right]_x \begin{array}{c} CH_3 \\ - O - Si - CH_3 \\ CH_3 \end{array}$$

*Cabot Corporation, Boston, Massachusetts.

the subscript x indicates the chain length, which determines viscosity. The Si-O "backbone" is thermally very stable, and the methyl (CH_3) groups are firmly bound, such that the fluid is very resistant to decomposition by either chemical or thermal means. For example, the flash point of 1,000 cstks, fluid is $> 600°F$, it resists attack by dilute acids and bases, and it is generally unreactive with metals and many organic compounds such as petroleum hydrocarbons. The various silicone fluids are considered to be very poor solvents, with the dimethylsilicones being the worst. Shelf life of the ablator composition should therefore be indefinite.

3. Ablative Ammunition

In the work, some effort was made to optimize the ablative ammunition design for practical applications to current rounds. In addition to change in ablator composition as described above, attempt was made to improve the performance and integrity of the ablator containment. The natural container which exists in the annular space between the projectile and the steel sealing sleeve of the AAI round was used to contain the ablator fill.

Figure 14 illustrates the essential ablative round components. For the earlier rounds tested, a short cutout in the steel sleeve as shown was required to accommodate the overlapping polypropylene cap so that assembly of the plastic case (not shown) can be made without interference. The cutout was acceptable to AAI and was incorporated in AAI's sleeve design drawings. Later ammunition, due to sleeve design change which incorporated a projectile shot start ring, required no cutout but necessitated no change in ablative components or loading procedure. Gas seal was obtained by use of two stacked plastic seal rings (rather than five as used in the non-ablative standard round). Containment of the ablator is provided by two polypropylene plastic covers which pass over the afterbody of the projectile. The method of assembly of the essential ablative components is as shown in Figure 15. First the projectile and seal rings are placed into the metal sleeve insuring that the projectile is at its proper forward location. The annular space is then filled with the silicone ablator. For many rounds this is best done using a high-

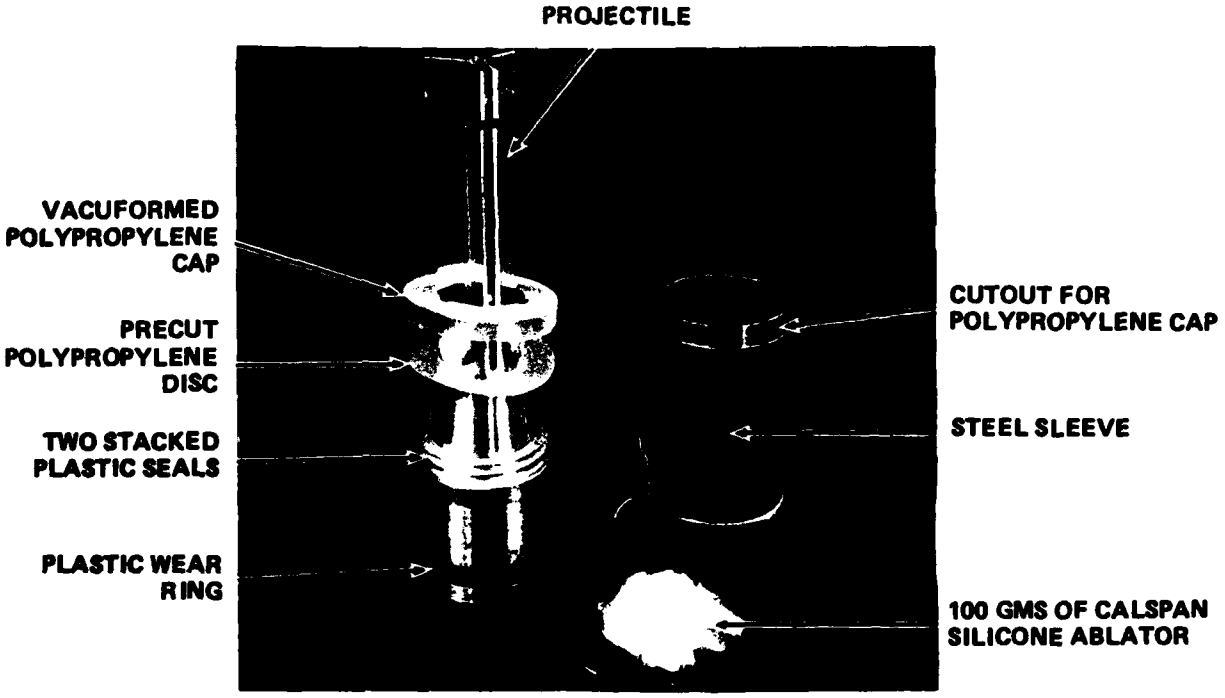

Figure 14 75mm ABLATIVE AMMUNITION COMPONENTS

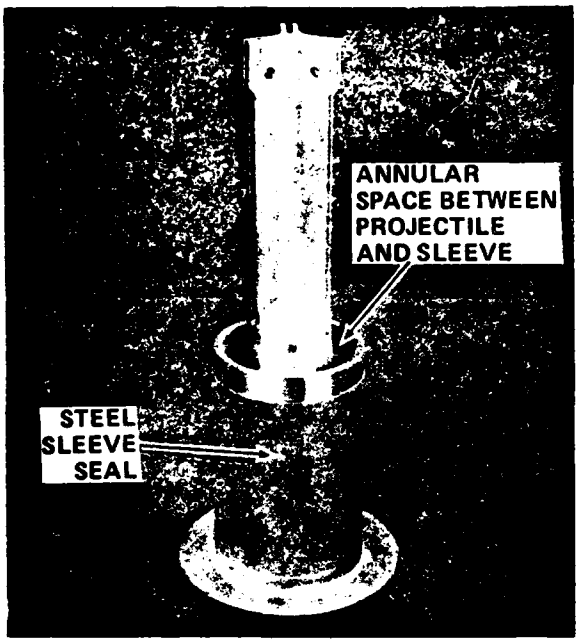

STEP 1. PROJECTILE AND PLASTIC SEALS INSERTED INTO FORWARD STEEL SLEEVE

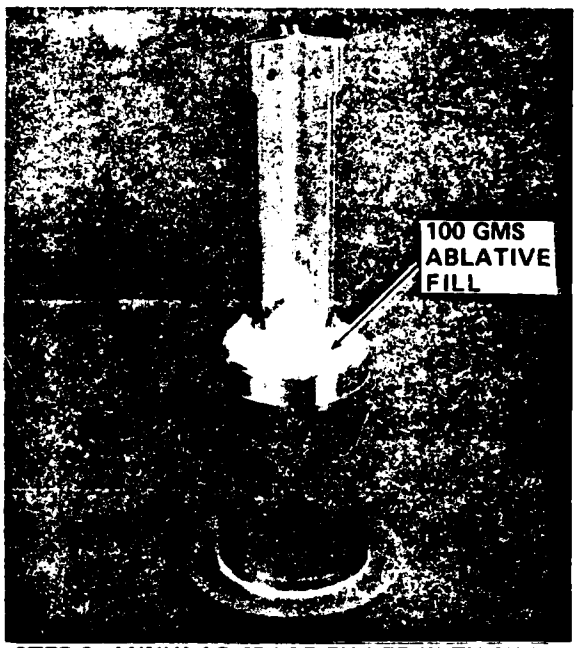

STEP 2. ANNULAR SPACE FILLED WITH SILICONE ABLATOR

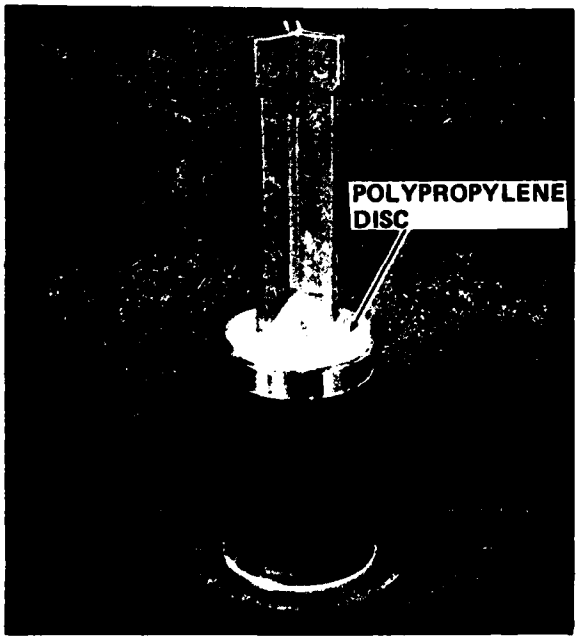

STEP 3. PRE-CUT POLYPROPYLENE DISC IN PLACE

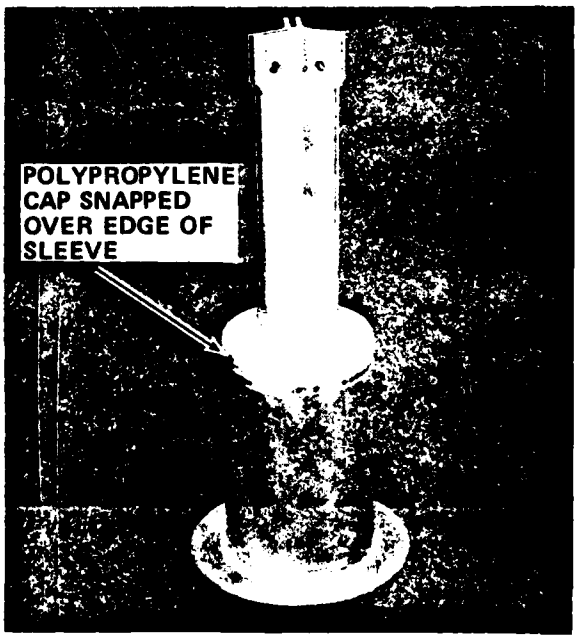

STEP 4. PRE-FORMED POLYPROPYLENE CAP IN PLACE. ASSEMBLY COMPLETE.

Figure 15 METHOD OF ASSEMBLY OF ABLATIVE ROUND COMPONENTS

pressure grease gun. The first polypropylene disc is placed into position on top of the silicone, a 45° rotation of this disc assures that the three cutouts in the disc, required to allow it to pass over the aft fin retainers, will be out of line with those in polypropylene cap which is snapped over the sleeve cutout as a final step. Seal of the silicone ablator is thus produced by the two internal gas seal rings on the tube side and by the polypropylene cap acting against the projectile cone on the propellant side. Due to the thick nature of the ablative substance, it has no tendency to flow, thus, only separation from the propellant is actually required. The present configuration and sealing method is believed totally adequate for long term storage. Figure 16 illustrates the ablative ammunition assembly in partial cross-section. All ablative rounds tested in this work utilized 100 gms. of ablator. The amount of propellant load was unchanged in the ablative rounds.

Throughout the work, ablative ammunition components and assembly methods were discussed with AAI personnel and sufficient components were supplied to AAI for fabrication of several hundred ablative rounds. These rounds were shipped to Ares for test firing in their rapid-fire cannon. As these rounds were fired, bore erosion was monitored at Ares and resulting data will later aid in assessing performance of the ablative round. Of course, this interim utilization of the ablative round in its present configuration also increases barrel life during the Ares cannon development.

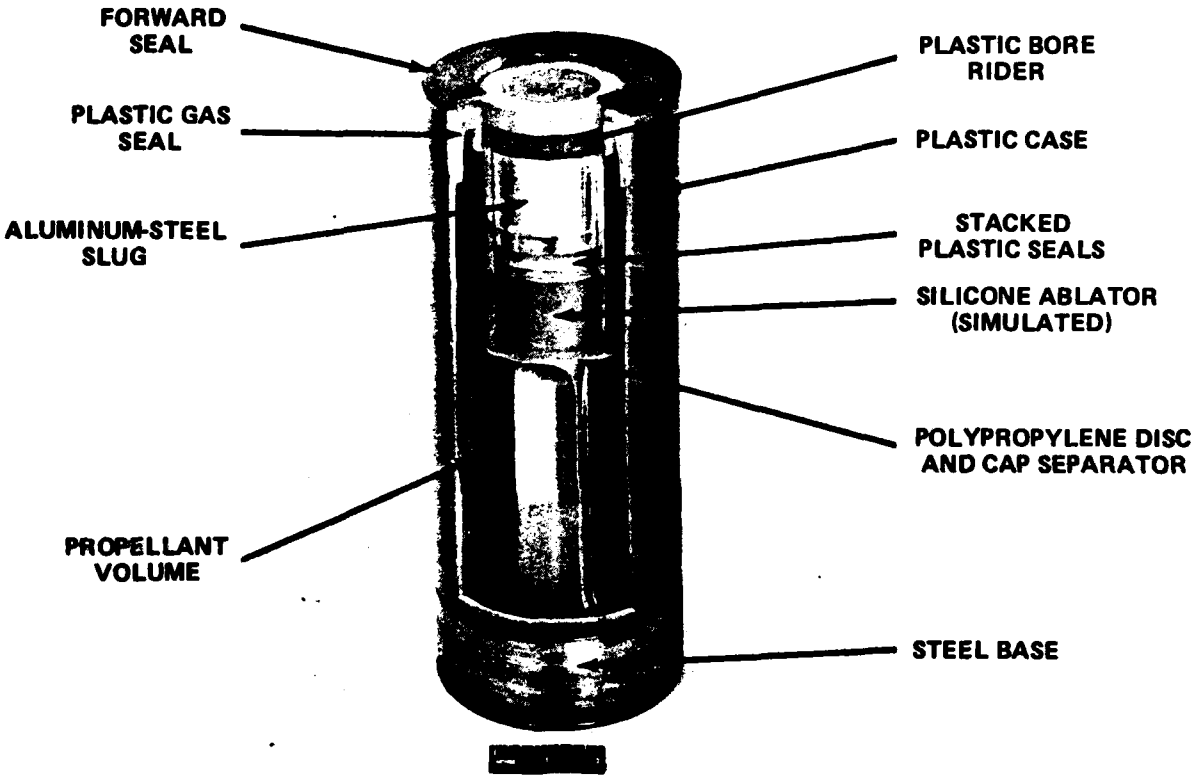

Figure 16 ABLATIVE AMMUNITION ASSEMBLY IN PARTIAL CROSS-SECTION

III. SINGLE-SHOT TEST RESULTS AND DISCUSSION

Single-shot testing performed in this work consisted of a total of 65 shots in which typical measurements included:

1. Chamber pressure;
2. Short barrel pressure;
3. Action time;
4. Ignition delay;
5. Muzzle velocity;
6. In-wall temperatures;
7. Barrel external temperatures; and
8. Erosion.

A. BALLISTICS PERFORMANCE

Ballistic test results for the 65 rounds are summarized in Tables III and IV. Pressures in each instance were obtained through the use of PCB Piezoelectric pressure transducers. Representative pressure histories are given in Figure 17 for both charge types tested. Ignition delay was taken as the time from initiation of voltage to the primer to measurable start of chamber pressure rise. Because the pressure rises continuously from its baseline value, the actual rise time is not specific and is judged from the recorded pressure histories with an accuracy of about $\pm$0.25 msec. Action time was determined as the time from initiation of primer voltage to projectile exit at the muzzle indicated by a muzzle break wire. The projectile velocity was obtained by measurement of projectile transit time over a 55 ft. distance from the muzzle.

In reviewing the ballistics data of Table III, one notes that within each charge type, pressure and velocity variations appear to be of similar magnitude. Furthermore, addition of the ablator appears to have minimal effect on either chamber pressure or velocity. As is summarized in Table IV, one notes the M26/M30 charge type to exhibit somewhat increased pressures over

TABLE III

BALLISTIC RESULTS

Test No.	Ammunition Type	Charge Wt. gms	Ablator Type	Chamber Pressure psi	Barrel Pressure psi	Ignition Delay msec	Action Time msec	Velocity Deviation From Nominal Ft/Sec
1	100 gm Subload-M26	2280	None	47,300	42,700	11.5	17.0	---
2	STD-M26	2380	None	47,300	45,300	6.0	12.0	-150
3	STD-M26	2380	None	53,500	44,000	8.5	14.5	-210
4	STD-M26	2380	None	47,200	42,500	6.5	12.5	-200
5	STD-M26	2380	None	52,400	45,500	6.0	12.0	-140
6	STD-M26	2380	None	48,400	44,000	6.0	12.0	-50
7	530 gm Subload-M26	1850	None	36,000	---	6.0	12.0	---
8	STD-M26	2380	None	51,400	---	5.0	11.5	-120
9	STD-M26	2380	None	50,500	---	---	---	-230
10	STD-M26	2380	None	53,500	---	7.0	12.0	---
11	STD-M26	2380	None	53,300	---	4.0	10.0	-50
12	STD-M26	2380	None	62,800	---	4.0	10.0	0
13	STD-M26	2380	None	51,300	46,500	4.0	10.0	-110
14	STD-M26	2380	None	51,000	48,000	3.0	9.0	-200
15	STD-M26	2380	None	51,000	46,500	4.5	10.5	---
16	ABL-M26	2380	I	50,500	46,500	5.0	11.0	+20
17	ABL-M26	2380	I	52,400	46,500	5.5	11.5	-200
18	ABL-M26	2380	I	51,300	46,500	6.5	12.5	---

TABLE III (CONT.)

BALLISTIC RESULTS

Test No.	Ammunition Type	Charge Wt. gms	Ablator Type	Chamber Pressure psi	Barrel Pressure psi	Ignition Delay msec	Action Time msec	Velocity Deviation From Nominal Ft/Sec
19	ABL-M26	2380	I	---	48,000	7.0	---	---
20	ABL-M26	2380	I	50,400	45,300	5.0	---	---
21	STD-M26	2380	None	51,450	---	5.5	---	---
22	STD-M26	2380	None	51,200	---	5.5	---	---
23	STD-M26	2380	None	51,200	---	6.0	---	---
24	STD-M26	2380	None	51,400	---	6.0	---	+100
25	STD-M26	2380	None	51,200	---	5.0	---	+50
26	STD-M26	2380	None	52,300	---	4.5	---	+75
27	STD-M26	2380	None	51,200	45,500	5.0	11.0	+0
28	STD-M26	2380	None	51,000	45,500	5.5	11.5	+30
29	STD-M26	2380	None	51,000	46,000	5.5	12.0	-50
30	STD-M26	2380	None	54,300	46,000	4.0	10.0	+50
31	STD-M26	2380	None	54,300	47,300	6.5	12.5	+30
32	STD-M26	2380	None	51,000	43,400	10.0	16.5	-170
33	STD-M26	2380	None	49,000	43,300	5.0	11.0	-100
34	STD-M26	2380	None	49,000	42,000	7.0	13.0	-150
35	STD-M26	2380	None	50,000	43,300	7.5	13.5	-100
36	STD-M26	2380	None	52,300	43,300	7.5	13.5	-130
37	ABL-M26	2380	I	52,200	44,700	6.0	12.5	-150
38	ABL-M26	2380	I	52,200	47,300	8.0	14.0	-100

TABLE III (CONT.)

BALLISTIC RESULTS

Test No.	Ammunition Type	Charge Wt. gms	Ablator Type	Chamber Pressure psi	Barrel Pressure psi	Ignition Delay msec	Action Time msec	Velocity Deviation From Nominal Ft/Sec
39	ABL-M26	2380	I	52,700	45,700	7.0	13.5	-100
40	ABL-M26	2380	I	52,200	46,000	6.0	12.5	-100
41	ABL-M26	2380	I	52,300	46,000	8.0	14.5	-100
42	STD-M26	2380	None	51,200	---	6.0	12.5	-80
43	STD-M26	2380	None	50,000	---	5.0	11.5	-150
44	STD-M26	2380	None	50,600	---	7.5	14.0	-150
45	STD-M26	2380	None	53,300	---	7.0	13.5	-50
46	ABL-M26/M30	2190	I	55,000	45,770	3.5	9.5	-430
47	ABL-M26/M30	2190	I	55,000	50,700	3.0	---	---
48	ABL-M26/M30	2190	I	55,110	44,360	5.0	11.5	-400
49	ABL-M26/M30	2190	I	55,330	46,470	3.0	9.0	-270
50	ABL-M26/M30	2190	I	---	46,470	6.0	---	-200
51	ABL-M26/M30	2190	I	55,000	46,470	4.5	10.5	-200
52	ABL-M26/M30	2190	I	---	---	---	10.0	-160
53	ABL-M26/M30	2190	I	54,460	47,180	4.0	10.0	+40
54	ABL-M26/M30	2190	I	56,640	46,750	4.0	9.5	-220
55	ABL-M26/M30	2190	I	57,180	46,470	6.0	13.0	-220
56	STD-M26/M30	2190	None	54,460	46,470	4.0	10.0	-160
57	STD-M26/M30	2190	None	60,400	45,910	2.0	8.0	-50

TABLE III (CONT.)

BALLISTIC RESULTS

Test No.	Ammunition Type	Charge Wt. gms	Ablator Type	Chamber Pressure psi	Barrel Pressure psi	Ignition Delay msec	Action Time msec	Velocity Deviation From Nominal Ft/Sec
58	STD-M26/M30	2190	None	54,460	46,470	4.0	10.0	-160
59	STD-M26/M30	2190	None	53,800	45,360	4.0	10.0	-160
60	STD-M26/M30	2190	None	53,260	45,070	5.0	11.0	-200
61	STD-M26/M30	2190	None	51,740	45,700	3.0	9.0	-160
62	ABL-M26/M30	2190	II	54,460	45,700	4.0	10.0	-270
63	ABL-M26/M30	2190	II	63,000	43,230	4.0	10.0	-220
64	ABL-M26/M30	2190	II	61,950	45,900	6.0	11.0	-160
65	ABL-M26/M30	2190	II	---	44,000	5.0	11.0	-170

TABLE IV

SUMMARY OF BALLISTIC RESULTS (AVERAGES)

Ammunition Basic Charge Type	Chamber Pressure psi	Barrel Pressure psi	Ignition Delay msec	Action Time msec	Velocity Deviation From Nominal Ft/Sec
M26	51,590	45,370	5.9	11.7	-87
M26/M30	55,955	46,025	4.2	10.0	-198

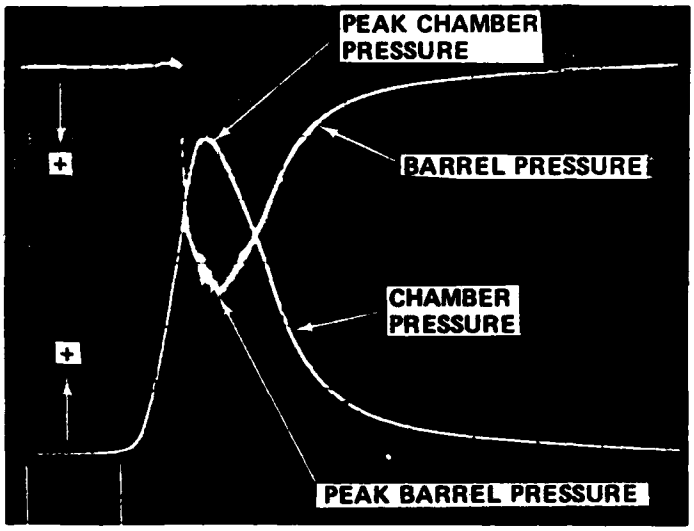

IGNITION DELAY

STD M26 CHARGE
SHOT NO. 14

CALIBRATIONS:
UPPER TRACE DRIVING DOWN: –
BARREL PRESSURE AT
13,330 psi/DIV, 2 ms/DIV
LOWER TRACE DRIVING UP: –
CHAMBER PRESSURE AT
10,280 psi/DIV, 2 ms/div

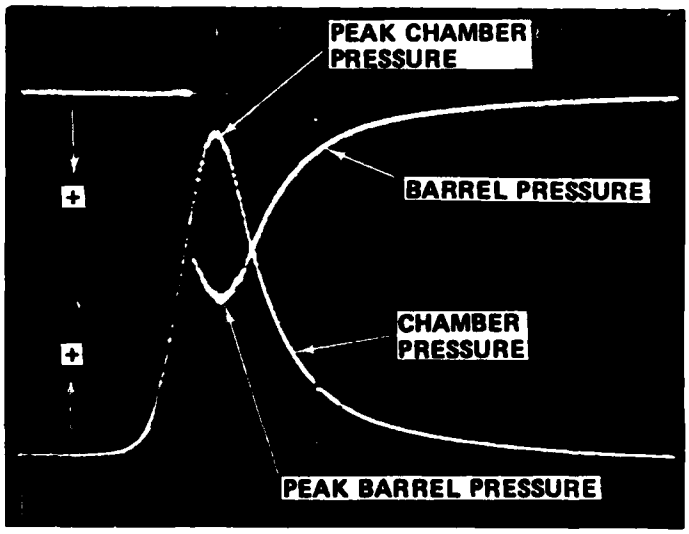

IGNITION DELAY

ABL M26/M30 CHARGE
SHOT NO. 49

CALIBRATIONS:
UPPER TRACE DRIVING DOWN: –
BARREL PRESSURE AT
14,080 psi/DIV, 2 ms/DIV
LOWER TRACE DRIVING UP: –
CHAMBER PRESSURE AT
10,890 psi/DIV, 2 ms/div

Figure 17 REPRESENTATIVE PRESSURE DATA FOR M26 AND M26/M30 CHARGES

that of the M26 charge. This is accompanied by improved ignition delay and action time but surprisingly with somewhat reduced muzzle velocity. In this connection, it must be noted that substantial velocity decay exists over the 55 ft. flight distance from the muzzle due to the high drag profile of the TP round configuration. Furthermore, changes in projectile orientation in flight can have measurable effect on velocity. Hence, velocity variations and deviations below the nominal are as expected, but the reduced velocity of the M26/M30 charge type compared with the M26 charge is as yet unexplained. Perhaps the lower charge weight of the M26/M30 charge, although apparently of greater combustion quickness, results in reduced "push" of the projectile as the projectile moves down the tube. This hypothesis is substantiated somewhat by the indicated short barrel peak pressures of only 82 percent of the peak chamber pressure compared with 87 percent for the M26 charge. Data are, however, insufficient to better explain velocity results obtained at Calspan.

In addition to the measurements noted in Table III, peak muzzle pressure was recorded in Shots No. 8-12 as an aid in assessing tube pressure requirements near the muzzle. Peak muzzle pressures were found to average 12,700 psi which was approximately the same pressure as recorded in the chamber at projectile exit. Therefore, in future, muzzle pressure can be estimated from recorded chamber pressure and action time.

The residual chamber pressure at periods much in excess of the muzzle time is also of importance in reliable weapon function. Therefore, at Ares' request, Calspan determined several residual chamber pressure histories to about 40 msec after firing. Resulting values are as shown in Table V. Note that chamber pressure approaches atmospheric at 40-45 msec. Some difficulty was found in determining chamber pressure at extended time due to drift of the transducer output, but the values of Table IV account for the drift and are believed to represent the maximum chamber pressure at the corresponding times. Communication with Mr. Duane Somers of Ares indicated that no greater precision is warranted, and the recorded data are sufficient for present use in analysis of weapon function.

TABLE V

RESIDUAL CHAMBER PRESSURES

Firing - Msec	Chamber Pressure - psia	
	Shot 44	Shot 45
15	7300	6300
20	2300	2200
25	1200	1200
30	440	450
35	110	160
40	~15	70
45		~15

B. HEAT INPUT

During each test shot, when possible, barrel temperature data were obtained and converted analytically to bore total heat input as described in Reference 1. Reduced test data for all shots are given in Table VI and are summarized in Table VII. Reviewing the test data one finds it in essential agreement with heat input data derived in the earlier work of Reference 1.

Highest bore heat input values were found for the standard charge containing M26 stick propellant. Heat input values are about equivalent to those found for the high energy round of the earlier work. Because the pressure histories are also nearly equivalent, one concludes the stress-deformation predictions of the earlier work (Ref. 1) remain valid for this charge.

There appears to be measurable reduction in heat input throughout the bore with change to the lower charge weight in the standard M26/M30 round. At the critical short barrel entrance region (1.375 in.), bore heat input for this charge is less than 90 percent of that for the standard charge containing only M26 stick propellant. There are even greater reductions evident down-bore. It must be noted here that some of the down-bore reductions observed

TABLE VI

BARREL HEAT INPUT

Test No.	Ammunition Type	Heat Input, Btu/Ft^2, at Given Distance from Breech End, In.			
		1.375	15.5	35.5	145
1	100 Gm. Subload	108	99	91	86
2	STD-M26 Stick	111	102	88	80
3	STD-M26 Stick	102	106	91	91
4	STD-M26 Stick	103	101	98	88
5	STD-M26 Stick	101	105	--	78
6	STD-M26 Stick	108	103	91	88
7	530 Gm. Subload	---	---	84	75
8	STD-M26 Stick	---	---	91	83
9	STD-M26 Stick	---	---	98	76
10	STD-M26 Stick	105	91	91	86
11	STD-M26 Stick	104	91	88	88
12	STD-M26 Stick	100	90	91	84
13	STD-M26 Stick	121	101	88	88
14	STD-M26 Stick	108	102	91	85
15	STD-M26 Stick	100	93	88	85
16	ABL-M26, I	90	90	98	85
17	ABL-M26, I	92	95	--	82
18	ABL-M26, I	101	93	91	77
19	ABL-M26, I	90	98	--	82
20	ABL-M26, I	95	95	77	79

TABLE VI (CONT.)

BARREL HEAT INPUT

Test No.	Ammunition Type	Heat Input, Btu/Ft^2, at Given Distance from Breech End, In.			
		1.375	15.5	35.5	145
21	STD-M26 Stick	110	98	77	90
22	STD-M26 Stick	106	95	77	77
23	STD-M26 Stick	108	97	84	75
24	STD-M26 Stick	111	102	80	80
25	STD-M26 Stick	108	98	88	86
26	STD-M26 Stick	108	97	84	84
27	STD-M26 Stick	110	98	91	84
28	STD-M26 Stick	106	97	91	84
29	STD-M26 Stick	106	98	--	78
30	STD-M26 Stick	108	97	--	84
31	STD-M26 Stick	106	97	88	82
32	STD-M26 Stick	106	98	84	93
33	STD-M26 Stick	108	98	98	88
34	STD-M26 Stick	110	101	91	95
35	STD-M26 Stick	110	99	84	93
36	STD-M26 Stick	106	99	84	87
37	ABL-M26, I	---	--	77	78
38	ABL-M26, I	95	96	73	81
39	ABL-M26, I	95	98	74	80
40	ABL-M26, I	90	98	73	82
41	ABL-M26, I	90	96	70	85

TABLE VI (CONT.)

BARREL HEAT INPUT

Test No.	Ammunition Type	Heat Input, Btu/Ft^2, At Given Distance from Breech End, In.			
		1.375	15.5	35.5	145
46	ABL-M26/M30, I	86	82	70	75
47	ABL-M26/M30, I	78	79	70	73
48	ABL-M26/M30, I	80	80	63	69
49	ABL-M26/M30, I	87	83	56	70
50	ABL-M26/M30, I	80	83	--	--
51	ABL-M26/M30, I	89	84	--	64
52	ABL-M26/M30, I	81	82	56	68
53	ABL-M26/M30, I	77	82	49	68
54	ABL-M26/M30, I	81	82	46	66
55	ABL-M26/M30, I	77	82	46	67
56	STD-M26/M30	93	85	46	67
57	STD-M26/M30	96	88	46	68
58	STD-M26/M30	95	87	53	62
59	STD-M26/M30	--	--	56	64
60	STD-M26/M30	98	89	56	65
61	STD-M26/M30	99	91	65	61
62	ABL-M26/M30, II	87	79	74	62
63	ABL-M26/M30, II	89	78	70	68
64	ABL-M26/M30, II	89	74	67	63
65	ABL-M26/M30, II	87	74	67	64

TABLE VII

BARREL HEAT INPUT SUMMARY (AVERAGES)

Ammunition Type	Heat Input, Btu/Ft^2, At Given Distance from Breech End, In.			
	1.375	15.5	35.5	145
STD-M26 Stick	107	98	88	85
STD-M26/M30	96	88	53*	64*
ABL-M26, TYPE I	93	95.5	79	81
ABL-M26/M30, TYPE I	81.5	82	57	68
ABL-M26/M30, TYPE II	88	76	69	64

at the 35.5 inch and 145 inch stations may be due to some residual effect of earlier ablative shots fired in the fixture. This would not account entirely for the much reduced heating at these points and there is clearly less down bore heating with the STD-M26/M30 charge.

Use of the ablator in either round is shown to result in a lowering of heat input in the short barrel. The combined change in propellant load and addition of the ablator as indicated by ABL-M26/M30 shows substantial heating reduction compared to the STD-M26 round. Comparison of Types I and II ablator shows some increased protection at the 15.5 inch point with use of the Type II ablator. This is derived at the expense of some protection at the entrance end (1.375 in.). In that change to the Type II ablator was for the purpose of improving down bore protection as well as aiding ablator loading operations, it appears that the "thinner" Type II composition is performing as desired within the short barrel.

Main barrel heating, as indicated in Table VI by results at the 35.5 and 145 inch positions, appears to steadily diminish with increased ablative firings, thus suggesting a buildup of protection from the ablator. This effect has also been noted in other work where similar ablator has been used (Ref. 3) and is therefore not unexpected. The main barrel protection by the ablator is furthermore observed to continue well into the firings of the non-ablative ammunition. Again, this type of residual effect has already been demonstrated (Ref. 3), but not to the extent here observed. Perhaps, the bore surface cracking of the present tube allows for greater adherence of any developed protective coating produced as a result of decomposition of the ablator. Maximum effect of the ablator in lowering of bore heating may not have been achieved in the limited number of rounds fired of each type. Indeed, the results of the burst fire tests discussed later suggest much greater protective effect of the ablator in the muzzle area of the cannon.

With respect to what might be considered modest heat input reduction associated with the ablative ammunition, one should note that corresponding effects on erosion can be dramatic. Bore erosion occurs in part by increase of bore temperature to a threshold point at which the materials' ability to

withstand the surface shear stresses of the gas flow is lost. At this threshold point, added heat load produces rapid loss of material. The ablator, due to its protective coating effect, not only results in a lowering in the rate of temperature rise to the threshold point, but also reduces the rate of heat input into the metal at the time of maximum bore shear stress. Heat absorbed in the ablative coating although later transferred to the bore, is not transferred to the metal at a rate and/or time which can result in serious damage to the bore material. Observe that the same magnitude of heating reduction achieved through simple change in propellant load without benefit of the ablator, would not result in the same effect on erosion.

C. EROSION

As discussed above, erosion measurements were made in the instrumented short barrel through the use of the erosion ring inserts. Erosion results obtained in the test firings are given in Tables VIII and IX for the entrance and exit ends of the short barrel. Tests were conducted to investigate both changes in bore material and changes in ammunition.

1. Entrance End - M26 Stick Propellant

At the entrance to the short barrel with use of STD-M26 ammunition, results indicate the erosion of the Vascomax 300 material to increase in rate for the first few shots to a limiting diametrical erosion rate of about 1.1 mils/shot. With introduction of the ablative composition in this round type, erosion is shown to be reduced from 10 to 30 fold depending upon whether average or limiting rates of erosion are compared. It is judged best to consider the limiting erosion rate as most significant inasmuch as this more nearly approximates actual gun usage. Based on this criterion, one estimates a diametrical erosion rate of about 0.04 mils/shot for the ABL-M26 (Type I), or about 0.040 inches in one thousand rounds. Hence, use of the ablator in this round reduces bore erosion to the extent that erosion should present little obstacle to weapon development and use. There is, of course, the need to insert the ablator in each round and to assure that all evolutionary rounds are designed to accommodate the ablator.

TABLE VIII

EROSION PERFORMANCE AT ENTRANCE TO SHORT BARREL

Designation	Type	Number of Shots	Diametrical Rate Of Erosion mils/shot	Purpose	Final Condition Of Specimen
R I	Vasco 300	1 STD-M26	0.28	To determine single round erosion of Vascomax	Obvious surface loss
R II	Vasco 300	1 STD-M26	0.32	Test Vascomax in successful shots first shot.	Significant surface loss, melting evident
R II	Vasco 300	2 STD-M26	1.10	Second and third shots.	
R II	Vasco 300	2 STD-M26	1.12	Fourth and fifth shots.	
R II	Vasco 300	3 Ablative-M26, I	0.12	Test ablative ammunition-three shots.	Minor erosion, little melting
R II	Vasco 300	7 Ablative-M26, I	0.04	Seven additional shots.	
R III	Vasco 300 with 0.005 in. plasma sprayed Tantalum	1 STD-M26	0.08	Test Tantalum coating.	Coating "blistered".
R IV	Vasco 300 with 0.005 in. plasma sprayed NiAl	2 STD-M26	2.9	Test NiAl coating.	Coating removed.
R V	4340	3 STD-M26	0.42	Test 4340 steel three shots	Obvious surface loss, surface flame polished.
R V	4340	2 STD-M26	0.46	Two additional shots.	

TABLE VIII (CONT.)

EROSION PERFORMANCE AT ENTRANCE TO SHORT BARREL

Designation	Type	Number of Shots	Diametrical Rate Of Erosion mils/shot	Purpose	Final Condition Of Specimen
R VII	1010 Steel Insert	2 STD-M26	0.04	Test 1010 steel liner. First 2 shots.	Minor erosion, no melting or cracking.
R VII	1010 Steel Insert	3 STD-M26	0.07	Three additional shots.	
R IX	Vasco 300 with 6.5 mils chrome (soft, low contraction)	3 STD-M26	+0.03	Test soft chrome. First three shots.	Negligible erosion, some surface cracking, protective oxide.
R IX	Vasco 300 with 6.5 mils chrome (soft, low contraction)	3 STD-M26	0.10	Ring inserted in reverse, three additional shots.	
R IX	Vasco 300 with 6.5 mils chrome (soft, low contraction)	2 STD-M26	0.025	Two additional shots.	
R XVI	Vasco 300	3 STD-M26/M30	0.51	Test Vascomax with standard M26/M30	General surface loss. Melting evident.
R XIII	Vasco 300	10 ABL-M26/M30, I	0.02	Test ablator Type I.	Negligible erosion.
R XIII	Vasco 300	4 ABL-M26/M30, II	0.05	Test ablator Type II.	Negligible erosion.
R XVII	1020 Steel	3 STD-M26/M30	0.11	Test 1020 Steel.	Erosion confined to sharp edges.

TABLE IX

EROSION PERFORMANCE AT EXIT OF SHORT BARREL

Ring Designation	Type	Number And Type of Shots	Average Diametrical Rate of Erosion mils/shot	Purpose	Final Condition Of Specimen
F I	Vasco 300	9 STD-M26	0.13	Test Vascomax with STD-M26	Some surface wash, no cracks
F I	Vasco 300	10 ABL-M26, I	0.12	Test Vascomax with ABL, I	Some surface wash, no cracks
F II	4340	19 STD-M26	0.06	Test 4340 with STD-M26	Some loss, extensive cracking
F IV	Vasco 300	3 STD-M26/M30	0.01	Test Vascomax with STD-M26/ M30	Negligible loss, some deposits
F IV	Vasco 300	10 ABL-M26-M30, I	0.009	Test Vascomax with ABL-M26/ M30, Type I	Negligible loss, some deposits
F IV	Vasco 300	4 ABL-M26/M30, II	0.007	Test Vascomax with ABL-M26/ M30, Type II	Negligible loss, some deposits

Erosion of the 4340 steel test ring was found to average about 0.43 mil/shot for the five STD-M26 shots fired. Limiting erosion rate was about 0.46 mils/shot or roughly 40 percent of that for the Vascomax. Figure 18 illustrates the surface condition of the 4340 test ring after the first three shots. As may be observed, there is evidence of surface "wash" with the surface essentially flame polished. A few adherent surface deposits are also visible. This is to be compared with the Vascomax ring as shown in Figure 19, where the rivulose surface and obvious surface melting indicates greater erosion. Compared, however, with the ablative ammunition, the improved performance associated with the 4340 steel is considered modest at best and is believed most applicable as a replaceable short barrel insert. This type of insert is discussed later in this report.

The two test rings having plasma sprayed coatings were found to perform poorly in the test firings. The tantalum was found to exhibit "blistering" in a single shot. This is illustrated in Figure 20. Furthermore, significant material loss was apparent. Because the coating is thin (<.005 in.), only negligible erosion may be tolerated. The plasma sprayed NiAl (Ring R IV) showed greater adherence but intolerably high erosion. Portions of the coating were completely removed after only two shots as shown in Figure 21.

The two plasma sprayed coatings tested in this work represent the best candidate materials available. Plasma spraying yields the greatest possible density in thermally applied coatings. The failure of these coatings strongly suggests that thermally applied coatings will not survive the environment of the present weapon. Failure is for the most part due to the porosity of the applied coating. The high porosity lowers both the coating strength and its thermal conductance. These combine to overcome the basic high-temperature resistance of the parent material, thus resulting in little or no improvement. Hence, no further investigation of thermally applied coatings was conducted. Rather, coating efforts were directed to those methods, such as electroplating, by which coatings of greater density and strength can be applied.

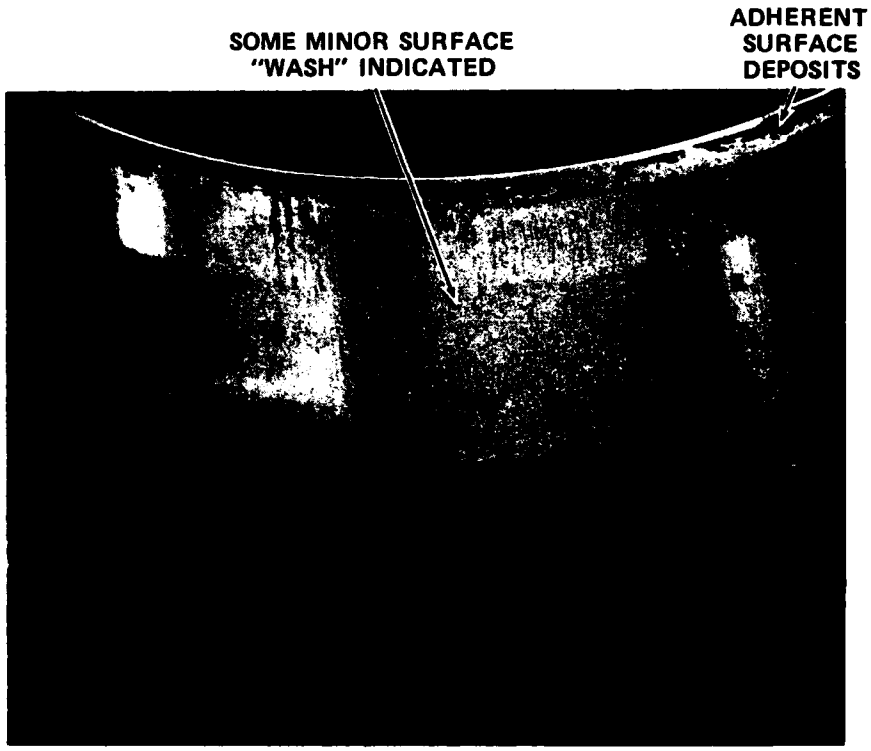

Figure 18 VIEW OF SURFACE OF 4340 ENTRANCE RING AFTER THREE SHOTS

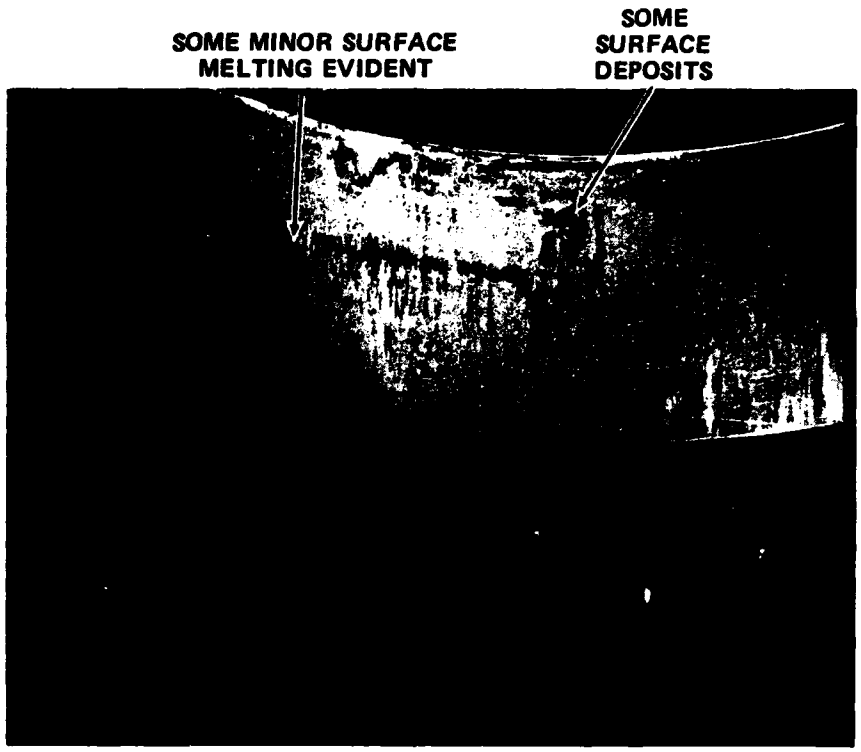

Figure 19 VIEW OF VASCOMAX ENTRANCE RING AFTER 5 STANDARD PLUS 3 ABLATIVE SHOTS

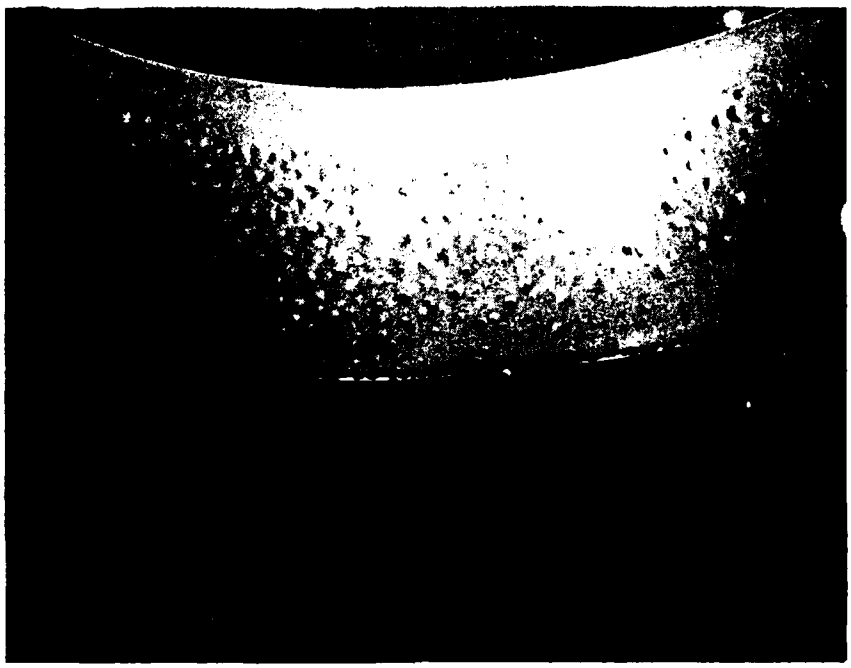

Figure 20 VIEW OF SURFACES OF PLASMA SPRAYED TANTALUM ENTRANCE RING AFTER ONE SHOT (SHOWS "BLISTERING" OF TANTALUM COATING)

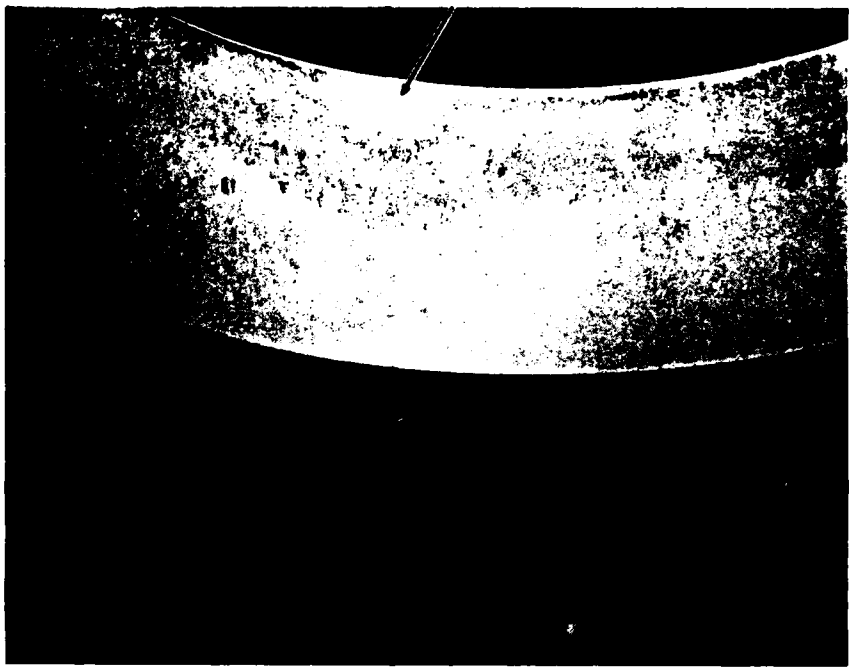

Figure 21 VIEW OF SURFACE OF PLASMA SPRAYED NiAl ENTRANCE RING AFTER 2 SHOTS

Erosion results for the 1010 steel lined test ring R VII indicate excellent performance compared to either Vascomax or 4340 steel. Erosion rate was found to be less than 0.07 mils/shot, or only about 7 percent of that for Vascomax, subjected to the same charge. As shown in Figure 22, surface condition of the 1010 steel after test and cleaning was essentially unchanged due to firing. The surface was relatively free of deposits and both scribe and polish marks were sharply visible. There was minor rounding of the entrance edge of the ring. This outstanding erosion resistance although not totally unexpected based on earlier discussion is encouraging and offers great promise for total solution of the erosion in the short barrel.

By contrast with refractory liners such as tantalum and columbium where thermal expansion differences from that of the Vascomax pose a major fabrication problem, less fabrication difficulties should arise in lining of the Vascomax short barrel with 1010 low carbon steel. For test, the 1010 test ring was fabricated by silver soldering a 0.085 in. thick 1010 liner into a Vascomax 300 support ring and then furnace treating at 900°F to reharden the Vascomax. Fabrication of an entire lined short barrel would best be performed by use of more sophisticated vacuum brazing techniques as discussed later in the Appendix.

As with the 1010 steel, negligible erosion was also found in the firings of the low contraction chrome plated Ring R IX. This ring is shown in Figure 23 as plated and after eight standard shots. Erosion indexing marks are clearly visible after test. Weight loss measurements indicate essentially no erosion in five shots. Some very minor material loss was experienced in three shots where the ring had been inadvertently inserted in reverse. This ring reversal (resulting in a sharp entrance edge) subjected the ring entrance edge to very severe heating and erosion conditions, much more severe than in normal operation. Due to this increased severity, some loss of the Vascomax 300 substrate material at the entrance edge was produced. With its loss, actually beneath the chrome plate, one would have expected the chrome to chip or break at this edge. Visual examination of the edge under a stereo microscope showed, however, little loss of the chrome, thus demonstrating the toughness of the low contraction chrome and the superior bond

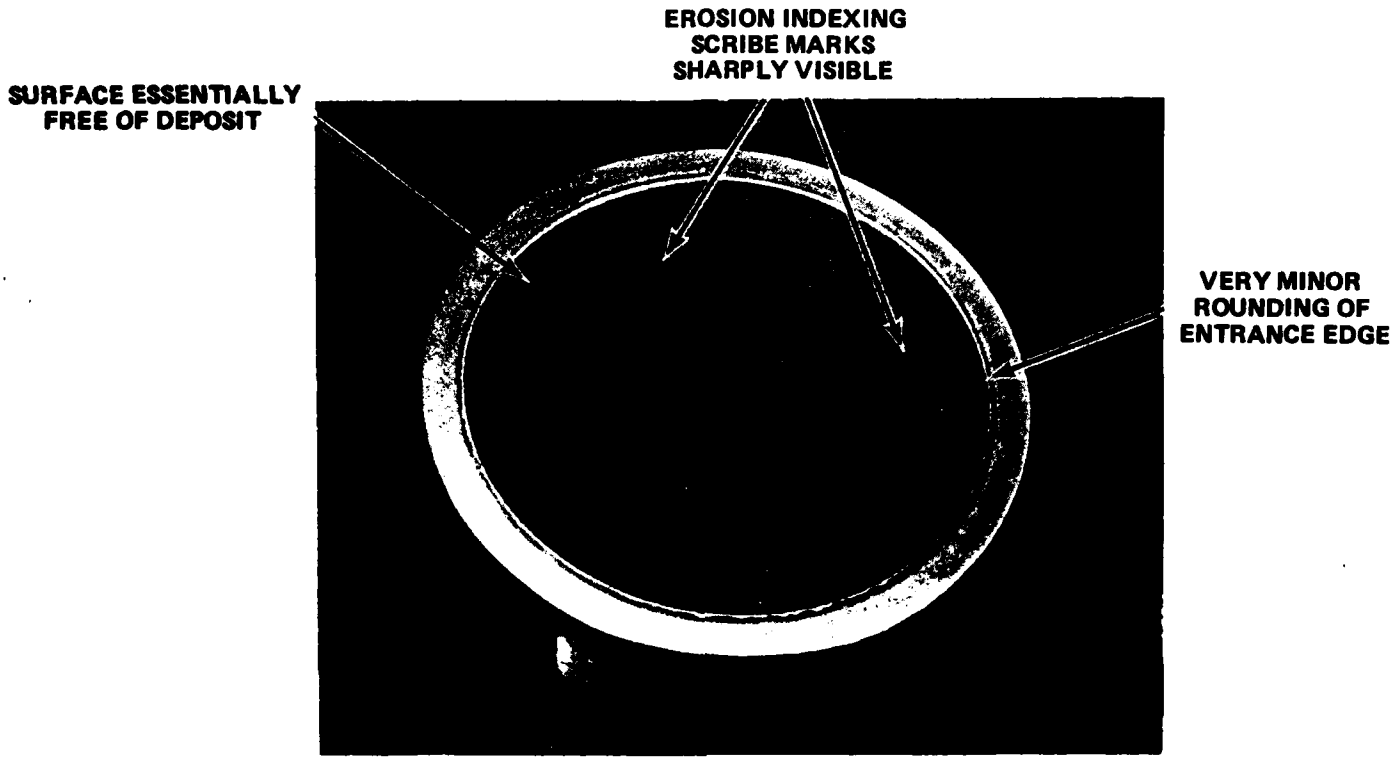

Figure 22 VIEW OF 1010 STEEL LINED ENTRANCE RING R VII AFTER 5 SHOTS (CLEANED WITH HOPPES NO. 9 SOLVENT)

TYPICAL SOFT (LC) CHROME RING-
AS PLATED

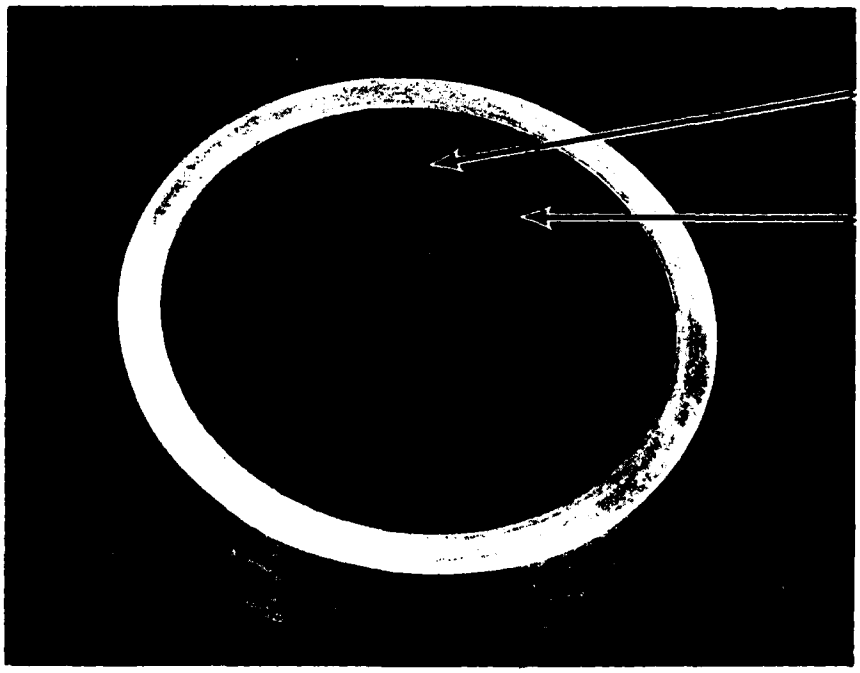

SOFT CHROME RING R IX
AFTER EIGHT SHOTS

Figure 23 VIEWS OF SOFT (LC) CHROME ENTRANCE RING

strength of the plating. Because of the ring reversal, erosion data in these three shots must be discounted, resulting in the conclusion that the low contraction chrome plate is not eroded under the single-shot conditions of firing. Testing of this ring was continued into the rapid-fire evaluation presented later.

A rather clear and concise illustration of the significant findings regarding the erosion of the M26 type ammunition is had by reference to Figure 24, which shows the surface condition in the vicinity of the indexing scribe marks for several entrance rings after test. Here, complete loss of the scribe marks is observed for both the Vascomax and 4340 steel specimens after only five standard M26 shots. For each of these specimens, complete loss of surface machining marks is also evident, with the smooth surface appearance of the 4340 specimen indicating a degree of surface flame polishing but probably a very thin melt layer. The rougher surface appearance of the Vascomax indicates greater depth of melt and resolidification. In fact, for the Vascomax ring, resolidified melt was clearly discernible at the down bore edge of the ring after removal from the short barrel.

By comparison with the standard-M26 ammunition, the erosivity of the ablative-M26 ammunition is shown to be strikingly less with inspection of the condition of the scribe marks. Little effect of firing on these marks is noted after as many as ten rounds containing ablator. Surface machining marks are, however, no longer visible thus suggesting some very minor erosion, but this amount of erosion should not interfere with weapon development and use.

With the standard-M26 round, most notable reductions in erosion are shown for the low contraction (soft) chrome plate and the 1010 low carbon steel liner. The chrome-plated ring specimen shows essentially no erosion after eight standard-M26 shots. In the chrome, the indexing scribe marks are clearly visible. There is, however, a surface crack pattern visible.

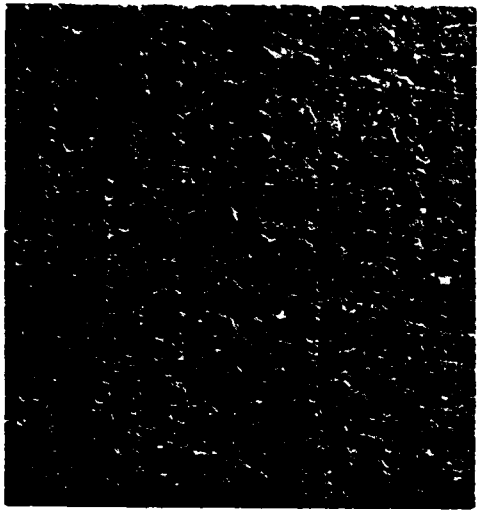

VASCOMAX 300 AFTER
5 STANDARD–M26
SHOTS

6.5 MILS LC CHROME
AFTER 8 STANDARD–M26
SHOTS

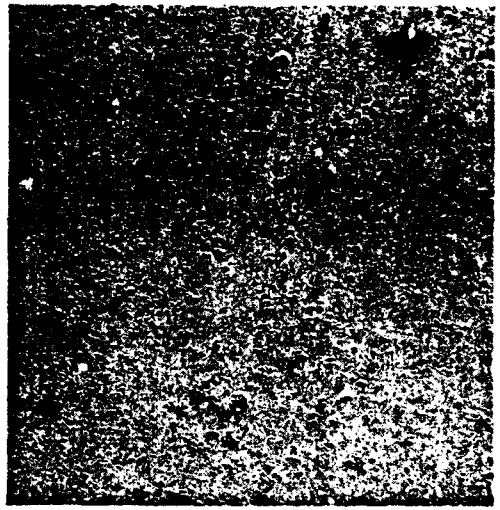

4340 STEEL AFTER
5 STANDARD–M26 SHOTS

VASCOMAX 300 AFTER
10 ABLATIVE–M26 SHOTS

MAGNIFICATION 40X

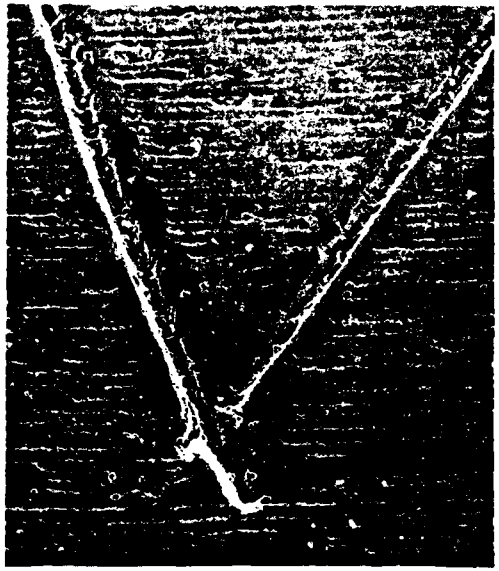

1010 STEEL LINER
AFTER 5 STANDARD–M26
SHOTS

Figure 24 SURFACE CONDITION OF TEST RINGS AFTER FIRING

Although this surface cracking in the plating is evident, the much increased pattern size compared to earlier microcracking of the hard chrome demonstrated in Figure 25, gives promise of improved bond integrity and performance.

Also shown in Figure 24 is the excellent surface condition of the 1010 low carbon steel lined ring after five standard-M26 shots. Although some very minor erosion is suggested by the smoothing of the surface machining marks, there is essentially no cracking or melting visible. The clarity of the indexing marks supports the results of Table VIII which indicate negligible loss.

2. Entrance End - M26/M30 Propellant

The final four entries of Table VIII summarize the erosion data generated as a result of a limited number of firings in which the propellant charge was changed (by AAI) from 2380 grams of M26 stick to 2190 grams of combined M26 stick and chopped M30 propellant as described in Section II. This change in ammunition as discussed above was found to result in a general lowering of bore heat input which apparently also results in a general lowering of erosion as shown in Table VIII. Here, rate of erosion for Vascomax was measured to be 0.51 mils/shot with STD-M26/M30 ammunition compared with the earlier amount of 1.1 mils/shot with the STD-M26 ammunition. Hence, it appears that the erosivity of the M26/M30 charge is roughly one-half of that of the earlier charge. This amount of erosion is, on the other hand, still very substantial and bore protection is needed. Use of the ablator in either the Type I or Type II formulations is again shown to lower erosion to a tolerable amount.

For these firings, the circumferential groove erosion indicating techniques discussed in Section II was used in addition to the 90° indexing scribe mark method. Replication of the surface grooves before and after test as shown in Figure 26 clearly demonstrates the superior performance of the ablative over the non-ablative round. The erosion with use of the Type I ablator is reduced by at least 25:1 based on weight loss, and much more based

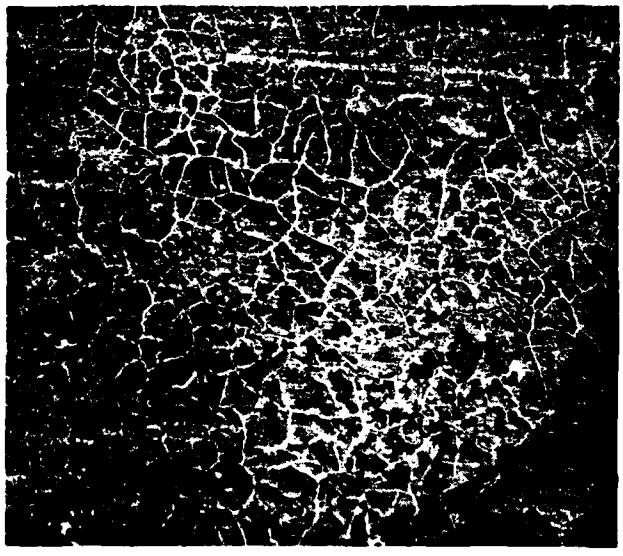

SURFACE OF HARD CHROME PLATED EROSION SENSOR
AFTER ONE SHOT
(100X, SEM)

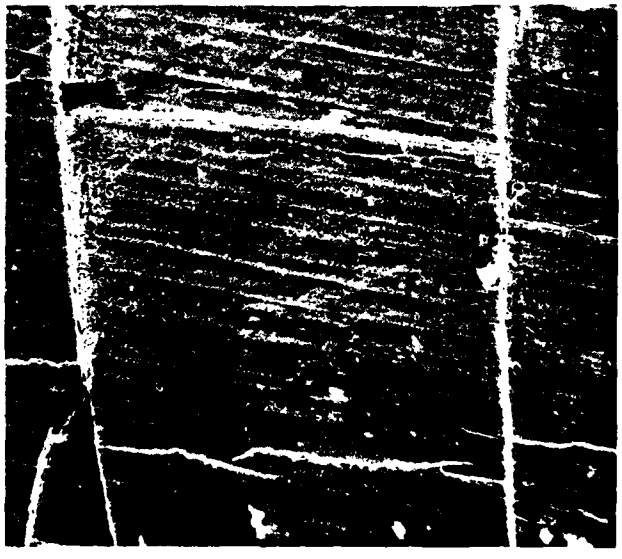

SURFACE OF SOFT LC CHROME PLATED
RING NO. IX AFTER THREE SHOTS
(100X SEM, INDIUM REPLICA)

Figure 25 COMPARSION OF SURFACE CRACKING

on general surface recession. For the ablative ammunition (Type I or II) erosion was confined chiefly to sharp edges such as those introduced by the erosion indexing grooves or the leading edge of the ring. General surface erosion was nil in 10 Type I ablative shots. Comparative surface condition of Vascomax entrance rings after the ablative and non-ablative firings are shown in Figure 26. The excellent performance of the ablator is graphically illustrated.

At the short barrel entrance, somewhat better erosion reductions were obtained with the Type I formulation, but test firings are too limited to judge whether differences are significant with the small material losses actually measured. Further testing of these two formulations is planned in future work.

In a three-round test of a 1020 low-carbon steel entrance ring using standard M26/M30 rounds, erosion was found to be considerably less than that for Vascomax. Although the results given in Table VIII based on weight loss suggest only a 5:1 reduction with the 1020 steel, actual examination of the 1020 test ring indicated erosion in these shots to be again confined to the sharp edges as above with little general surface loss as found with the Vascomax. Hence, continuation of testing of this material might indicate much improved performance over the Vascomax 300 once the sharp edges have rounded due to erosion. Further testing of this material is planned in the future.

3. Exit End

Erosion results obtained at the exit end of the short barrel are summarized in Table IX for all charges tested. At this location in the short barrel, erosion conditions are clearly less severe than at the entrance end. There is, nonetheless, substantial erosion of the unprotected Vascomax with use of the Standard-M26 charge. At this location results suggest only minor improvement in erosion performance with use of the Type I ablator, but because the actual erosion is much less than that at the short barrel entrance end, less protection is needed. Increased protection at the exit end could no

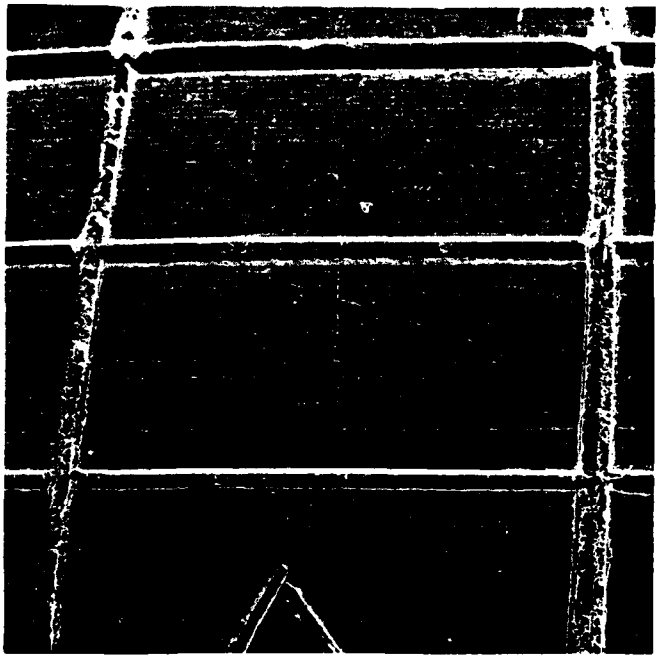

VASCOMAX 300 RING R XIII BEFORE FIRING MAG = 30 X

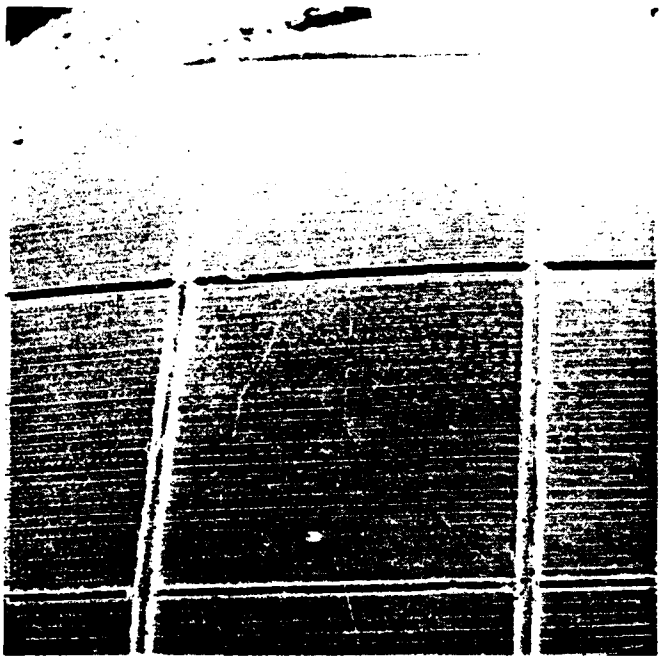

VASCOMAX 300 RING R XVI BEFORE FIRING MAG = 20 X

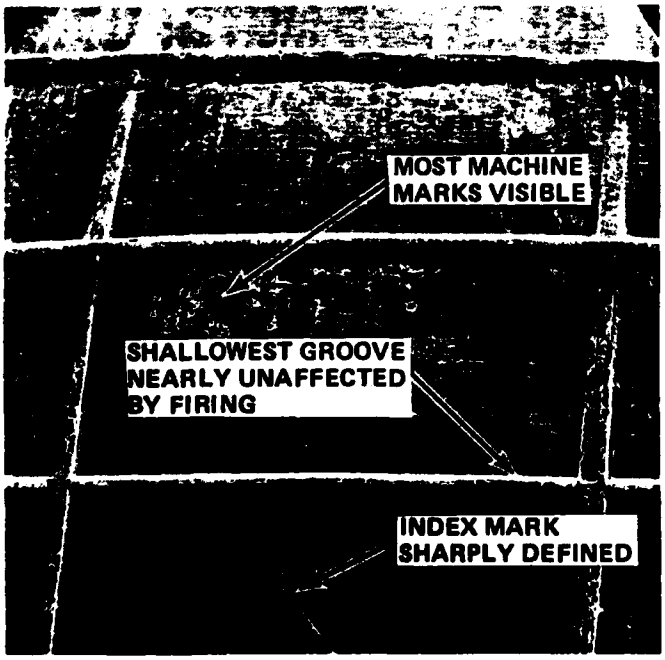

SAME AREA OF VASCOMAX 300 RING R XIII AFTER 10 ABLATIVE–M26/M30 ROUNDS, MAG = 30 X

SAME AREA OF VASCOMAX 300 RING R XVI AFTER 3 STD–M26/M30 ROUNDS, MAG = 20 X

Figure 26 SURFACE CONDITION OF VASCOMAX 300 ENTRANCE RINGS BEFORE AND AFTER FIRING

doubt have been obtained by change in ablator composition. The shift in basic charge from the M26 stick to M26/M30 propellant combination precluded examination of ablator composition change with the standard-M26 charge. Indeed, the reduced erosion shown for the standard-M26/M30 charge nearly obviates the need for short barrel protection at the exit end in that the indicated erosion for this charge at this location is small enough to be considered no present factor in short barrel life. On the other hand, use of the ablator so necessary to reduce entrance erosion for this charge, does also show a favorable down bore effect as noted in Table IX.

Tests of the 4340 steel at the short barrel exit end were conducted only with the standard-M26 charge and indicated reduction in erosion to about one-half that of the Vascomax. There was extensive fatigue cracking of this material observed after only 19 shots which may limit its usefulness in extending actual short barrel life; especially where the material would be used to produce a monolithic short barrel. Because the exit location of the short barrel is adjacent to the main barrel entrance, observations regarding erosion and fatigue of the 4340 material should apply also to the 4340 steel main barrel. Therefore, future testing will be conducted with 4340 material subjected to the improved ablative round containing the combined M26/M30 propellant load.

D. FATIGUE

Whenever very high-strength steels are employed in guns, low-cycle fatigue properties must be given careful consideration. This is true primarily because fracture toughness decreases with increasing yield strength and because some high-strength alloys exhibit low fracture toughness. Given the combined conditions of high applied pressure stresses (for which the designer selects a high strength steel in the first place) and low fracture toughness, catastrophic fatigue failure becomes a possibility even when bore surface cracks are rather small. Such failures have taken place in the past in cannon tubes made of conventional "quench and temper" low-alloy, medium-carbon gun steels tempered to yield strengths in the range 170,000-190,000 psi. More recently a combination of cleaner gun steels, tempering to lower yield strength

(hence higher fracture toughness), autofrettaging, and the use of thicker sections is said to have eliminated the possibility of catastrophic failure in fielded cannons. That is, if and when a crack is eventually propagated completely through the tube wall, fragmentation still does not result.

The high strength maraging steels such as the forerunners of Vascomax 300 and Vascomax 250 suffered during their early development in the nineteen-sixties from unreliable fracture toughness with the result that certain large rocket motor cases failed catastrophically. Extensive research showed that two factors were crucial; titanium content, and cleanliness (inclusion and gas content) as determined by melting practice. Lowering the titanium content from 1.4 percent to 0.8 percent produced a two-fold increase in fracture toughness at the 250,000 psi yield strength level and double vacuum melting produced another very significant increase as shown in Figure 27. Current Vascomax 250 and 300 alloys contain 0.4 percent titanium and 0.6 percent titanium respectively, and both are double-vacuum melted to minimize inclusion and interstitial impurity content.

Fracture mechanics theory has contributed greatly to the understanding of gun tube fatigue during the past decade. While Calspan has to date undertaken no comprehensive study of fatigue in the short barrel, certain observations of bore surface cracking in short barrel insert test rings have been made and appear to be significant in the context of qualitative fracture mechanics considerations. It is important to note, however, that the surface cracking observed to date is primarily the result of thermally and metallurgically induced surface stresses; it is clear from the firing of several hundred rounds at Ares that the rates of cyclic crack growth that might be inferred from the surface crack data do not prevail as firing continues.

Gun barrels (and other structures) fail at applied stress levels below the expected gross yield strength when surface cracks of sufficient size are present such that the stress concentration effect of the defect raises the local stress intensity at the crack tip above the effective yield strength at the same location. In other words, if we consider a shallow bore surface crack which is deepening slightly with each shot fired, this crack will become a running crack when it reaches the critical size at which

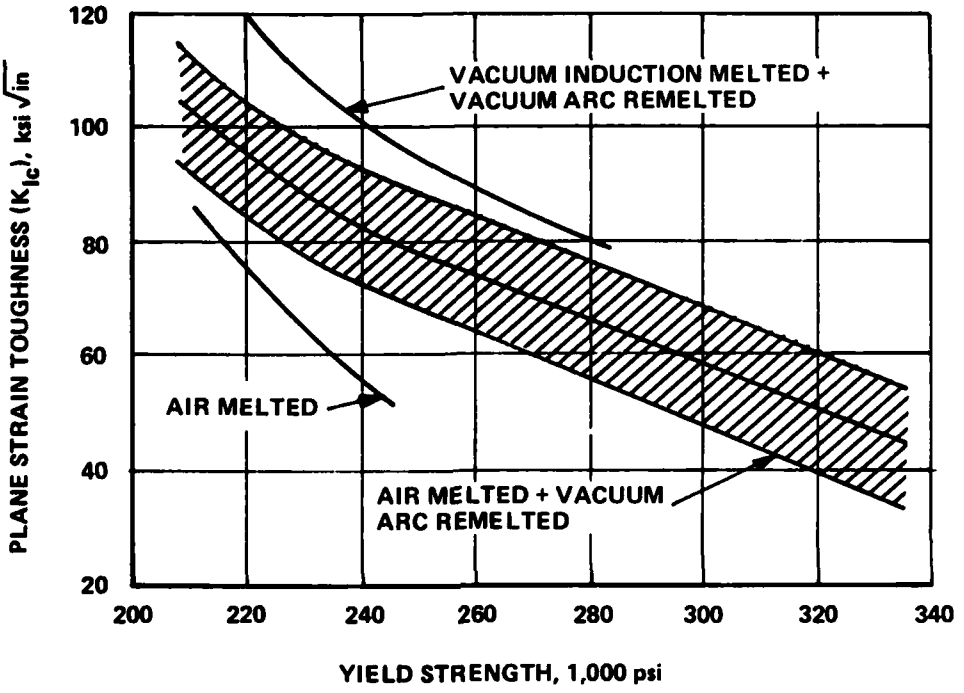

Figure 27 FRACTURE TOUGHNESS vs YIELD STRENGTH IN THE 18 PERCENT NICKEL MARAGING STEELS (AFTER HALL[4])

the stress intensity factor K becomes equal to the fracture toughness K_{IC}* of the material. The stress intensity factor can be expressed as[5]

$$K = K_p + (\sigma_{max}) Y \sqrt{b} \quad (1)$$

where K_p = the contribution to the stress intensity due to the pressure acting within the crack cavity itself;

σ_{max} = the tangential stress in the barrel wall due to pressure

Y = a non-linear function of the relative crack depth (b/B) and the crack shape ratio (b/2a), where

b = crack depth

a = crack length

B = barrel wall thickness

For the purpose of the present discussion, equation (1) is presented only to suggest how the stress intensity factor K increases with crack depth. For example, in the 175mm cannon studied extensively by Watervliet Arsenal, assuming a crack shape such that b/2a = 0.25, 50,000 psi peak pressure, and a wall thickness of 3.5 inches, it is calculated that K = 70 ksi $\sqrt{in}$ when the crack depth is about 0.4 inch, and K = 140 ksi $\sqrt{in}$ when the crack depth is about 2.2 inches. If the tube material of the above example actually has a fracture toughness (K_{IC}) of 70 ksi $\sqrt{in}$, it will fail catastrophically when it develops a bore surface crack 0.4 inches deep and 1.6 inches long. This failure will occur despite the fact that the apparent tangential stress due to pressure is only 80,000 psi and the yield strength of gun steel exhibiting a K_{IC} of 70 ksi $\sqrt{in}$ is about 190,000, as shown in Figure 28.

*The subscript IC refers to plane strain conditions; such conditions generally apply to thick test specimens and to thick members such as gun tube walls.

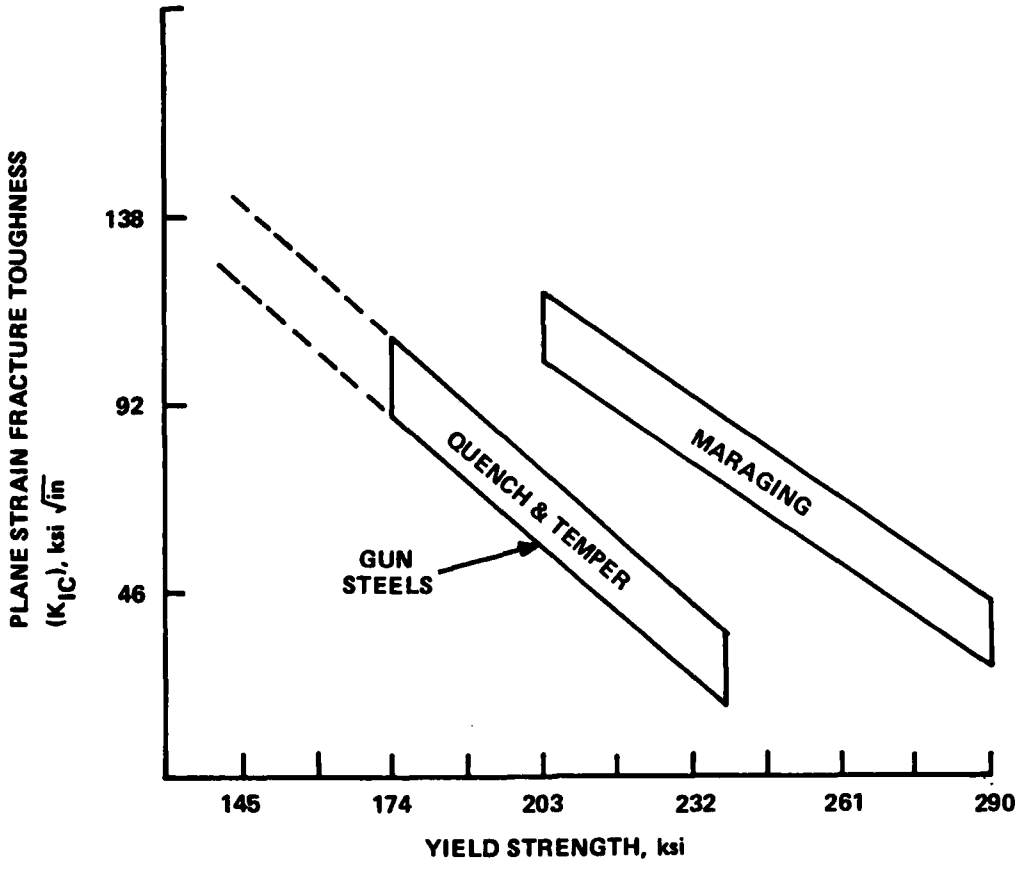

Figure 28 FRACTURE TOUGHNESS vs STRENGTH FOR "GUN STEELS" AND VACUUM MELTED MARAGING STEELS (AFTER ZACKAY, et.al.[6])

In the Ares 75mm short barrel design, constraints are such that wall thickness must be limited; while the short barrel does not experience maximum chamber pressure, tangential pressure stress in the wall may exceed 120,000 psi. Taking into account the need for adequate safety factors, a yield strength near 180,000 psi was chosen for initial 4340 short barrels. Figure 28 indicates that at this and higher yield strength levels maraging steels have a very pronounced advantage in fracture toughness over conventional gun steels. For example, Vascomax 250 CVM grade having a yield strength of 250,000 psi has a fracture toughness of about 70 ksi $\sqrt{in}$ according to Figure 28, or 80 to 90 ksi $\sqrt{in}$ according to Figure 27. In any case, the fracture toughness for quench and temper gun steels, estimated by extrapolation of Figure 28, would be less than 30 ksi $\sqrt{in}$ at a yield strength level of 250,000 psi, and does not reach the 80 ksi $\sqrt{in}$ level in such steels until they are tempered down to a yield strength near 180,000 psi.

In view of the above discussion, it can be concluded that since both Vascomax 250 heat-treated to a yield strength of 250,000 psi and 4340 steel heat-treated to a yield strength of 180,000 psi have a fracture toughness near 80 ksi $\sqrt{in}$, both would fail catastrophically at similar rather small critical crack depths in the short barrel application. No attempt has been made to calculate the precise critical depth, but by analogy with the above discussed 175mm example where tangential stress was only 80,000 psi, it is estimated that a crack very substantially less than one-half inch deep could result in catastrophic failure.

1. Short Barrel Insert Ring Surface Cracking

a. 4340 Steel Observations

If cracks only a fraction of an inch deep can cause failure of the short barrel, it becomes very important to examine in some detail any available information on crack initiation and early growth. Looking first at 4340 steel, Figures 29 and 30 show extensive surface cracking in a 4340 front (exit) ring after firing 19 non-ablative single shots, and Figures 31 and 32 indicate that those cracks lying in the axial direction show some gas "washing."

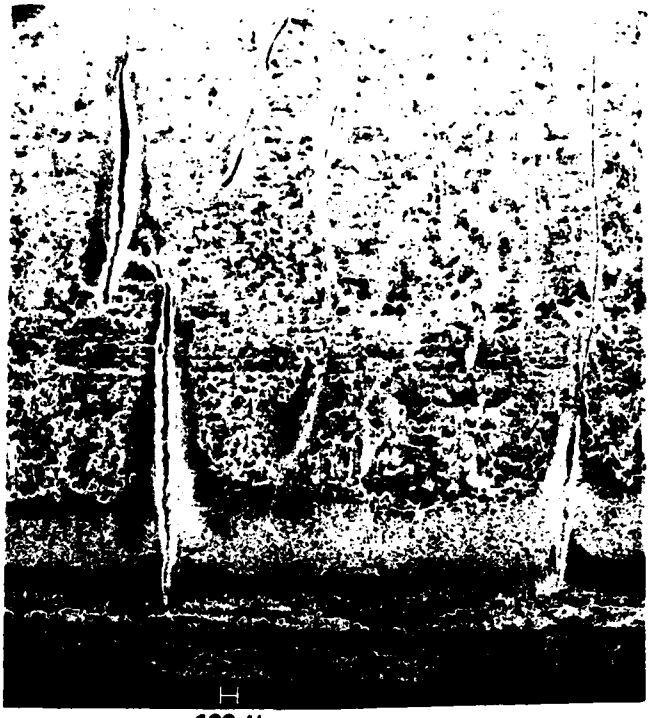

Figure 29 4340 STEEL EXIT RING (F II) SHOWING EXTENSIVE FATIGUE CRACKING AFTER 19 SHOTS (SEM)

Figure 30 SAME SPECIMEN AS ABOVE AT HIGHER MAGNIFICATION (SEM)

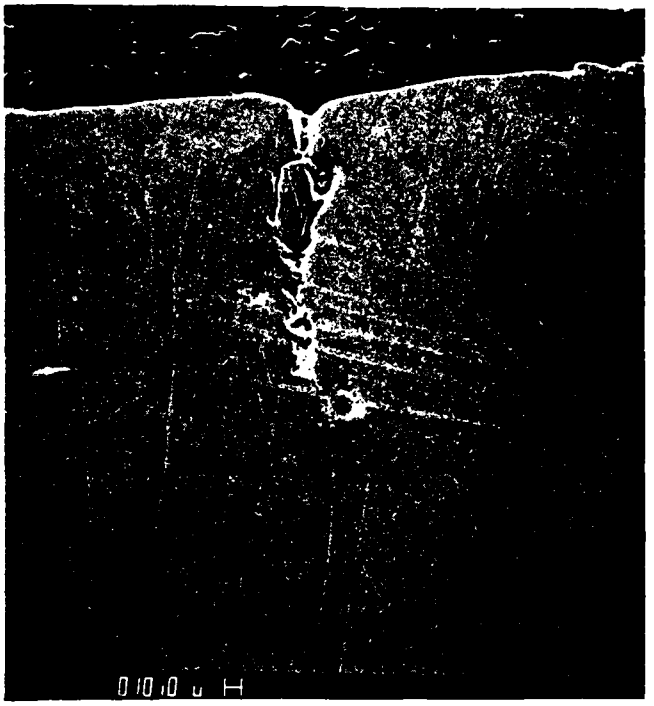

Figure 31 4340 EXIT RING NO. II LATERAL SECTION SHOWING TYPICAL CRACK APPEARANCE IN THE SEM

Figure 32 SAME CRACK AS ABOVE AT 1000X. PROPELLANT GASES HAVE ERODED CRACK WIDTH TO 10-15 μ = 0.5 MIL

Figures 33 and 34 show very clearly the presence of a hard martensite layer about three mils deep at the bore surface. This layer which stands in polishing relief in Figure 33 (which is not etched), is shown to have a hardness of K740 (R_c 60) in Figure 34, and is shown in Figure 35 to be the white etching layer mentioned in World War II vintage gun research literature. This layer is undoubtedly present on the bore surface of all carbon steel cannon barrels where heating is sufficient to drive the surface temperature above the 1500-1600°F range. While the layer may become enriched in carbon and nitrogen as firing continues, it is known that initially it is simply the fine-grained martensite one would expect to find as a result of the extreme thermal cycling of the bore surface.

Unfortunately, untempered hard martensites have extremely low fracture toughness and as seen in Figures 29 through 33, the hard layer cannot support without cracking the large tensile stresses which can be shown as follows to develop during the rapid cooling portion of the ballistic cycle.

1. In high performance guns the bore surface temperature exceeds 2000°F during each ballistic cycle and the thermal expansion of a thin layer of surface, is, therefore, of large magnitude. Since the yield strength of the hot surface layer is very greatly reduced at high temperature in all steels, and the <u>elastic</u> thermal expansion of the surface is prevented by a strong, cold mass of steel beneath the surface, the surface <u>must</u> deform by <u>plastic</u> compression (thickening) in order to remain attached to the cold substrate. The instant when maximum compressive deformation (strain) is reached will approximately coincide with the instant in the ballistic cycle when maximum surface temperature is reached. In addition to the plastic

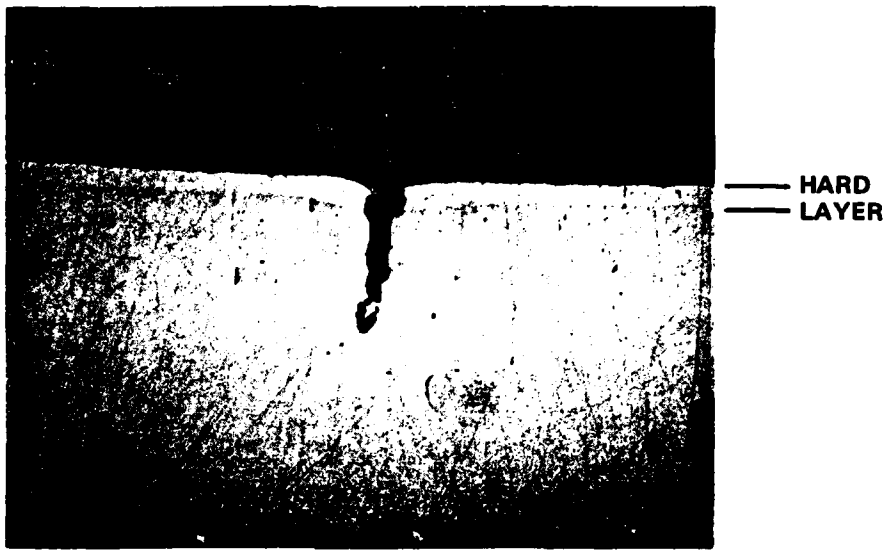

Figure 33 4340 STEEL EXIT RING NO. II, LATERAL SECTION SHOWING FATIGUE CRACK AFTER 19 SHOTS (ALSO SHOWS HARD MARTENSITE LAYER ABOUT 75 μ DEEP) (LIGHT MICROSCOPE, 40X, NO ETCH)

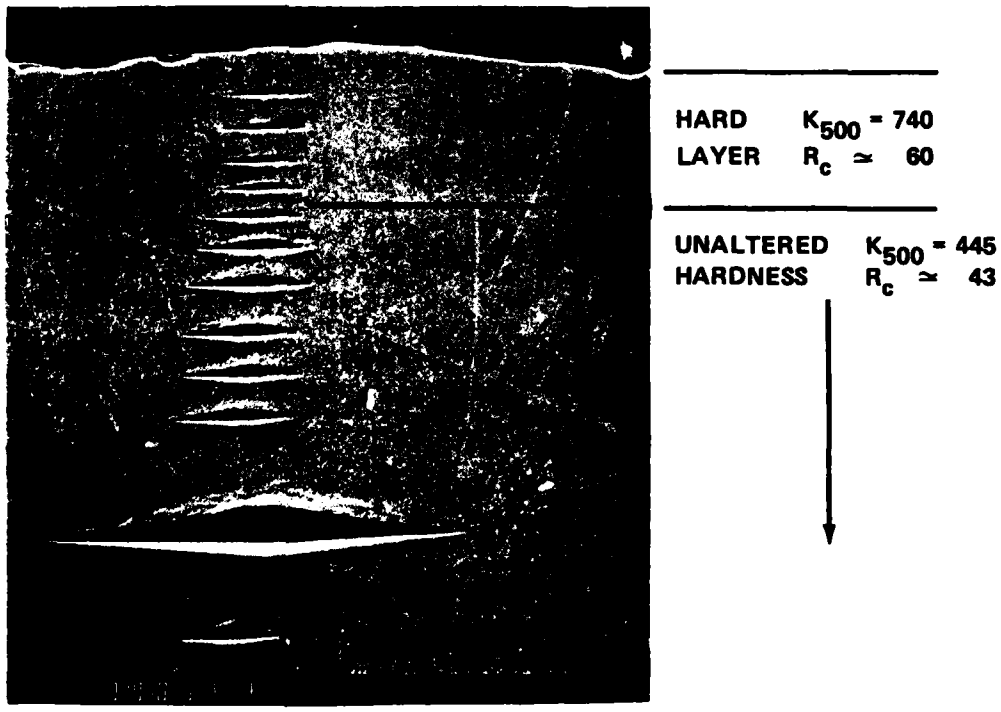

Figure 34 SAME SPECIMEN AS ABOVE SHOWING REDUCED LENGTH OF MICRO HARDNESS INDENTATIONS NEAR SURFACE (SEM)

Figure 35 4340 STEEL ENTRANCE RING V, LATERAL SECTION SHOWING WHITE – ETCHING LAYER AT BORE SURFACE (LIGHT MICROSCOPE, 130X, NITAL ETCH)

strain, there will exist elastic compressive strain up to whatever level of yield strength the metal retains at the applicable peak temperature.

2. In the period following peak temperature, the strained surface layer cools. The first segment of thermal contraction "wipes out" the elastic compressive strain that was present and from that temperature on down, large tensile stress (both circumferential and axial) must develop in the surface layer. At the tip of certain pre-existing microcracks or flows the stress intensity, K_c, will be above the effective fracture toughness, K_{IC}, and these cracks will grow until the stress is relieved.

3. Superimposed on the above thermal stress cycling will be the effects of metallurgical phase changes. Upon firing, the surface will transform to austenite when it reaches 1500-1600°F. The transformation is accompanied by a ~0.2 percent linear contraction but since the hot surface is under compression, and is somewhat soft as outlined above, it is not likely that tensile cracks would form at this time. Upon cooling from the peak temperature, the austenite phase will be retained to temperatures below 900°F where it transforms to hard martensite. Very large thermally induced tensile stresses develop during this cooling period and it is possible that cracking takes place even before brittle martensite is formed.

The above explanation of bore surface crack initiation points up the fact that in carbon steels, cracks of the order of several mils deep (i.e., the thickness of the hard martensite layer) must form in one or two shots. Furthermore, Figure 36 shows that in 19 shots at the short barrel exit station, the maximum crack depth has already reached about 30 mils, and the key questions become whether growth will continue at this rate in

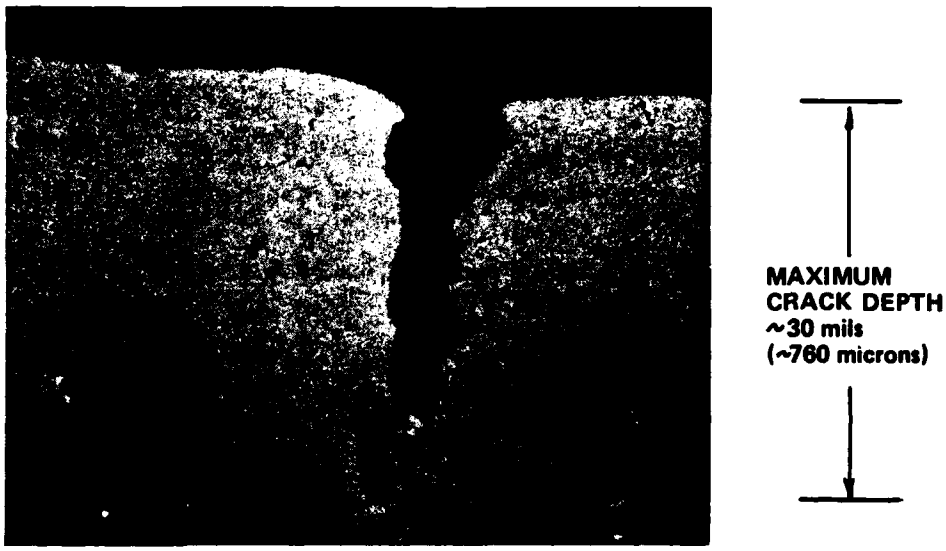

Figure 36 4340 STEEL EXIT RING CROSS-SECTION AFTER 19 SINGLE SHOTS (80X)

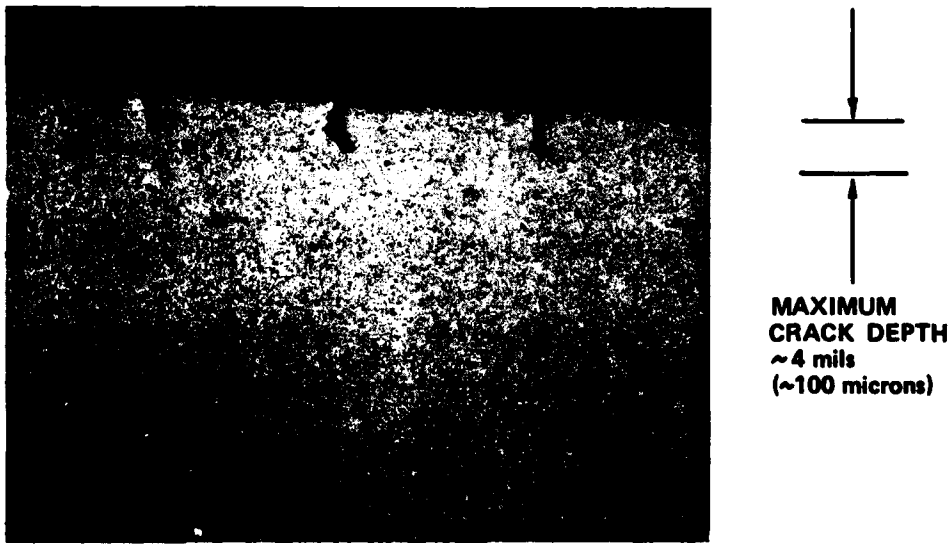

Figure 37 VASCOMAX 300 EXIT RING CROSS-SECTION AFTER 19 "BURST" SHOTS (80X)

subsequent firing or whether conversely, there is a probability that growth will slow greatly. These questions are to some extent amenable to empirical fracture mechanics analysis as outlined below but probably cannot at present be treated when the cracks are still so small that the crack tip lies in the depth region in which thermally-induced stresses and metallurigcal transformations determine the effective stress intensity and fracture toughness.

A fracture mechanics expression relating incremental crack growth to fracture toughness applicable when cracks reach greater depths where the crack tip stress intensity is determined simply by the applied pressure (see equation 1 given previously) is[5]

$$\frac{db}{dN} = \frac{C(\Delta K)^m}{ES_y K_{IC}} \qquad (2)$$

where db/dN = the increment in crack depth per stress cycle applied

C = a material constant

ΔK = the change in stress intensity factor in going from zero pressure to maximum pressure

m = an empirical exponent ranging from two to four

E = the elastic modulus

S_y = the tensile yield strength

K_{IC} = the plane strain fracture toughness of the material.

Here it may be seen that the cyclic growth rate will be minimized when the product, $S_y K_{IC}$, (yield strength times fracture toughness) is maximized. By inspection of Figure 28, the slope of the "curve" for quench and temper steels such as 4340 is such that the product, $S_y K_{IC}$, is increasing as yield strength decreases. The clear implication is that very soft steel might resist crack growth very well, but the only practical implementation of this concept lies in the use of a soft low carbon steel liner in a high strength housing which can stand the applied pressure stress. Experiments along this line are discussed later herein.

Before turning to the discussion of Vascomax test ring surface changes, it should be noted (Figure 35) that 4340 entrance rings show practically

no cracking when fired under the conditions causing extensive exit ring cracking. This implies that over the length of the short barrel the somewhat lesser heating and lower erosion rate conditions that prevail toward the exit end somehow favor crack initiation.

b. Vascomax 300 Observations

The higher fracture toughness of Vascomax 250 relative to Vascomax 300 has recently prompted a decision to switch from the 300 grade to the 250 in the 75mm short barrel application. No Vascomax 250 rings have yet been tested by Calspan as of this writing, but the following observations on the initial microscopic bore surface changes in Vascomax 300 rings are not expected to change significantly when Vascomax 250 is tested.

Figures 36 and 37 show, respectively, the previously described largest crack in a 4340 exit ring and the largest cracks found in a Vascomax 300 exit ring. Both are shown at the same magnification and both rings fired 19 shots of "non-ablative" ammunition. While the initial crack growth rate is clearly far less in the Vascomax, it would be of great interest to carry Vascomax ring testing of this type on to the extent of say 50 shots or more. If such extended testing is carried out it should, however, employ the low-erosion ablative-modified ammunition which is currently employed in all program testing.

The effect on Vascomax 300 of 15 burst shots of ablative ammunition is shown for an exit ring in Figure 38 and entrance ring in Figure 39. Changes in the exit ring surface are of about the same size scale as they were with non-ablative ammunition but the shape of the surface "cracks" appears desirably rounded rather than sharp. The entrance ring surface is almost smooth as was the case for 4340 steel entrance rings.

Figure 40 shows qualitatively that the effect of firing on the surface of Vascomax 300 is a softening rather than the hardening found for 4340. This is as expected since the maraging steels form a soft nickel martensite on cooling from high temperatures. It is possible that a very desirable high

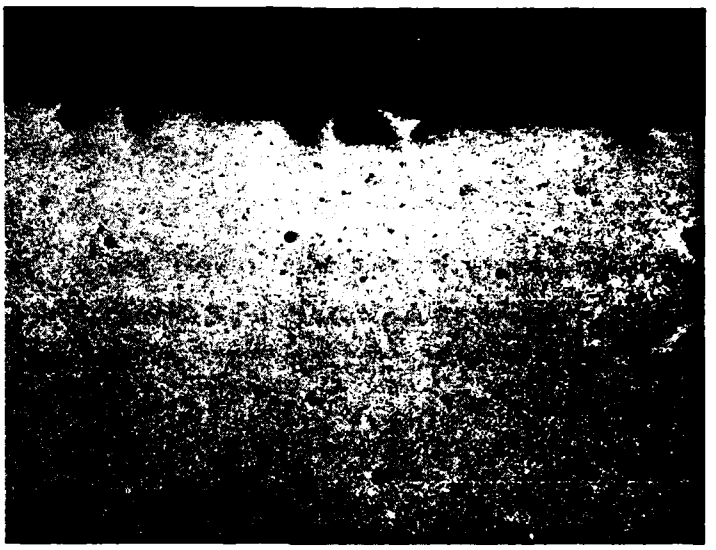

Figure 38 VASCOMAX 300 EXIT RING CROSS-SECTION AFTER 15 "BURST" SHOTS WITH ABLATIVE AMMUNITION (80X)

Figure 39 VASCOMAX 300 ENTRANCE RING CROSS-SECTION AFTER 15 "BURST" SHOTS WITH ABLATIVE AMMUNITION (80X)

AD-A131 118 HEAT TRANSFER AND EROSION IN THE ARES 75MM HIGH VELOCITY CANNON VOLUME 2(U) ARES INC PORT CLINTON OH F A VASSALLO ET AL. OCT 77 DAAA09-76-C-2082 2/2

UNCLASSIFIED F/G 20/13 NL

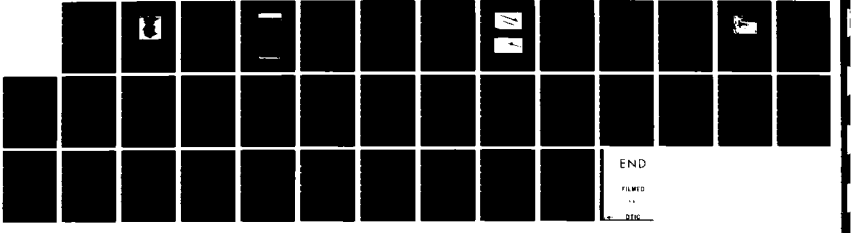

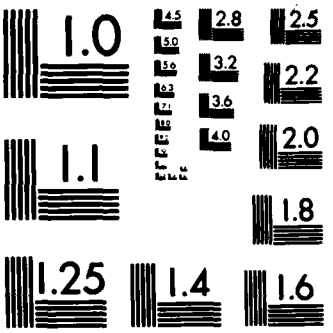

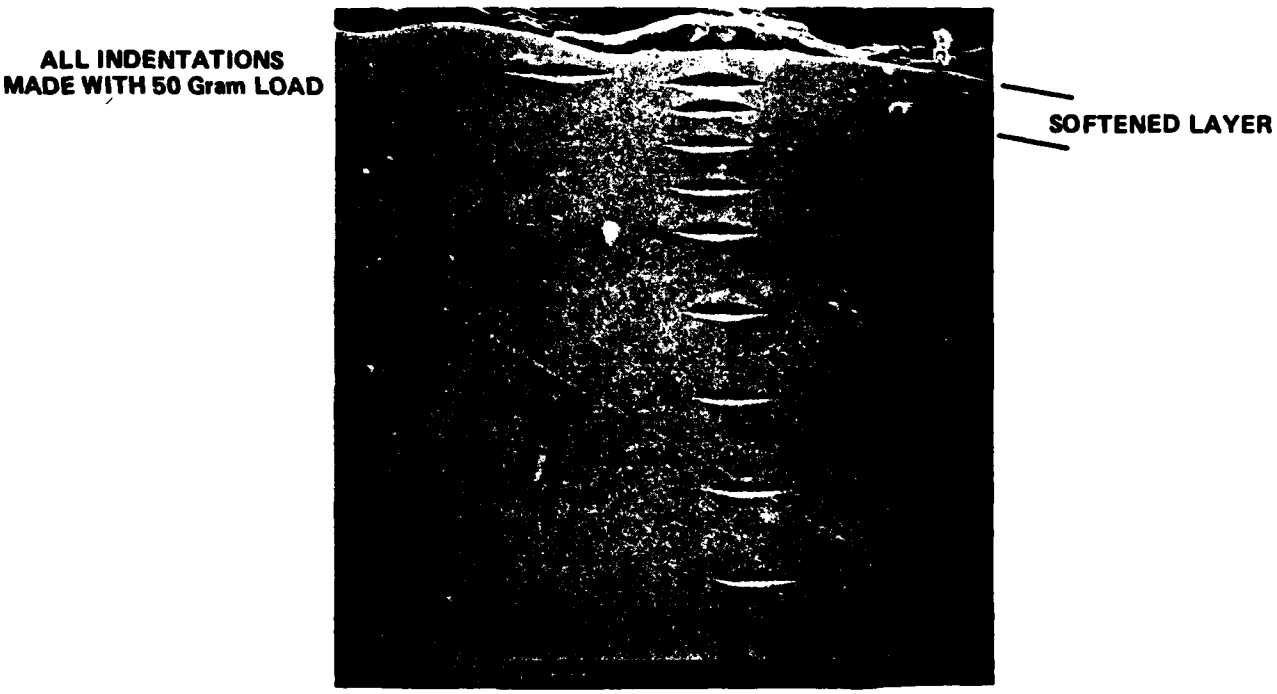

Figure 40 VASCOMAX ENTRANCE RING CROSS SECTION SHOWING SURFACE SOFTENING AFTER 15 SHOTS SEM

fracture toughness in the surface layer and at the "crack" tips would result from such softening.

c. Extended Short Barrel Firing Experience

A Vascomax 300 short barrel at Ares has fired over 500 rounds to date. Inspection indicates that crack depth is much less than that which could be calculated by linear extrapolation of the rate of growth implied in Figures 37 and 38 above where the depth reaches about four mils in 15 to 19 shots. This observation supports the view that surface crack initiation and early growth may be dominated by thermally induced processes while the later cyclic crack growth rate is of a lower magnitude, more simply dependent upon stress and material properties as indicated by equation (2) given previously.

2. Low Carbon Steel Liners

As alluded to previously, pure iron or low carbon steel liners should have extremely high fracture toughness such that cyclic crack growth should be extremely slow. In addition, crack initiation should not take place by the mechanism of hard martensite formation previously described for steels containing 0.4 percent carbon.

In brief, testing of short barrel insert rings found that:

1. A 1010 steel exit ring was of insufficient yield strength to remain in position during firing and no data on surface cracking were obtained;
2. A 1010 steel entrance ring consisting of a liner brazed into a Vascomax ring housing exhibited no hard, white martensite layer and no cracking when sectioned after five shots, as shown in Figure 41. Note, however, that neither 4340 nor Vascomax 300 entrance rings show surface cracking, so this result is not definitive.

Figure 41 LOW CARBON (1010) STEEL ENTRANCE RING NO. VII SECTION SHOWING NO CRACKING AFTER FIVE SHOTS (130X LIGHT MICROSCOPE, NITAL ETCH)

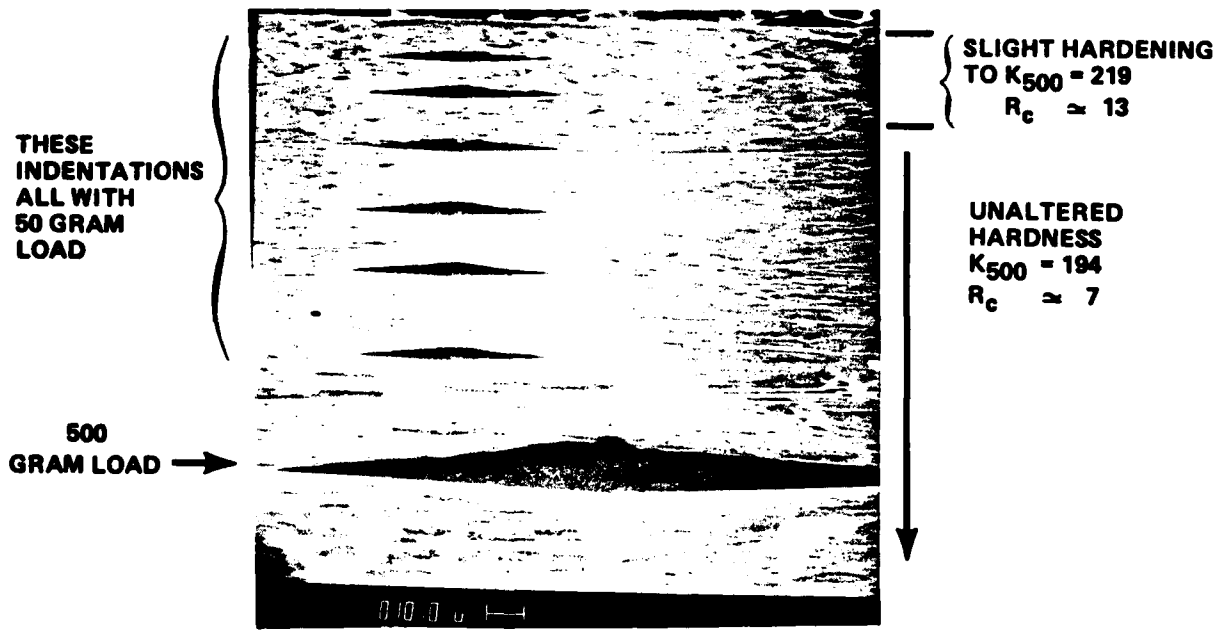

Figure 42 SAME SPECIMEN AS ABOVE SHOWING LITTLE INCREASE IN MICROHARDNESS NEAR SURFACE (500X SEM)

It may be seen in Figure 42 that surface hardening is very slight after five shots. There is, however, evidence of some surface microstructural change in both Figures 41 and 42 and substantial further testing will be required to establish whether any carbon is picked up from the propellant gases. Such carbon pickup has been observed in some steel cannon tubes. The surface hardness shown in Figure 42 is roughly equivalent to a yield strength of 60,000 psi which would indicate very high fracture toughness.

3. Main Barrel Fatigue

a. Surface Cracking

The surface cracking seen in 4340 short barrel exit rings would be expected to continue into the adjacent entrance of the main barrel which is fabricated of 4340 steel. No insert rings have been installed in the main barrel to date but photographs of the bore surface supplied by Ares have been reviewed at Calspan. These photographs show the expected surface cracking and heat checking of the type typically seen in unplated carbon steel cannon bores.

Crack growth should proceed more slowly in the main barrel than it would in the exit end of a 4340 short barrel because stress intensity is somewhat reduced due to increased wall thickness and decreased peak pressure, and fracture toughness is much increased due to the fact that the main barrel is not heat treated to 180,000 psi yield strength but is tempered down to a yield strength level near 150,000 psi. The actual crack growth rate remains, however, to be documented by sectioning a main barrel at several points along its length.

b. Extended Main Barrel Firing Experience

A 4340 main barrel has accumulated over 700 rounds at Ares with nc evidence of severe crack growth. This suggests that, as in the case of the short barrel, the surface crack penetration found initially slows to much lower growth rate as firing goes on.

4. Summary of Fatigue Considerations

Observations of surface crack depth in test rings which have fired say five to twenty shots indicate that the 18 percent nickel maraging steels are superior to conventional gun steels such as 4340 with respect to crack initiation and early growth. Extended firing experience with a Vascomax 300 short barrel and a 4340 main barrel indicates that the cyclic crack growth rates seen in the first twenty shots are primarily thermally induced and that these rates decline markedly as the cracks deepen slightly when firing is extended to several hundred rounds. Fracture toughness data indicate that current maraging steels are, at any given yield strength level, superior to conventional steels in resistance to crack growth. This appears to be supported by the extended firing experience at Ares where both the 4340 main barrel and the more highly stressed Vascomax 300 short barrel appear to be capable of meeting a fatigue life goal of 2000 rounds.

If improvement in fatigue life is found necessary, special high quality grades of 4340 or similar steels may eventually prove to be the best choice for the main barrel application. For example, electro-slag-remelted (ESR) 4340 steel exhibited no greater erosion resistance than did aircraft quality 4340 but is said to have improved fracture toughness due to better control of inclusion content and size, lower oxygen and sulfur content, smaller grain size and less directionality in strength properties. It is believed that Watervliet Arsenal personnel may have pertinent data on improvements in fracture toughness and fatigue life in ESR steel tubes. It would be readily possible to obtain crack initiation data suitable for direct comparison with regular grade 4340 by testing the ESR grade as a short barrel exit ring.

Autofrettaging to place the bore surface in compression is known to be effective in slowing crack growth in guns where improvement in fatigue life is sought without weight (wall thickness) increases. Autofrettaging can be viewed as a markedly reducing ΔK and hence db/dN in equation (2) given previously. Available data on the effects of autofrettage in high strength steels should be reviewed carefully before deciding to employ this technique.

Additional study of crack initiation and growth in high-strength steel gun bores can be efficiently carried out by means of insert rings subjected to a combination of actual firing and firing stress simulation. In this way the crack growth rate as a function of depth could be determined for any individual material, plated material, or liner candidate of interest.

E. LINER TESTS

1. Tantalum Liner

The tantalum-2 1/2% tungsten liner was subjected to three test firings (Shots 7, 8, and 9). The first, utilized a test round containing 530 gms. less propellant. This was for the purpose of investigating the behavior of the liner under less than the maximum pressure. Actual chamber pressure in this test was 36,000 psi and no noticeable deterioration of the liner was evident, although some forward motion of the liner in the housing was observed as permitted by a length tolerance allowed between liner and short barrel at the exit end. The liner was then subjected to two standard shots. After the second of these shots, inspection of the fit between liner and housing at the entrance end revealed a gap of 0.002-0.003 inches to be present. At first, it was believed that gun gases had gotten behind the liner, collapsing it as the bore pressure later decreased. Later review of the temperature history measured for the liner, however, where average liner temperatures of nearly 300°F were found, suggested that compression of the liner after firing may have been induced by its thermal expansion.

Diametrical expansion of the liner at a rise of 230°F would be as much as 0.0025 in. Because the relatively soft liner was already near its elastic limit through the heat shrink fit, this expansion would all result in strain beyond the elastic limit and on cooling would result in a measurable gap. Lack of contact between liner and housing in later shots could result in higher liner temperature due to gas flow behind the liner and, hence, correspondingly greater thermal expansion. The actual condition of the liner after test and demonstration of loss of interference is shown in Figure 43 . As shown, removal of the liner after test presented little difficulty. The

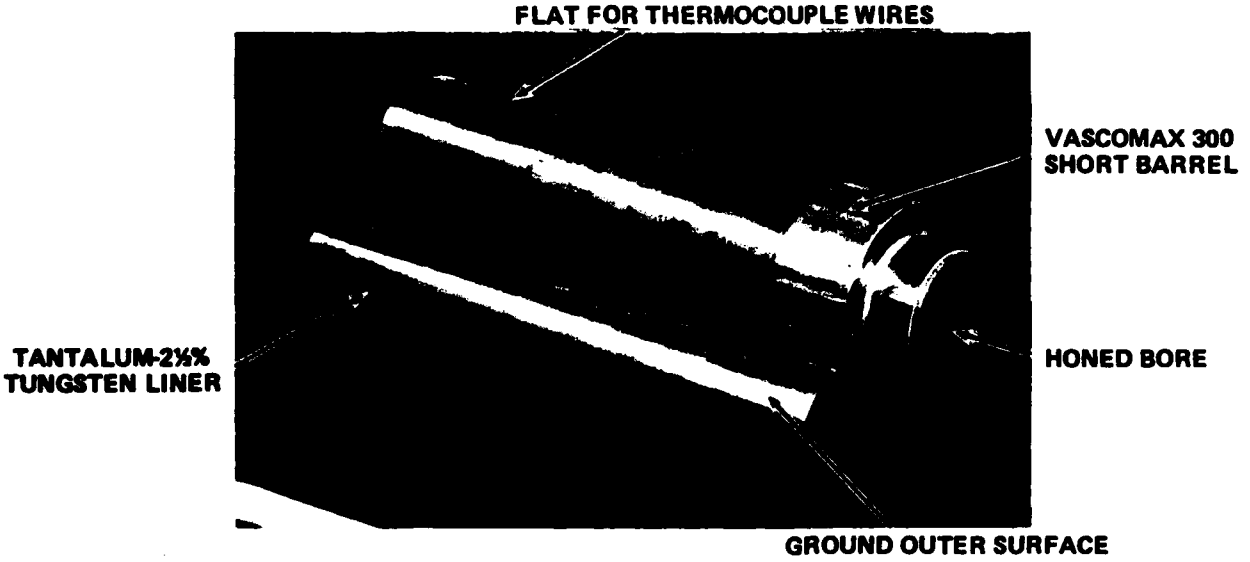

BEFORE HEAT SHRINK ASSEMBLY

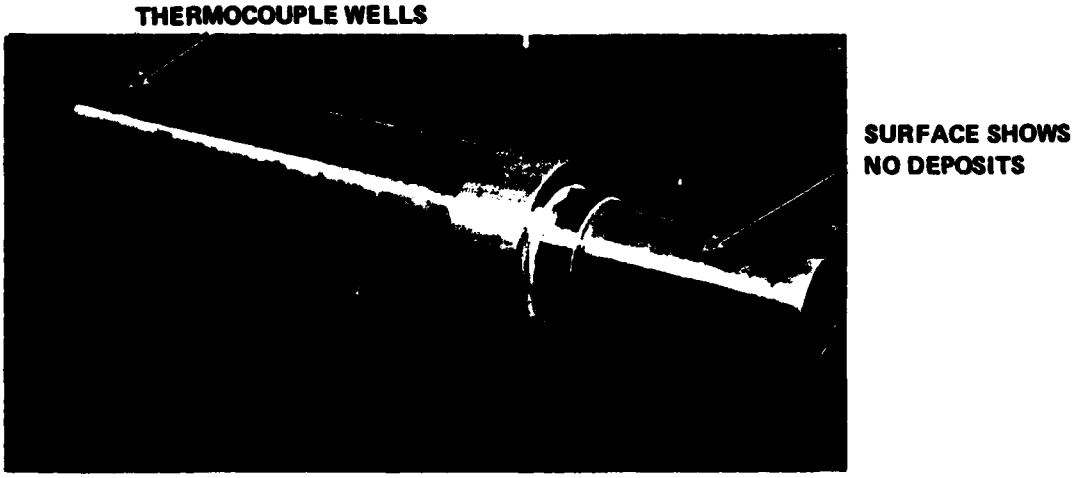

DURING REMOVAL AFTER FIRING

Figure 43 SPECIAL VASCOMAX 300 SHORT BARREL AND ASSOCIATED TANTALUM-2½% TUNGSTEN LINER

ground outer surface showed no significant deposits, although some minor indication of propellant gas leakage at the ends was noted. As anticipated, negligible erosion of the liner was indicated by inspection of the erosion indexing scribe marks.

Failure of the liner to maintain interference with the housing is primarily a consequence of its very low yield strength. Recall that the initial desire to fabricate a tantalum-10% tungsten was compromised to only 2 1/2% tungsten in order to secure a cost-effective test liner. Had a tantalum-10% tungsten liner been used, its increased yield strength would have allowed it to survive the single-shot tests without loss of interference. On the other hand, under burst fire conditions, due to increased heating and temperature, it too would lose interference and hence, positional stability. For this reason, and because excellent erosion performance was indicated in these tests, some future effort should be devoted to investigation of means by which the liner may be fixed in the housing. Vacuum brazing or explosive forming are prime candidate methods by which this may be achieved. Study of these techniques has been beyond the scope of the present study but is recommended for later work.

2. Replaceable 4340 Liner

Preliminary proof tests of the replaceable liner-housing assembly were conducted in several full charge firings in the single-shot fixture (shots No. 42, 43, 44, and 45). The liner was removed and inspected after shots No. 42, 43, and 44 and found to be in nearly original condition with very minor erosion at the entrance end. No leakage in the area of the "O" rings was noted. Review of the temperature data taken on the liner in these shots indicated an average liner temperature rise of 38°F at the entrance end. Cooling of the liner due to contact with the housing was found to be about 1.5 °F/sec. Therefore, at high rate firing conditions, say 2 rds/sec, only little heat will be lost by conduction to the housing. Thus, liner thermal expansion is expected to approach 0.005 inches/shot in rapid fire, compared to less than 0.0015 inches/shot for the entire assembly. Although

the liner can tolerate this expansion without failure due to axial loading, it was considered prudent to investigate means of eliminating the resulting liner projection at the breech as shots are fired. In this direction, test number 45 was conducted with the liner shifted 0.040 inch forward relative to the housing. This firing was totally successful with no damage evident in either case or short barrel. Hence, it appears that thermal expansion for burst fire up to 10 rounds can readily be accommodated by reduction of liner length. This burst length capability should be sufficient for present weapon developmental efforts.

Present plans for this lined short barrel include shipment to Ares for rapid-fire evaluation of erosion and fatigue life.

IV. RAPID FIRE RESULTS

A number of heating/erosion tests were performed using the Ares 75mm rapid-fire test fixture. These tests were conducted at Ares and were attended by Calspan personnel.

The purpose of these tests was to gather heating and erosion data under burst-fire conditions in an effort to validate earlier Calspan predictive methods of Reference 2 and to obtain additional comparative erosion data in the expected weapon operational mode. For these tests, the instrumented short barrel discussed in Section II was installed in the Ares fixture as shown in Figure 44. Short barrel in-wall temperatures were obtained at the two instrumented short barrel locations shown; namely, 1.375 and 15.5 inches from the breech end. Additionally, the barrel external temperature at 145 inches from the breech end was measured.

A total of 34 shots were fired in the rapid-fire tests. Of these, 19 were non-ablative rounds having a 4 percent charge subload. The remaining were ablative rounds having the same charge but containing 100 gms. of Type I ablator. All rounds were loaded and supplied by AAI.

A. BARREL TEMPERATURES AND HEAT INPUT

Temperatures in the short barrel were obtained in all but Test No. 70 where loss of thermocouple signal took place. In most tests, 5 round bursts were attempted, but only one complete burst (Test No. 71) was obtained. Reduced temperature data derived for this test are shown in Figures 45 and 46 . Figure 45 shows the recorded temperature rise as a function of time as indicated by the in-wall thermocouple at the breech end of the short barrel. This thermocouple was located 0.030 inches from the bore. Although the temperature excursions shown are of some interest in establishing thermal gradient near the bore, the residual temperatures as indicated in Figure 45 are of most significance in that they determine the bore temperature and gross barrel thermal gradient at the time of firing. Furthermore, these can be used as a

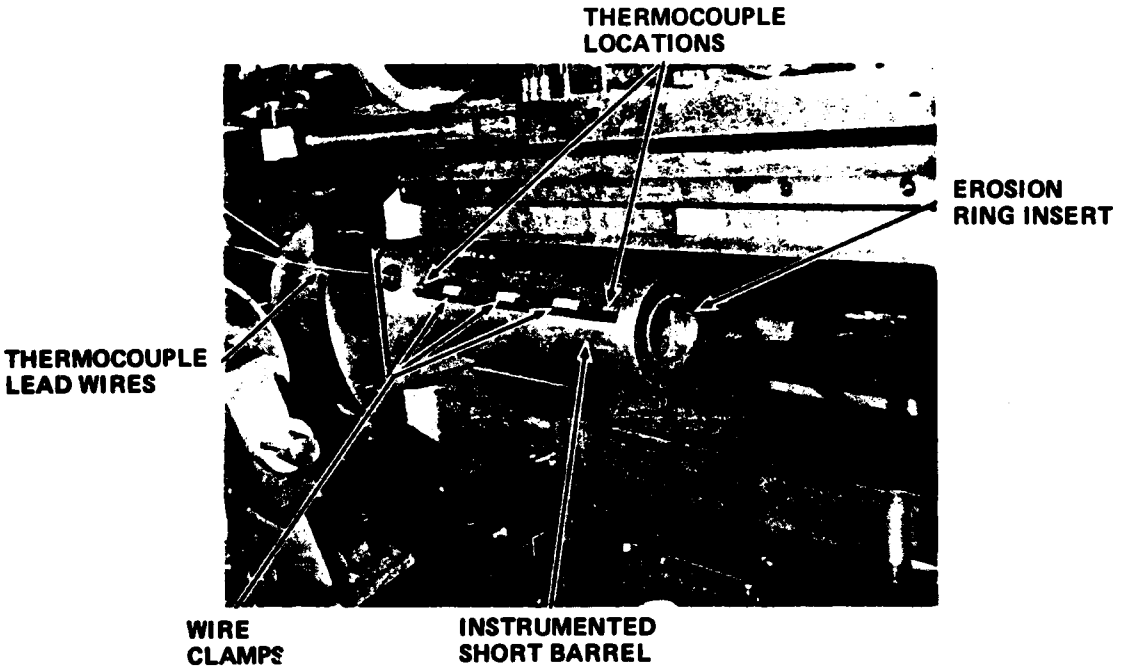

Figure 44 VIEW OF INSTRUMENTED SHORT BARREL AS INSTALLED IN ARES RAPID FIRE FIXTURE

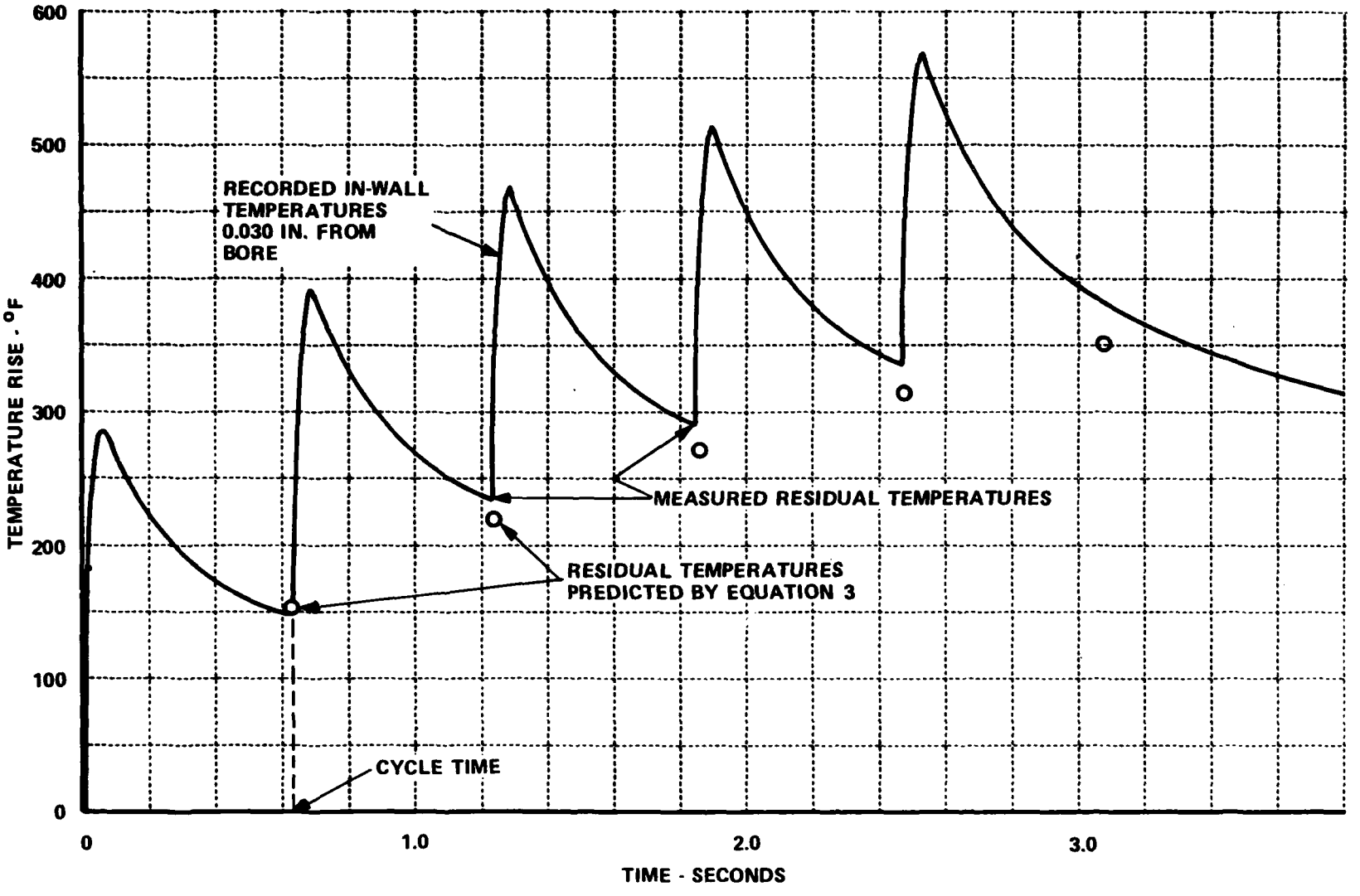

Figure 45 TEMPERATURE HISTORY DURING BURST FIRE AT ENTRANCE END OF SHORT BARREL (5 ROUNDS - NON-ABLATIVE)

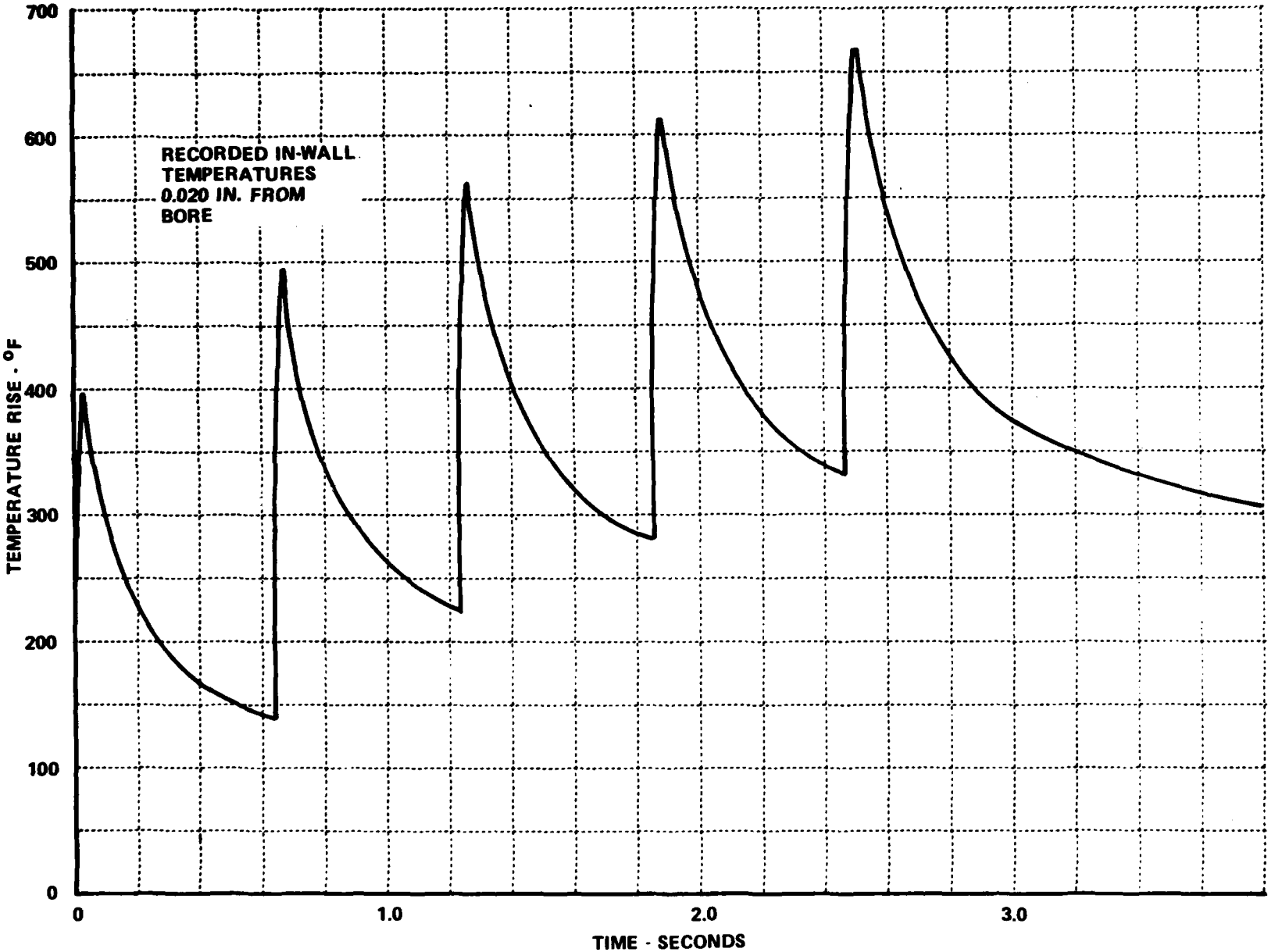

Figure 46 TEMPERATURE HISTORY DURING BURST FIRE AT EXIT END OF SHORT BARREL (5 ROUNDS - NON-ABLATIVE)

measure of the validity of the stress deformation analysis of Reference 1, where it was shown that no stress deformation failure of the Vascomax short barrel was likely in burst lengths up to 50 rounds. For these predictions, the residual temperature at the entrance was found to be given by the relation

$$T_R = \frac{170\sqrt{\frac{R}{120}N} + 9.5N + T_i}{(1 + 0.0405\sqrt{\frac{R}{120}N} + 0.0023N)} \qquad (3)$$

in which N is the number of rounds fired
R is the firing rate - rpm
T_i is the initial temperature - °F

Figure 45 demonstrates the excellent agreement between the test data and the predictions of this equation. Hence, one concludes that the stress deformation conclusions of the earlier work based upon predicted thermal gradient remain valid.

Analysis of the recorded temperature data results in bore heat input values as given in Table X. Comparison with the single shot results of Table VII discussed earlier indicates reasonable agreement except at the 145 inch location where considerably less heating was found in the rapid-fire tests. The slight subload of the ammunition used in the burst tests could account for minor differences in heating observed in the short barrel but would not be expected to account for the great difference in heating indicated at the muzzle end. One explanation, however, might be that the tube bore at the muzzle, having fired a large number (several hundred) of ablative rounds, has been "coated" irreversibly by ablative constituents as suggested by the earlier single-shot tests. Recall that those tests indicated a general lowering of heating in the muzzle area with successive shots. Here, the limited firings of the rapid-fire series may have been unable to eliminate the residual effect of these earlier ablative rounds. Another explanation is that the 4340 steel barrel at the bore surface has developed substantial surface oxide deposits the low thermal conductance of which provides similar insulation of the bore. In either situation, "aging" of the tube is needed to achieve the reductions in

TABLE X

BARREL HEAT INPUT DURING RAPID-FIRE TESTS

Test No.	Number Of Shots	Ammunition Type	Nominal Charge Weight Gms.	Heat Input/Shot, Btu/Ft^2 At Given Distance, In., From Breech		
				1.375	15.5	145
66	1	Subload-M26/M30	2110	89	95	47
67	2	Subload-M26/M30	2110	92	95	47
68	2	Subload-M26/M30	2110	94	94	47
69	2	Subload-M26/M30	2110	92	94	45
70	3	Subload-M26/M30	2110	--	--	42
71	5	Subload-M26/M30	2110	97	92	44
72	4	Subload-M26/M30	2110	92	89	46
73	1	ABL-M26/M30	2110	85	86	49
74	1	ABL-M26/M30	2110	82	85	52
75	1	ABL-M26/M30	2110	78	86	52
76	1	ABL-M26/M30	2110	79	82	52
77	1	ABL-M26/M30	2110	79	82	53
78	2	ABL-M26/M30	2110	78	84	47
79	2	ABL-M26/M30	2110	83	84	43
80	2	ABL-M26/M30	2110	72	87	46
81	2	ABL-M26/M30	2110	68	80	47
82	2	ABL-M26/M30	2110	81	81	45
AVERAGES		Subload-M26/M30		93	93	45
		ABL-M26/M30		79	84	48

heating . The number of "aging" rounds required is likely to be much less if the reductions are due to ablative deposits than due to protective oxide. Indeed, existence of protective surface oxide cannot be assumed in the weapon design because practical field application may involve use of new "unaged" barrels. Determination of factors leading to the tube heating reductions observed should, however, be made in order that appropriate account of such reductions may be made in future weapon design considerations. Future testing in this direction is planned.

Figure 47 illustrates the effect of this lowered heat input on predicted multishot temperatures compared with earlier predictions for the higher heating level of the standard M26 charge. As shown, the resulting average temperatures are significantly less than the earlier predictions of Reference 1. In fact, the temperatures are lowered to the extent that little loss of barrel strength should be anticipated at this location in the barrel in bursts up to 40 rounds. As discussed above, however, caution is advised in accepting the lowered heat input for general design purposes without further test confirmations.

B. EROSION

Through utilization of the instrumented short barrel and the ring insert technique, some evaluations of erosion were made during the rapid-fire tests. Both non-ablative ammunition and ablative ammunition having the subloaded M26/M30 charge were used in evaluations of erosion or Vascomax 300 and soft (LC) chrome plated test rings. Burst lengths ranged from a single shot to five rounds at a rate of about 100 rpm. Resulting erosion data are as presented in Table XI. Generally, it is found that results are in agreement with those of the single-shot tests. Erosion of the Vascomax entrance ring with non-ablative M26/M30 ammunition after seven shots was found to average 0.32 mils/shot compared with a single shot (3 round) measurement of 0.5 mils/shot. The difference in indicated erosion is most likely due to the 4 percent subload of the rounds used in the rapid-fire evaluations for which some bore heating reductions have already been mentioned. At the entrance to the short barrel, it is notable that the ablative component essentially eliminates

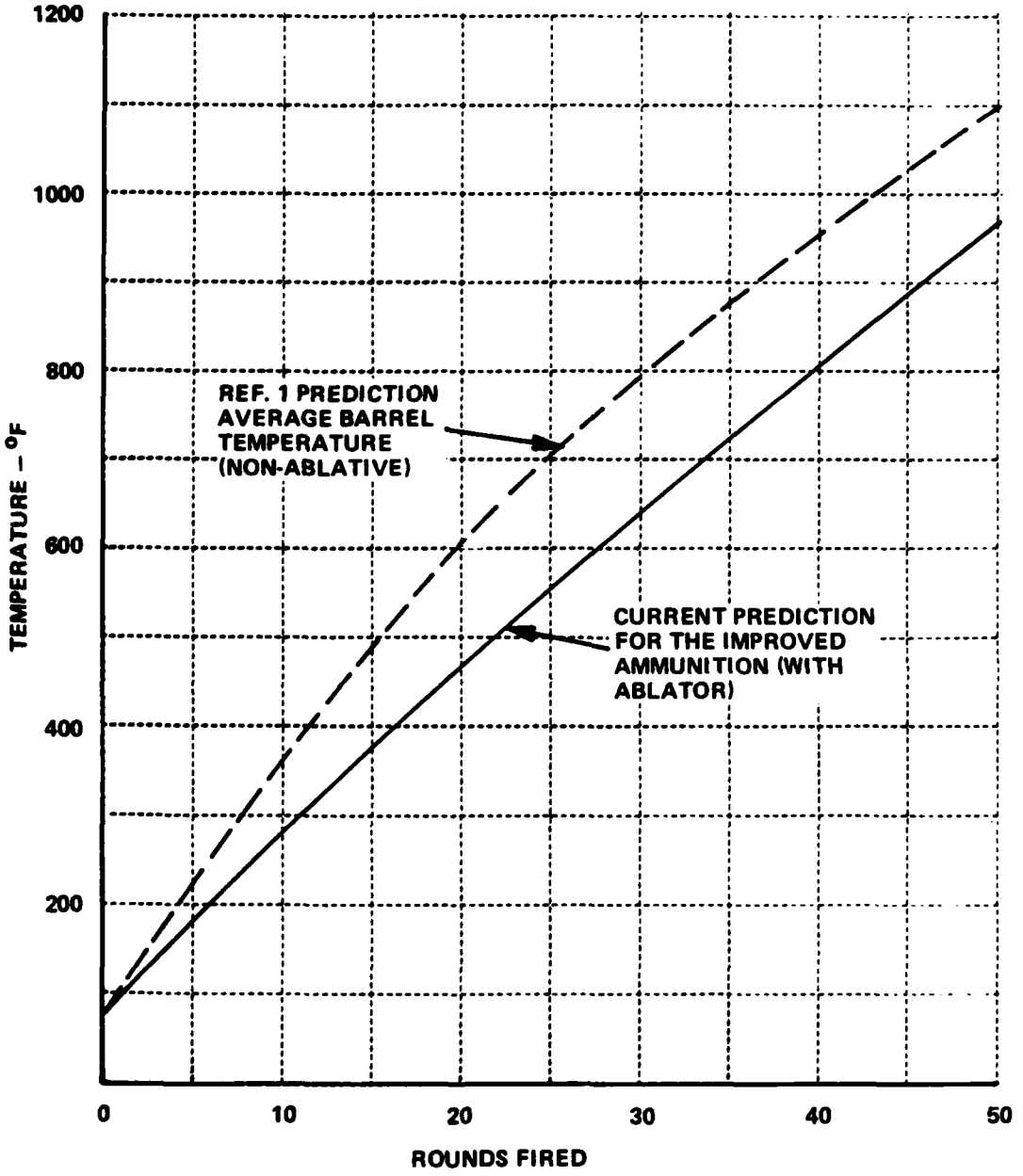

Figure 47 PREDICTED AVERAGE BARREL TEMPERATURES DURING RAPID FIRE AT 120 RPM – 145 INCHES FROM BREECH END OF SHORT BARREL

TABLE XI

RAPID-FIRE EROSION RESULTS

At Entrance of Short Barrel

Test Ring	Ammunition Type	Test Series	Diametrical Erosion Rate Mils/Shot	Comment
Vasco RXVI	Non-Ablative Subload-M26/M30	Single Shot Followed By Three Two Round Bursts - 7 Shots Total	0.32	Very Smooth Eroded Surface - No Cracking - Some Melting
Soft Chrome	Non-Ablative Subload-M26/M30	One Three, One Four, and One Five Round Burst - 12 Shots Total	None	Surface Condition and Adherence Excellent. Slight Washing of Vasco Substrate at Entrance Face.
Vasco RXIII	Ablative Subload-M26/M30	Five Single Shots, Five Two Round Bursts - 15 Shots Total	0.002	Thick Silica Surface Coating (1 Mil Thick). Underlying Surface Shows Slight Erosion. No Cracking

At Exit of Short Barrel

Vasco FI	Non-Ablative Subload-M26/M30	One Single Shot, Three Two Round Bursts, One Three, One Four, and One Five Round Burst - 19 Shots Total	0.011	Shows Axial and Circumferential Cracks. Some Checking and Pitting
Vasco FIV	Ablative Subload-M26/M30	Five Single Shots, Five Two Round Bursts - 15 Shots Total	0.000	No Measurable Erosion. Has Thin Adherent Silica Coating

erosion in this charge. Here, 100 gms. of the Type I ablator was used. Inspection of the ring after the 15 shot sequence indicated a 1 mil thick silica coating to be present on the surface. The presence of this type of coating was observed in the single-shot testing and is no doubt partially responsible for erosion reductions observed.

As expected, the low contraction "soft" chrome plated ring survived the burst testing with no measurable loss. As indicated, this test ring was exposed to 3, 4, and 5 round bursts of non-ablative ammunition. Critical examination after test indicated no change in surface condition or adherence as a result of the burst testing. The dark surface oxide and surface cracking experienced as a result of the single-shot tests were still in evidence but unchanged. This demonstrates superior performance and leaves little doubt that solution of short barrel erosion is possible through utilization of soft chrome. Further testing of this approach is planned for future work where more fully plated short barrels will be used.

Erosion conditions at the exit end of the short barrel are clearly less severe than at the entrance end. In fact, as suggested in the single-shot testing, the rapid-fire results also indicate that erosion at this location should impose little limitation on short barrel life whether or not the ablator is used. Basic reduction in the erosion at this end of the short barrel appears to result from the change in charge type and amount. Of course, addition of the ablative component helps rather than hinders erosion performance with the indicated result that erosion of Vascomax is essentially nil in 15 recorded shots.

In sum, the rapid-fire tests show that erosion throughout the short barrel will be very minimal with use of ablative ammunition having the M26/M30 charge combination. Change in charge type or weight could, however, alter this conclusion. Therefore, one must avoid indiscriminate change in charge without consideration of effects on erosion.

REFERENCES

1. Vassallo, F.A., "Heat Transfer and Erosion in the Ares 75mm High Velocity Cannon," Calspan Report No. VL-5645-D-1, (For Ares, Inc.), October 1975.

2. Vassallo, F.A., "Mathematical Models and Computer Routines Used in Evaluation of Caseless Ammunition Heat Transfer," Calspan Report No. GM-2948-Z-1, June 1971.

3. Adams, D.E., Brown, W.R., Sterbutzel, G.A., and Vassallo, F.A., "Design Studies of the XM140 Barrel, Volume II," Calspan Report No. GA-2446-Z-1, October 1967.

4. Hall, R.C., "Processing the Maraging Steels," Metal Progress, p. 41, June 1974.

5. Davidson, T.E., Throop, J.A., and Reiner, A.N., "The Role of Fracture Toughness and Residual Stresses in the Fatigue and Fracture Behavior of Large Thick-Walled Pressure Vessels," Watervliet Report No. WVT 7148, October 1971.

6. Zackay, V.F., Parker, E.R., Fahr, D., and Busch, R., Trans, ASM, Vol. 6, p. 252, 1967.

APPENDIX

In the course of the work, some Calspan effort was devoted to study of brazing techniques as applied to maraging steels. Results of that study to date are given in this Appendix. Also described in some detail is a simplified analysis of maximum aiming corrections needed to overcome the thermally induced barrel bending associated with non-uniform cooling of the barrel cross-section in field use of the weapon.

A. BRAZING STUDIES

Calspan has shown certain alloys such as low carbon steels to be very promising as erosion-resistant liners for the maraging steel short barrel. Of the possible methods of bonding such liners to the short barrel, brazing would be expected to be relatively straightforward, but Calspan's efforts to braze liners into Vascomax 300 erosion insert test rings have not been entirely successful to date. The main difficulties arise in the areas of thermal size change differences and in securing wetting of the Vascomax alloy by the molten braze. These and other aspects of the brazing experiments conducted to date are discussed in turn below.

Considering first the selection of brazing temperature, the heat-treating characteristics of the Vascomax 300 dictate that the brazing temperature must lie in the range 1400°-1750°F. The region below 1400°F (but above the 900°F normal age-hardening temperature of the alloy) is ruled out because austenite reversion occurs in this range. This reverted austenite, in contrast to the age-hardenable austenite obtained on solution-annealing above 1400°F, does not respond well to the subsequent aging treatment at 900°F.

An upper bound on practical brazing temperatures is imposed by increasing diffusion rates which promote grain growth with attendant mechanical property deterioration. This leaves, conservatively, the range 1500°-1750°F in which the only effect of heating on Vascomax 300 is to form the normal, heat-treatable austenite phase which responds extremely well to a subsequent age-hardening treatment at 900°F.

Braze alloys possibly suitable for use in the range 1500°-1750°F can conveniently be categorized as follows:

1. General purpose "silver solders," i.e., American Welding Society type Ag-1 alloys containing silver, copper, zinc and cadmium.

2. Silver-copper base alloys formulated primarily for vacuum brazing, i.e., free of high vapor pressure elements such as zinc and cadmium.

3. Special vacuum brazing alloys containing "wetting enhancers" to facilitate good wetting of stainless steels and of other alloys which are difficult to wet.

Representatives of types (1) and (2) brazes were tried initially under flux-brazing, air-atmosphere conditions on rings and small coupons of Vascomax 300 and 1020 (low carbon) steels; in some cases pure nickel and 18-8 stainless steel coupons were also tested in contact with the braze alloy in order to study wetting tendencies. Pure nickel has an easily-reduced oxide layer and is, therefore, aggressively wetted by most braze alloys under a wide range of furnace atmosphere conditions. Stainless steels containing chromium are, conversely, difficult to wet due to the resistance of chrome oxide to "reducing" furnace conditions. The use of small flat coupons also facilitates control of the clearance at the braze joint such that wetting effects can be distinguished at least reasonably well from effects due to joint clearances existing at the brazing temperature.

The first series of brazing trials was done with fluxes in an air-atmosphere furnace primarily because Calspan hoped to fabricate at least one 1020 steel-lined Vascomax insert test ring by this simple technique. (It was assumed at the outset that when the time came to line a complete short barrel-it would be necessary to employ suitable vacuum or other protective-atmosphere brazing facilities). These initial trials of "silver solder" with borax-based and other fluxes resulted in moderately strong joints between 1020 steel and Vascomax 300 but when these joints were pulled apart and examined microscopically, substantial percentage areas of flux inclusions were invariably found.

Consultation of pertinent literature reveals that a few investigations have recognized this. Reference A1 notes that even under the most favorable and carefully controlled laboratory conditions it is not possible to produce braze joints which are free of flux inclusions. Joints which appeared perfectly filled when inspected externally turned out (on destructive examination) to contain ". . . large numbers of defects. The use of pre-placed foil filler metals was . . . helpful in overcoming this" but only to the extent that foil ". . . produced small, regularly shaped defects whereas capillary flow (or wire braze) produced very erratic joint quality, defect size, and defect distribution." Calspan noted little improvement in a brief trial of pre-placed foil braze in flux brazing.

One 1020 steel/Vascomax 300 "rear ring" assembly was flux-brazed (before turning to vacuum brazing) and put aside for future single-shot proof testing. In view of the above-discussed findings, the probable braze joint quality in this ring is considered to be marginal at best.

Vacuum brazing totally avoids the flux inclusion problem, but it is known that at the brazing temperatures of interest the best practical vacuums do not dissociate the more stable oxides of chromium, titanium, aluminum and the like. Vascomax 300 contains no chromium but does contain 0.6 percent titanium, 0.1 percent aluminum, 0.02 percent zirconium, 0.05 percent calcium, and up to 0.1 percent silicon, all of which might contribute to difficult wetting in vacuum brazing.

A paper by Bennett, et. al.[A2] prompted trial of certain brazes of the (3) category alluded to previously; these authors present very useful information on the problem of securing complete wetting in vacuum brazing two high chrome steels; namely, a 21Cr--6Ni--9Mn--0.3N alloy and ordinary type 304 (18Cr--8Ni) stainless steel. In the absence of similar data on Vascomax 300, the chrome in these alloys can be presumed to cause wetting

---

*45% silver, 15% copper, 16% zinc, and 24% cadmium, i.e., American Welding Society grade BAg-1 alloy.

problems very similar to those engendered by the titanium and other elements listed above for Vascomax 300. Bennett and his co-workers first conducted extensive wetting tests in which a wetting index was obtained by multiplying the measured wetted area on a standardized coupon/braze perform assembly by the cosine of the observed contact angle, according to the method of Feduska.[A3] In these tests a wetting index of 0.05 was considered good and values above 0.10 indicated excellent wetting.

The majority of the tests of Reference A2 employed copper-silver eutectic (72Ag + 28Cr) with various elements added to enhance wetting; most of the alloys are commercially available and many are useful in the temperature range which must be employed on Vascomax 300. Pertinent results may be summarized as follows:

1. Wetting index increases strongly with temperature for most braze alloys but not for silver-copper eutectic; the wetting index for this braze on 304 stainless was only about 0.003 at 1650°F.

2. Palladium is a strong wetting enhancer such that the index on 304 stainless steel was 0.06 at 1750°F for the braze alloy 58Ag--32Cu--10Pd and was 0.11 at the same temperature for the braze alloy 65Ag--20Cu--15Pd.

3. Manganese and tin are wetting enhancers such that the index on 304 stainless was above 0.10 at 1560°F for 57Ag--33Cu--7Sn--3Mn alloy.

4. Four commercial braze alloys containing lithium or indium wetting enhancers failed to wet the subject steels.

5. Gold-based and certain other brazes gave good wetting but the temperatures required were over 1800°F and tendencies to penetrate grain boundaries were sometimes pronounced.

Considering both wetting data and the results of careful metallographic studies, the authors concluded that the silver-copper-palladium alloys were well suited for brazing austenitic stainless steels in the range 1650°F to 1830°F. For the range below about 1540°F, which was of special interest to the authors, the 57Ag--33Cu--7Sn--3Mn alloy was the only one exhibiting sufficient wetting.

Vacuum brazing trials in Calspan's small cold-wall vacuum furnace (at pressures below 5 X 10^{-5} torr) confirmed that Vascomax 300 presents about the same degree of difficulty in wetting as does 18Cr--8Ni stainless steel. Silver-copper eutectic without a wetting enhancer did not wet well. A source for the silver-copper palladium alloys of Reference A2 is the Western Gold and Platinum Company of Belmont, California. Their 58Ag--32Cr--10Pd (Palcusil 10) alloy was obtained as one mil foil and tested on a Vascomax 300/1020 steel coupon assembly. Good wetting and bonding was achieved at 1650°F and it is planned in the future to vacuum braze an erosion test ring assembly using this alloy. Examination of the 1020 steel side of the brazed joint (after destruction) indicates, however, that Palcusil 10 reacts somewhat aggresively with the low carbon steel at 1650°F. To reduce the amount of reaction it is planned to lower the brazing temperature to 1600°F, and to keep the time above the braze solidus temperature (1520°F) to a minimum. To ensure complete wetting under these conditions, Calspan has had the Vascomax 300 rings brush-plated with 0.2 mils of nickel by Dalic Sifco Metachemical Company of Cleveland, Ohio.

Another much-used type vacuum brazing alloy tried briefly was Nicobraze 10, a nickel-phosphorous alloy produced by Wall Colmonoy Corporation of Detroit, Michigan. Excellent wetting and bonding was obtained at 1700°F but destructive examination revealed a very brittle joint as might be expected with phosphorous.

While the wetting problem reduces to a matter of careful selection of braze alloy and perhaps of pre-plating of parts, the thermal size change behavior of Vascomax 300 has presented unexpected difficulties which still remain to be more fully explored. Both Vascomax 300 and low carbon steel

are known to transform to the austenite phase above 1200°F with a large size change as shown in Figure A1. Despite differences in these size changes and in the thermal expansion coefficients (considered apart from the phase changes) analysis of Figure A1 indicated that, given proper initial clearance between the O.D. of the 1020 steel liner and the I.D. of the Vascomax ring, the joint clearance at braze temperature could be three mils on a side or less. Very strong joints can generally be made at clearances of this order and if joint strength is sufficient, the tensile stresses arising below 400°F (when the Vascomax expands, see Figure A1) will be tolerated. Of course, good strength will also be required of the braze joint during the ballistic cycle.

In the first attempt to furnace braze a Vascomax 300/1020 steel insert ring, the initial clearance was made 6.5 to 7.0 mils on a side. On examination, the joint was found to be imperfectly filled, the width of the joint varied from less than one mil to more than five mils, the O.D. of the outer Vascomax ring was as much as ten mils smaller than it was before brazing, and there was substantial out-of-roundness in both the Vascomax 300 and the 1020 liner.

As a result of these findings, it was clear that unexpected size changes were occurring; accordingly, a Vascomax ring was machined and measured expressly as a size-change test piece and was then subjected to five consecutive cycles above 1500°F in the vacuum furnace. Results were as tabulated in Table A1.

In short, it is seen that starting with new, as-received, annealed round stock, the O.D. and I.D. increase and the height decreases every time it is heated above 1500°F. Moreover, the diameter increase reaches a maximum along one particular "azimuth" while it is almost nil along another azimuth located approximately 90° from the first.

Taking into account all size-change observations to date, the following picture emerges:

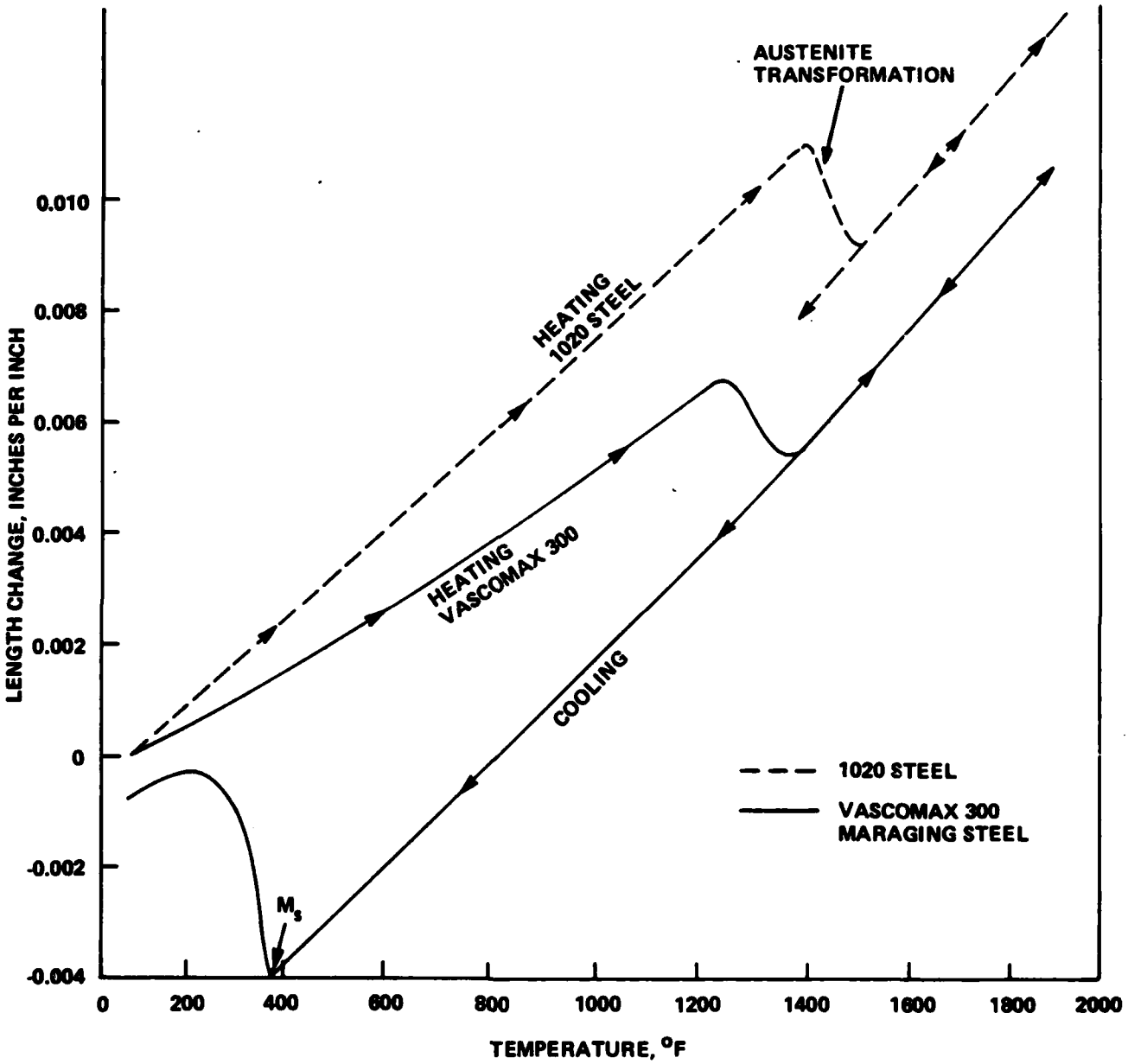

Figure A1 THERMAL SIZE CHANGES IN VASCOMAX 300 AND LOW CARBON STEEL

TABLE A1

IRREVERSIBLE THERMAL SIZE CHANGES IN VASCOMAX 300

Treatment	Change in 3.5 Inch Outside Diameter		Change in 3.0 Inch Inside Diameter		Change In Height 1.1" Nominal
	Direction A	Direction B	Direction A	Direction B	
1/2 Hour at 1575°F	+3.5 mils*	-0.5	+3.5	0.0	-2.0
1/2 Hour at 1600°F	+5.5	-0.5	+6.5	-0.5	-3.5
1/2 Hour at 1600°F	+8.5	+1.5	+8.0	+1.0	-5.0
1/2 Hour at 1600°F	+10.5	+1.5	+12.0	+1.0	-5.0
1/2 Hour at 1700°F	+12.5	+1.5	+13.0	+0.0	-8.0

*All dimension changes are cumulative; direction A vs. B indicates out-of-roundness and maximum vs. minimum size changes at different "azimuths."

1. When Vascomax 300 is heated for a brief time to 1500°F (but not higher) some of the austenite formed is of the type (discussed previously) which does not transform well to martensite on cooling below 400°F; to the extent that it does not transform to martensite, it does not expand, and the net effect is a diameter shrinkage at room temperature. This takes place to some extent whether the stock was, before heating to 1500°F, in the as-received, solution-annealed soft martensite condition or in the age-hardened (hard) martensite condition. This shrinkage may differ in different azimuths.

2. When Vascomax 300 is heated (see Table A1) to 1575°F or higher there is formed essentially 100 percent austenite of the type which later transforms completely to martensite, and no net diameter shrinkage takes place. Calspan's tests show, however, that with each excursion of 1575°F or higher, there is an irreversible and directional expansion such that upon cooling to room temperature a previously round part will be as much as 1.2 mils per inch larger along one azimuth, but along an azimuth at 90° to the first, the net expansion will be about nil. In the axial direction, there will be a net contraction of roughly 2.0 mils per inch.

In view of the above, it is believed necessary to minimize distortion of the Vascomax member by pre-heating the stock once to 1700°F. Furthermore, the development of large joint clearances due to the residual distortion of the Vascomax at the brazing temperature can be prevented by fitting a Vascomax mandrel inside the 1020 liner ring such that the 1020 member will be "captive" between two Vascomax 300 rings. Work in this area is continuing.

B. THERMALLY INDUCED BARREL BENDING

In this work, some consideration was given to a suggested problem area concerning thermally induced barrel bending and its effect on weapon accuracy.

It is known that if a gun barrel has a temperature variation around its circumference, forces will tend to bend the barrel due to differential thermal expansion. Guns presently in the field are known to have significant aiming errors under solar heating conditions where the top of the barrel is hotter than the bottom. A knowledge of the magnitude of displacement of the Ares 75mm muzzle is desired to aid gun fire control design. To obtain information on the barrel bending and muzzle displacement, some estimates and measurements have been made of the magnitudes to be expected. These are presented in the following.

The magnitude of bending is dependent on the temperature distribution around the barrel. As a first approximation, the barrel can be assumed to be at one temperature over half of its circumference and a different temperature over the other half of its circumference. The bending radius, R, under this circumstance is given by

$$\frac{1}{R} = \frac{A\alpha(T_2 - T_1)(D_o + D_1)}{4\pi I_c} \qquad A1$$

where α is the coefficient of thermal expansion of the barrel. (Derived from a rectangular section solution given by F.R. Shanley, Strength of Materials, McGraw-Hill Book Company, Inc., 1957, p. 320).

For the barrel, the following apply:

$$A = \frac{\pi(D_o^2 - D_i^2)}{4} = \text{Tube Cross-Sectional Area} \qquad A2$$

$$I_c = \frac{\pi}{64}(D_o^4 - D_i^4) = \text{Bending Moment of Inertia} \qquad A3$$

Substituting equations A2 and A3 in equation A1 and rearranging, results in the following solution for the radius of curvature of the barrel:

$$R = \frac{\pi(D_o^2 + D_i^2)}{4\alpha(T_2 - T_1)(D_i + D_o)} \qquad A4$$

Inserting the values for the Ares 75mm in equation A4 provides the following relation for barrel radius of curvature, R, as a function of the temperature difference between the two halves of the barrel, $T_2 - T_1$.

$$R = \frac{4.5 \times 10^5}{T_2 - T_1}, \text{ R in inches, } T_2 - T_1 \text{ in } °F \qquad A5$$

The bend calculated from equation A5 would cause a displacement of the muzzle from a straight line by an amount given by:

$$\delta = \frac{4.5 \times 10^5}{T_2 - T_1}\left[1 - \cos\frac{L(T_2 - T_1)}{4.5 \times 10^5}\right], \quad \delta \text{ and } L \text{ in inches, } T_2 - T_1 \text{ in } °F, \text{ the angle in radians} \qquad A6$$

where L is the unsupported length of barrel.

Required for the completion of the estimate of muzzle deflection is the temperature difference between the two halves of the barrel. To determine the limits of muzzle deflection, three heat transfer conditions were considered: natural convection, forced convection (wind), and liquid cooling (rain). Conditions which would cause most severe bending were calculated. That is, a barrel was assumed to be heated to 1000°F (approximately that produced by a 40 round burst)* and then allowed to cool according to the relation

$$\frac{\Delta T}{\Delta T_o} = e^{-\frac{4hD_o\tau}{c\rho(D_o^2 - D_i^2)}} \qquad A7$$

*Standard-M26 (Non-Ablative).

where ΔT_o is the initial temperature rise above ambient, ΔT is the temperature rise above ambient at time τ, h is the heat transfer coefficient (combined convective and radiative), and c and ρ are the specific heat and density of the barrel material, respectively. Equation A7 was solved by stepping time forward and adjusting h for the calculated temperature level. Average values of heat transfer coefficient were determined for opposite halves of the barrel.

For natural convection, the convection heat transfer coefficient was taken from R. Herman, NACA TM 1366, November 1954. The calculated temperatures for the top and bottom halves of the barrel are as shown in Figure A2.

The maximum temperature difference under these conditions would be 22°F which, by equation A6 with a free barrel length of 50 in., would cause a muzzle deflection of 0.06 in. Numerical calculations have indicated that conduction around the barrel would not be significant in this case and therefore the calculated deflection of 0.06 inches should be a good approximation of what may be expected in the field.

For liquid cooling (rain), the heat transfer coefficient on the region struck by the rain would be so great that the water would boil off as fast as it struck the surface (c.f. Gebhart, B., Heat Transfer, McGraw-Hill Book Company, Inc., 1961, p. 285). Therefore, the cooling rate is limited by the rainfall rate. A rainfall rate of 1.9 in./hr. corresponds to 10,000 Btu/hr.-ft^2. This value was used to represent a very high rainfall rate. Using this heat transfer rate for the top half of the barrel results in the temperature shown in Figure A2.

The maximum difference between the rain cooled top and the natural convection cooled bottom would be about 700°F. For such a large temperature gradient around the barrel, there would be significant conduction so that this full temperature difference would not be realized but it may be useful to consider this value as an upper limit. For a 700°F temperature difference, the muzzle deflection would be 1.9 inches.

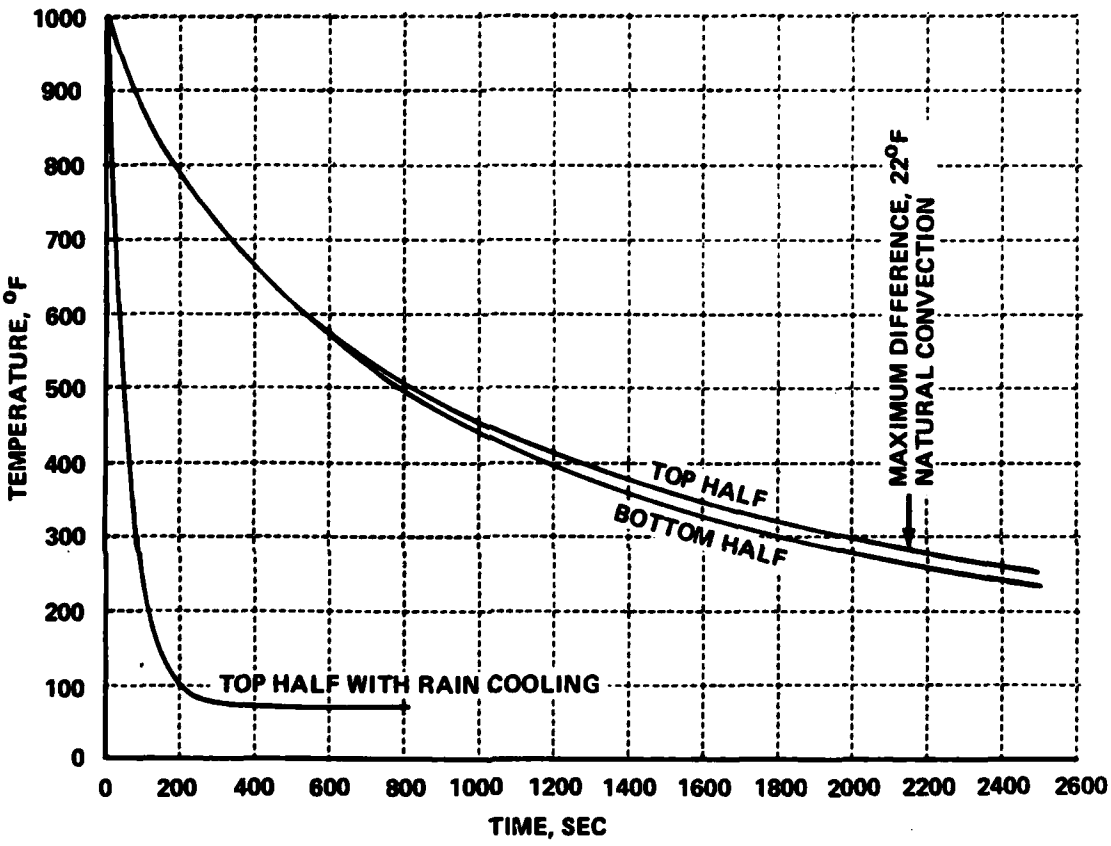

Figure A2 ARES 75mm BARREL COOL-DOWN, NATURAL CONVECTION, RADIATION LOSS INCLUDED

With wind blowing on the barrel, the heat transfer varies around the barrel such that there is a temperature variation during cooling. The heat transfer coefficient for each half of the barrel for equation A7 was taken from Giedt, H., Transactions of ASME, Vol. 71, p. 375, 1949. Figure A3 shows the cooling in a 60 ft/sec (40 mph) wind; a rather high wind condition and therefore a rather severe bending condition. The maximum temperature difference would be 72°F which would produce 0.2 inches of muzzle deflection.

The calculated muzzle deflections are quite substantial and require substantial aiming corrections as indicated by the following calculation of the aiming error of the muzzle. The barrel slope at the muzzle in mils of error is given by:

$$\sigma = 1000 \tan \frac{L}{R} \qquad \text{A8}$$

where R is the bending radius given by equation A5. Substituting equation A5 in equation A8 gives:

$$\sigma = 1000 \tan \frac{L(T_2 - T_1)}{4.5 \times 10^5} \qquad \text{A9}$$

At the 22°F temperature differential calculated for natural convection and a 50 inch unsupported length of barrel, the barrel slope at the muzzle would be 2.4 mils downward and at 72°F differential for a 60 ft/sec wind, it would be 8 mils toward the wind. Of course, rain could produce as much as 75 mils aiming error.

As a demonstration of barrel bending, actual deflection at the muzzle of the single-shot fixture was recorded at the completion of a five-round test series. For this deflection test, the muzzle end of the barrel was insulated so that heat introduced in the five-round sequence would not be totally lost and would result in an increase in the average barrel temperature near the muzzle. At the completion of 5 shots and prior to removal of the insulation, the barrel temperature at the muzzle region was measured to be about 180°F. At this time, a dial indicator stand was placed in contact with the farthest forward free end of the muzzle. Insulation was removed and a thermal gradient

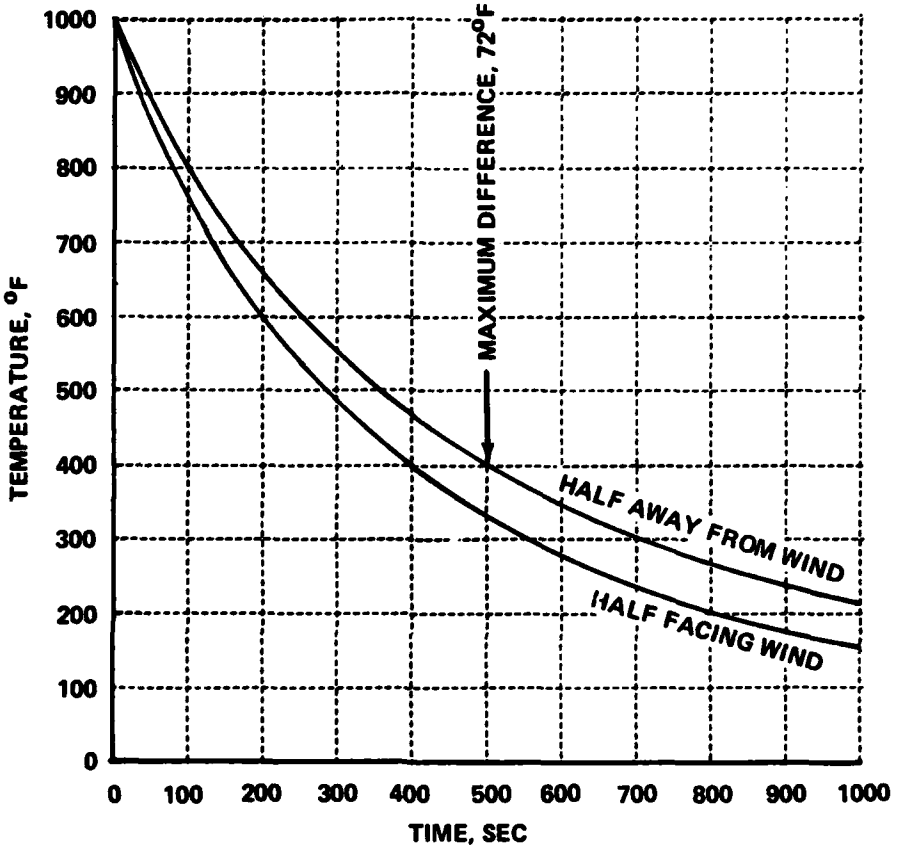

Figure A3 ARES 75 mm BARREL COOL-DOWN, 60 FT/SEC WIND VELOCITY, RADIATION LOSS INCLUDED

was induced by wiping the lower half of the barrel with a wet sponge. A maximum downward deflection at the muzzle end of 0.070 inches was recorded with a top-to-bottom temperature difference of no more than 40°F. This compares favorably with estimates given by equation A6 above and provides real evidence of thermally induced barrel bending.

Based upon the analysis given above and the brief confirmation test, there is reason to consider methods by which aiming errors caused by barrel bending may be overcome. One such method is to accommodate bending within the aiming system itself. Another is to reduce thermal gradient through insulation or cooling and thus reduce barrel bend. A third would be to increase the barrel wall thickness at the muzzle region, inasmuch as this reduces the thermal gradient while increasing the barrel's resistance to bending. Insulation techniques are definite candidates inasmuch as weapon performance in limited ammunition supply requires little barrel cooling. It is recommended that future consideration be given to the insulative approach combined with barrel wall thickness increase as a partial solution of thermally induced barrel bending. Sighting techniques which can accommodate the reduced bend can then provide a final solution.